# The Institute of Paper Chemistry

Appleton, Wisconsin

## Doctor's Dissertation

Polymer Production from Aqueous Solutions of D-Glucose by High Energy Radiation

John B. Snell

June, 1964

# POLYMER PRODUCTION FROM AQUEOUS SOLUTIONS OF D-GLUCOSE BY HIGH ENERGY RADIATION

A thesis submitted by

John B. Snell

B.S. 1959, University of Wisconsin
M.S. 1961, Lawrence College

in partial fulfillment of the requirements
of The Institute of Paper Chemistry
for the degree of Doctor of Philosophy
from Lawrence College,
Appleton, Wisconsin



June, 1964

TABLE OF CONTENTS


SUMMARY 1

INTRODUCTION 4

Historical Background 4

Choice of Sugar and Radiation Source 7

THE EFFECT OF RADIATION ON MATTER 8

Irradiation of Matter in General 8

Irradiation of Specific Compounds 13

Water 13

Alcohols 17

Carbohydrates 19

EXPERIMENTAL METHODS 21

Radiation Source 21

Preparation of Solutions for Irradiation 22

Analysis of Whole Irradiated Solutions 24

Isolation of Polymers 25

Analysis of Polymers 26

Light Scattering 26

Choice of Solvent 26

Clarification of Solvent 28

Clarification of Solutions 28

Light-Scattering Apparatus 29

Calculations 29

Refractive Index Gradient 33

Osmometry 34

Osmometer 34

Solutions 35

Membranes 36

Calculations 36

Viscometry 36

Chemical Measurements 38

Fractionation 39

Fractionation Procedure 39

Analysis of Fractions 40

RESULTS AND DISCUSSION 41

The Effect of Different Conditions of Irradiation 41

Dose 41

Dose Rate 43

Oxygen Content of the Solutions 45

Glucose Concentration 45

The Physical Nature of the Molecules 46

Molecular Weight 46

Evidence for Branching 54

The Polyelectrolyte Effect 57

Osmometry 57

Light Scattering 58

Viscometry 60

Fractionation 63

The Chemical Nature of the Molecules 66

Comparison of the Polymers with those of Barker *et al.* 66

Analysis of Fractions 70

Carboxyl Content 70

Infrared Absorption Spectra 71

Ultraviolet Absorption Spectra 73

Elemental Analyses 74

Fractionation of the Supernatant from Ethanol Precipitation 79

Miscellaneous New Chemical Information 79

Molisch Test 80

Optical Rotation 80

Treatment with Hydrobromic Acid 80

CONCLUSIONS 82

SUGGESTIONS FOR FUTURE WORK 83

POLYMER NOMENCLATURE 84

ACKNOWLEDGMENTS 85

LITERATURE CITED 86

APPENDIX I. IRRADIATION DATA 91

APPENDIX II. SOLUBILITY DATA 94

APPENDIX III. LIGHT-SCATTERING DATA ON POLYSTYRENE 96

APPENDIX IV. REFRACTIVE INDEX GRADIENT DATA 97

APPENDIX V. LIGHT-SCATTERING DATA ON FRACTIONS OF POLYMER 11 99

APPENDIX VI. DETERMINATION OF MOLECULAR WEIGHTS WITH THE VAPOR PRESSURE OSMOMETER 103

## SUMMARY

Recent work by Barker, et al. (1) indicated that a high yield of nondialyzable material (i.e., material retained by a dialysis membrane) could be obtained by irradiating deaerated aqueous solutions of glucose with gamma-rays from a cobalt-60 source. As a result of several chemical tests conducted on the material, they suggested that the nondialyzable material was a polymer of gluconic acid linked together by carbon-carbon bonds. No indication of the size and shape of the molecules was given.

In this thesis, 1.0% aqueous glucose solutions were irradiated with high energy electrons. The yield of polymer, measured as either nondialyzable material or ethanol precipitate, increased with both the dose and the dose rate. This would be expected in view of Barker's proposed mechanism which involves hydrogen abstraction from the sugar molecules followed by coupling of the resulting sugar free radicals. Increasing the dose rate would be expected to increase the concentration of hydrogen and hydroxyl free radicals, which in turn would increase the concentration of sugar free radicals and thus increase the liklihood of radical coupling.

The weight average molecular weights of the whole polymers isolated by ethanol precipitation were measured by light scattering in water solution. The molecular weights ranged from 9800 to 5,000,000, and hence are much larger than previously imagined. Measurement of the number average molecular weight of one of the polymers by osmometry established an $\overline{M}_w/\overline{M}_n$ ratio of 4.9, thus indicating a broad distribution of molecular weights within the polymer.

The polymers exhibited intrinsic viscosities in the range of 0.02 to 0.26 dl./g. in water at 30.000 $\pm$ 0.005°C., and are therefore thought to be very highly branched.

A marked polyelectrolyte effect was encountered in osmometry, a slight effect in light scattering, and no apparent effect in viscosity measurements. The results can be explained on the basis of a highly branched, weak polyelectrolyte. Apparently, the molecule is too highly branched to allow the charges to expand the molecule upon dilution, thus preventing the usual polyelectrolyte effect in viscometry.

In order to gain insight into the structure, one polymer was fractionated on a column of Sephadex, and the chemical composition of the fractions compared. Fractionation by molecular weight was demonstrated by molecular weight determinations on the fractions by light scattering and osmometry. The carboxyl content of the fractions, measured by titration with dilute sodium hydroxide, increased regularly with molecular weight. The carboxyl groups are therefore thought to be the result of secondary oxidative attack which takes place on the molecule as it grows in size. This is opposed to the earlier hypothesis that the repeating monomer unit in the initial stages of polymerization was gluconic acid.

Infrared absorption spectra of the fractions showed a single carbonyl peak at 1760 $cm.^{-1}$ for the low molecular weight material and peaks at 1760 and 1720 $cm.^{-1}$ for the higher molecular weight material. The peak at 1760 $cm.^{-1}$ was attributed to lactone formation and that at 1720 $cm.^{-1}$ to carboxyl formation.

Elemental analysis of the fractions showed that the composition of the low molecular weight material was similar to that of gluconolactone. Despite the increase in carboxyl content, the hydrogen and oxygen content decreased with molecular weight. To account for the loss of oxygen, it is proposed that, as polymerization proceeds, oxygen-rich fragments such as carbon dioxide or formic acid are lost from the polymer.

Ultraviolet absorption spectra indicated that unsaturated chromophoric groups are formed as the polymer increases in molecular weight. These groups are possibly of the enediol type proposed by preceding workers.

# INTRODUCTION

## HISTORICAL BACKGROUND

This thesis was undertaken as a sequel to the work of Barker, Grant, Stacey, and Ward (1), who reported the production of nondialyzable material (i.e., material retained by a dialysis membrane) upon irradiation of deaerated aqueous solutions of certain sugars and organic acids. Barker, et al. irradiated 0.1% solutions with gamma-rays from a 200 curie cobalt-60 source, and found the amount of nondialyzable material to vary with both the compound irradiated and the conditions of irradiation. This is shown in Table I.

TABLE I (1)

YIELDS OF POLYMERS

| Substrate | Dose Rate, rad./min.[a] | Dose, megarad | Yield, % nondialyzable |
|---|---|---|---|
| Maltose | 610 | 7.10 | 1.4 |
| Glucose | 610 | 2.34 | 1.3 |
| Glucose | 610 | 7.10 | 45 |
| 1,4-Gluconolactone | 2280 | 7.26 | 51 |
| Lactic acid | 2280 | 7.26 | 4.8 |
| Glycolic acid | 2280 | 7.26 | 4.5 |
| Glycolic acid | 610 | 1.46 | 0 |
| Glycolic acid | 610 | 6.88 | 2.2 |
| Glycolic acid[b] | 610 | 14.8 | 6.4 |

[a] A rad is defined as the absorption of 100 ergs of energy per gram of material irradiated. A megarad is $10^6$ rads.

[b] The concentration of this solution was 0.15%, the balance were 0.10%.

Although no molecular weights were obtained, the authors assumed the material was polymeric, and devoted most of their work to a chemical characterization of the material. The work on the polymer formed by the 7.10 megarad (Mrad) treatment of glucose is of particular interest to this thesis, and may be summarized as follows:

a. The material was acidic, having an equivalent weight of 328, or a carboxyl content of 13.7%.

b. The polymer had an aldehyde content of 16.0%, as measured by alkaline hypoiodite.

c. The polymer was resistant to acid hydrolysis. In fact, most of the polymer precipitated in hot acid. The precipitate had an infrared absorption spectrum similar to that of the original polymer, and the soluble portion showed no mobile components with paper chromatography.

d. The polymer contained 51.91% carbon and 5.07% hydrogen.

e. The polymer exhibited absorption at approximately 265 mμ in the ultraviolet.

f. The polymer reacted with sodium metaperiodate; about one-third of the material remained nondialyzable.

From the above information, the authors concluded that the polymeric linkage was neither that of a glycoside nor an ester. Instead, they proposed a carbon-carbon linkage similar to that formed upon irradiation of alcohols (2, 3). The proposed mechanism involved the production of H· and ·OH radicals from the water, which in turn abstracted a hydrogen atom from the carbohydrate substrate. Coupling of the sugar free radicals was then thought to produce the polymer. A similar mechanism has been used to explain polymer production from mannose (4), sorbitol (5), and glycolic acid (6). In all cases, the presence of an excess of

oxygen inhibited polymerization, as would be expected by the proposed free radical mechanism.

Since a high yield of gluconic acid was obtained in another study (7), and a high yield of polymer was obtained from 1-4 gluconolactone, Barker, Grant, Stacey, and Ward suggested that the main route of polymerization was through gluconic acid. In a later paper, Barker, Lloyd, and Stacey (8) proposed that, in the early stages of polymerization, the repeating unit was gluconic acid, as shown in Fig. 1.

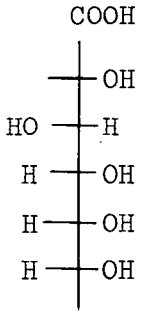


Figure 1. Proposed Monomer Unit (8)

On further irradiation, this unit would undergo radiation damage, and the chemical composition of the polymer would be expected to change.

Up to this time most of the work on radiation-induced polymers of carbohydrates had been chemical analyses of the polymer. Nothing was known about the physical properties, such as size and shape, of the molecules. This thesis represents what the author believes is the first contribution which concerns the molecular size and shape of polymers produced by high energy radiation of carbohydrate solutions. It also represents the first time such a polymer has been fractionated by molecular weight, followed by the study of the chemical composition of the fractions to yield information on the structure of the polymer.

## CHOICE OF SUGAR AND RADIATION SOURCE

Although the radiation-induced polymerization of any carbohydrate would be of interest from a purely scientific viewpoint, glucose was chosen because of the prior work of Barker, et al. (1), and because of its relationship to cellulose and the broader problem of crosslinking of cellulosic materials. Several authors (9-11) have reported the crosslinking of cellulosic materials by radiation, but the chemistry of the process is not understood. Since the crosslinking mechanism in this case is believed to be similar to that of the polymerization of the monomer, it seems logical to first study the simpler case of the polymerization of glucose.

Electrons were chosen rather than gamma-rays mainly because of the higher dose rates available with electrons. Irradiations that would have taken weeks with conventional gamma-ray sources such as cobalt-60, were conducted in a matter of hours. Also, the use of electrons extended the work into an area of dose rates never used before for the polymerization of glucose. One final advantage of electrons was that the actual irradiation procedure was simpler because the accelerator could be shut off and approached while the samples were handled by the operator. Penetration was the main problem encountered with electrons, but this was overcome by proper design of the sample container.

# THE EFFECT OF RADIATION ON MATTER

## IRRADIATION OF MATTER IN GENERAL

The passage of a gamma-ray through a material produces one or more fast electrons and a photon of lower energy. Since the ejected electrons then cause subsequent ionization and excitation of molecules, the net chemical effect is considered to be similar for gamma-rays and high energy electrons (12). In fact, the effect is considered to be similar for all types of ionizing radiation (alpha particles, protons, x-rays, gamma-rays, etc.) except for the penetration of the radiation and the density and distribution of the ions and excited molecules produced by the radiation. Since electrons were used in this thesis, this discussion will deal specifically with the interaction of electrons with matter. The information has been taken largely from Charlesby (12), Chapiro (13), Hollaender (14), and a bulletin from the High Voltage Engineering Corporation (15).

The penetrating ability of electrons varies directly with the energy of the electrons and indirectly with the density of the material being irradiated, as shown in Fig. 2.

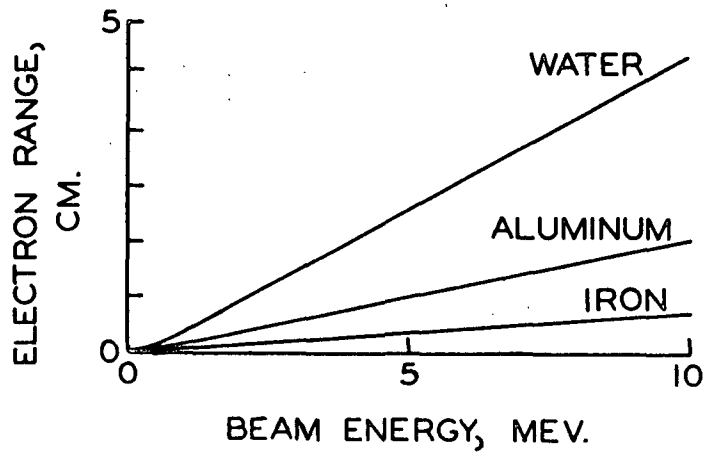


Figure 2. The Penetration of Electrons (15)

While the total beam energy is all delivered within the range shown in Fig. 1, the dose is not uniform at all depths. Several factors contribute to cause the characteristic dose-depth relationship shown in Fig. 3.

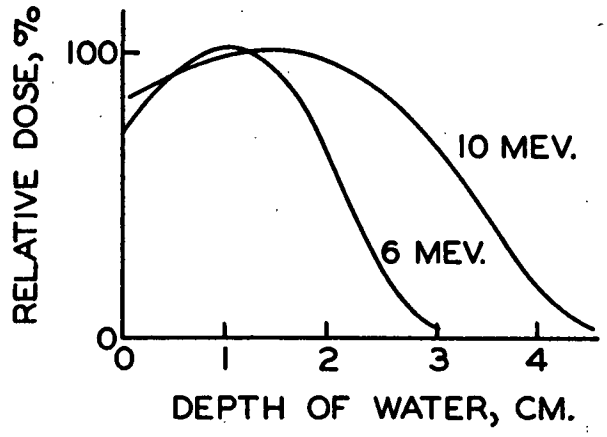


Figure 3. Dose-Depth Curves for Electrons (13)

After scattering of the incident beam, the electrons are, on the average, moving obliquely to the forward direction of the beam and thus leave more energy behind in a thin layer normal to the beam direction. Also, the rate of energy loss per unit length of path, $\underline{dE}/\underline{dx}$, increases as the electrons slow down, as shown by the following equation (12):

$$\frac{dE}{dx} = -\frac{2\pi e^4 NZ}{m V^2} B \qquad (1)$$

where $\underline{N}$ is the number of atoms of atomic number $\underline{Z}$ per cubic centimeter, $\underline{V}$ is the velocity of the electron, $\underline{e}$ and $\underline{m}$ are the charge and mass of the electron, and $\underline{B}$ is the stopping number of the medium. After a depth of about one-third the total range, most of the electrons have been scattered, so the dose starts to fall off again, and at a depth about two-thirds the total range, the dose is equal to that at the surface. This particular depth is significant because it is

the optimum thickness of sample to use. Here the best balance is obtained between minimizing overdosage and maximizing the total use of the beam's penetration.

A further complication involved in trying to irradiate a sample uniformly is that the electron beam produced by the accelerator is circular in cross section with the most intense portion in the center. To remedy this, the target is scanned by magnetic deflection of the beam. The result is a thin slot-shaped beam of nearly uniform intensity, as shown in Fig. 4.

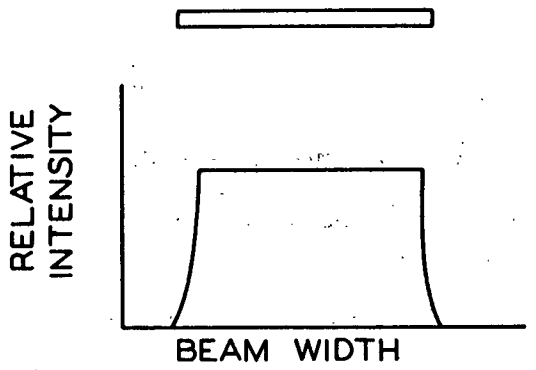


Figure 4. Scanned Electron Beam (15)

In passing through a specimen each electron loses energy by reaction either with the orbital electrons or with the nuclei of the atoms encountered. Since the masses of the electron and the nucleus are so different, only a small percentage of the electron's energy is transferred to the nucleus, and the main effect of electron-nucleus interaction is simply the scattering it causes the incident beam. Electrons lose most of their energy by reacting with orbital electrons. The primary electron is deviated and the bound electron may either be given sufficient energy to leave its parent atom completely (ionization) or move into an orbit of higher energy (excitation). In the former case a secondary, or $\delta$ electron, is produced which can in turn cause further ionization and excitation. For lack of definite knowledge, it is generally assumed that the energy lost through ionization equals that lost through excitation.

The path of the charged particle as it passes through a condensed medium is believed to be similar to that observed in a gas by means of the Wilson Cloud Chamber. The size of the track would, of course, be reduced according to the relative densities of the liquid and gas. The track of an electron may therefore be pictured as a string of randomly spaced spurs, as shown in Fig. 5.

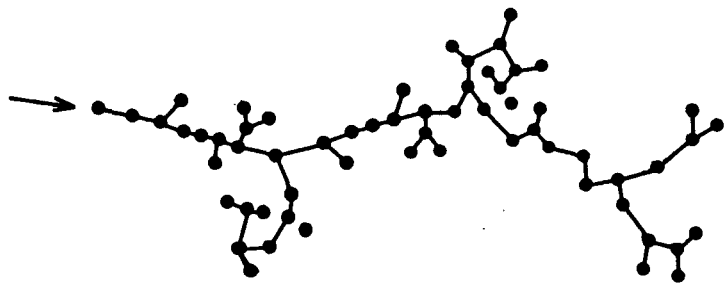

Figure 5. Schematic Diagram of the Track of a Fast Electron (13)

Since the frequency of the spurs depends on the speed and charge of the particle, the spurs become more closely spaced as the particle slows down. For 1 million electron volt (Mev.) electrons it is estimated that an elastic collision occurs at about every micron along the path of the electron in most solids and liquids. Branching off from the main string of spurs are other strings caused by δ electrons. Secondary electrons are believed to dissipate most of their energy within 10 A. of their point of origin in most solids and liquids.

Initially each spur contains only the primary products of irradiation, but the nature and concentration of the active species soon changes due to chemical reaction and diffusion.

The species produced in the primary event (ions, excited molecules, and secondary electrons) react with each other in the spurs or with nearby normal

molecules. The ions may react with other molecules, but more commonly they react with electrons or negative ions according to the following reactions (13):

a. Ion – electron recombination.

$$AB^+ + e^- \longrightarrow AB^* \qquad (2)$$

where AB* is an excited molecule.

b. Positive ion – negative ion interaction.

$$AB^+ + CD^- \longrightarrow AB^* + CD^* \qquad (3)$$

The excited molecules generally dissociate as follows (13):

a. Dissociation into free radicals.

$$AB^* \longrightarrow A\cdot + B\cdot \qquad (4)$$

b. Dissociation into molecular products.

$$AB^* \longrightarrow C + D \qquad (5)$$

Some authors have also suggested that excited molecules react with nonexcited molecules, but little is known about such reactions.

The eventual fate of the electrons after they lose their ability to ionize and excite molecules has been the subject of much speculation. It seems to be generally agreed that they probably become attached to neutral molecules or combine with positive ions as shown (13):

$$AB + e^- \longrightarrow AB^- \qquad (6)$$

$$AB^+ + e^- \longrightarrow AB^* \qquad (7)$$

Although other active species such as ions are responsible for some specific effects, the predominant radiation-chemical changes are believed to be caused by free radicals. The radiation induced polymerization of carbohydrates is therefore most likely due to free radicals produced in the solution.

When a single substance is irradiated, all the reactions must be due to primary ionizations and excitations of the substance itself. If a substance is irradiated in solution, though, the question arises as to whether the reactions are due to direct hits on the solute molecules or to hits on the solvent molecules which then react with the solute. The first is referred to as direct action and the second as indirect action. The proportion of solute molecules affected by a given dose will be independent of their concentration if the action is direct, but the actual number of affected molecules will be proportional to the concentration. If the action is indirect, however, the number of solute molecules reacted is independent of the concentration, and consequently the relative number reacted decreases as the concentration is increased (16). In other words, if the action is direct, the per cent yield should be independent of concentration, but if the action is indirect, the per cent yield should fall off as the concentration increases.

## IRRADIATION OF SPECIFIC COMPOUNDS

In the preceding section, the interaction of radiation with matter was discussed in a general sense. In this section, the effect of radiation on molecules of specific interest to this thesis will be discussed.

### WATER

Early work on the radiolysis of water indicated that hydrogen and hydrogen peroxide are decomposition products. Upon long exposure, oxygen is also formed,

but this has been shown to be a secondary product formed upon decomposition of the hydrogen peroxide (17, 18).

Although the net result of the irradiation of water is very simple, namely, the production and recombination of hydrogen and hydroxyl radicals, the different steps leading to these products are very complex. The preceding section, though, provides a guide for understanding the phenomenon.

In the initial step, a primary or secondary electron ionizes or excites a water molecule according to one of the following equations (19):

$$H_2O + e^- \longrightarrow H_2O^+ + e_s^- + e'^- \quad \text{(ionization)} \quad (8)$$

$$H_2O + e^- \longrightarrow H_2O^* + e'^- \quad \text{(excitation)} \quad (9)$$

where $e_s^-$ is a secondary electron and $e'^-$ is simply a lower energy state of the electron $e^-$. This initial step is often referred to as the physical stage, and has a duration of $10^{-13}$ sec. or less (20).

In the second stage, the ions, secondary electrons, and excited molecules formed in the primary act react with each other in the spurs or with nearby neutral water molecules. The ions formed may react by ion – electron recombination, positive ion – negative ion interaction, or ion – molecule reactions (13) according to the following equations:

$$H_2O^+ + e_t^- \longrightarrow H_2O^* \quad (10)$$

$$H_2O^+ + OH^- \longrightarrow H_2O^* + \cdot OH \quad (11)$$

$$H_2O^+ + H_2O \longrightarrow H_3O^+ + \cdot OH \quad (12)$$

where $e_t^-$ is a thermal electron. The thermal electron occupies the lowest position in the energy scale $e^- > e'^- > e_s^- > e_t^-$, and hence represents the last stage before the electron disappears by reaction with other active species in solution. The excited water molecule dissociates immediately:

$$H_2O^* \longrightarrow H\cdot + \cdot OH \qquad (13)$$

The secondary electrons continue to ionize and excite water molecules until they are reduced to thermal electrons. At this time they react with neutral water molecules or positive water ions (13). The equations are given as

$$e_t^- + H_2O \longrightarrow e_{aq}^- \qquad (14)$$

$$e_t^- + H_2O^+ \longrightarrow H_2O^* \qquad (15)$$

where $e_{aq}^-$ is the hydrated electron. The hydrated electron is simply an electron with one or more water molecules associated with it. The positive ends of the polar water molecules tend to line up toward the electron, thus creating a shell or cage of water molecules around the electron.

This second stage, in which the energetically unstable species undergo a series of transformations, establishes thermal equilibrium in the system and is referred to as the physical-chemical stage (20). It lasts about $10^{-11}$ sec. (20). The net result of the first two stages is, therefore, the production of H· and ·OH radicals, with perhaps small amounts of $H_3O^+$ and $e_{aq}^-$.

In the third, or chemical stage, the hydrogen and hydroxyl radicals react with each other or diffuse out of the spurs and react with other solvent molecules to eventually establish chemical equilibrium. The duration of this stage is $10^{-8}$ sec. or longer (20). At the start of this stage the spurs are 20 to

50 A. in diameter and consist of 2 to 12 radicals (20), which can take part in any of several reactions. Some of these reactions are given (19):

$$H\cdot + H\cdot \longrightarrow H_2 \quad (16)$$

$$\cdot OH + \cdot OH \longrightarrow H_2O_2 \quad (17)$$

$$H\cdot + \cdot OH \longrightarrow H_2O \quad (18)$$

$$\cdot OH + H_2 \longrightarrow H_2O + \cdot H \quad (19)$$

$$H\cdot + H_2O_2 \longrightarrow \cdot OH + H_2O \quad (20)$$

$$\cdot OH + H_2O_2 \longrightarrow H_2O + HO_2\cdot \quad (21)$$

$$2\ HO_2\cdot \longrightarrow H_2O_2 + O_2 \quad (22)$$

$$HO_2\cdot + H_2O_2 \longrightarrow H_2O + O_2 + \cdot OH \quad (23)$$

The hydrated electron has a half life of only 16 microseconds, but is believed to be an important intermediate in the radiolysis of aqueous solutions. For example, the water ion and a secondary electron may produce hydrogen and hydroxyl radicals by the following processes (19):

$$H_2O^+ + H_2O \longrightarrow H_3O^+ + \cdot OH \quad (24)$$

$$H_2O + e_s^- \longrightarrow e_{aq}^- \quad (25)$$

$$e_{aq}^- \longrightarrow H\cdot + OH^- \quad (26)$$

$$OH^- + H_3O^+ \longrightarrow 2H_2O \quad (27)$$

The net reaction is:

$$H_2O^+ + e_s^- \longrightarrow H\cdot + \cdot OH \quad (28)$$

In order for the radicals to react with solute molecules they must diffuse out of the spurs. Typical reactions with organic solute molecules are given:

$$H\cdot + RCH_2OH \longrightarrow \dot{R}CHOH + H_2 \qquad (29)$$

$$H\cdot + HCHO \longrightarrow \dot{H}CO + H_2 \qquad (30)$$

$$\cdot OH + RCH_2OH \longrightarrow \dot{R}CHO + H_2O \qquad (31)$$

$$\cdot OH + HCHO \longrightarrow \dot{C}HO + H_2O \qquad (32)$$

ALCOHOLS

The effect of ionizing radiations on alcohols is to cause fission of one of the alpha carbon – hydrogen bonds to give a hydrogen atom and a radical which can either give a dimer or be oxidized to give a carbonyl compound. This pattern seems to apply to irradiation of either the pure alcohol or solutions of the alcohol (2, 3, 21-24).

McDonell and Newton (3) irradiated several liquid, air-free, aliphatic alcohols with 28 Mev. alpha particles (helium ions) and obtained aldehydes and glycols from primary alcohols, and aldehydes, ketones and glycols from secondary alcohols and ketones with minor amounts of glycols from tertiary alcohols. Water, carbon monoxide, hydrogen, and saturated hydrocarbons of one less carbon atom than the parent alcohol were also formed. Principal bond rupture was at the carbinol carbon atom, with the reactivity of the carbinol groups exhibiting the order $H > C_2H_5 > CH_3$.

Burr (2) irradiated several deuterated ethanols and proposed the following mechanism to account for the products butane-2,3-diol, butane-1,4-diol, acetaldehyde, diethyl peroxide, 1-hydroxyethyl ethyl ether, and 2-hydroxy ethyl ether.

$$CH_3CH_2OH \longrightarrow CH_3\dot{C}HOH + H\cdot \qquad (100\%) \qquad (33)$$

$$H\cdot + CH_3CH_2OH \longrightarrow H_2 + CH_3CH_2O\cdot \qquad (80\text{-}90\%) \qquad (34)$$

$$H\cdot + CH_3CH_2OH \longrightarrow H_2 + \dot{C}H_2CH_2OH \qquad (10\text{-}20\%) \qquad (35)$$

$$2\ CH_3\dot{C}HOH \longrightarrow (CH_3CHOH)_2 \qquad (36)$$

$$2\ CH_3\dot{C}HOH \longrightarrow (CH_3CHOH)_2 \qquad (37)$$

$$2\ CH_3CH_2O\cdot \longrightarrow CH_3CHO + CH_3CH_2OH \qquad (38)$$

Jayson, Scholes, and Weiss (23) and Allen, Hayon, and Weiss (24) irradiated aqueous solutions of ethanol and obtained acetaldehyde and butane-2,3-diol with deaerated solutions. With oxygen-saturated solutions, no butane-2,3-diol was obtained. The mechanism postulated involved hydrogen abstraction from the $\alpha$ carbon atom as shown:

$$H_2O \longrightarrow H\cdot + \cdot OH \qquad (39)$$

$$CH_3CH_2OH + \cdot OH \longrightarrow CH_3\dot{C}HOH + H_2O \qquad (40)$$

$$CH_3CH_2OH + \cdot H \longrightarrow CH_3\dot{C}HOH + H_2 \qquad (41)$$

In the absence of oxygen, the ethanol radicals react:

$$2\ CH_3\dot{C}HOH \longrightarrow CH_3\overset{H}{\underset{OH}{C}} - \dot{C}\overset{H}{\underset{OH}{}}CH_3 \qquad (42)$$

$$CH_3\dot{C}HOH + \cdot OH \longrightarrow CH_3CHO + H_2O \qquad (43)$$

In the presence of oxygen, they react:

$$CH_3\dot{C}HOH + O_2 \longrightarrow CH_3\overset{\dot{O}_2}{\underset{}{C}}HOH \qquad (44)$$

$$H\cdot + O_2 \longrightarrow HO_2\cdot \qquad (45)$$

$$CH_3\overset{\overset{\cdot O_2}{|}}{C}HOH + HO_2\cdot \longrightarrow CH_3CHO + H_2O_2 + O_2 \qquad (46)$$

$$2\ CH_3\overset{\overset{\cdot O_2}{|}}{C}HOH \longrightarrow CH_3\overset{\overset{H}{|}}{\underset{\underset{OH}{|}}{C}}\text{-O-O-}\overset{\overset{H}{|}}{\underset{\underset{OH}{|}}{C}}CH + O_2 \qquad (47)$$

CARBOHYDRATES

Work other than that of Barker, et al. described in the introduction will be discussed in this section. Phillips (25) gives a summary of the work done up to 1960 in Advances in Carbohydrate Chemistry.

The precise nature of the products of irradiation has been studied in considerable detail for carbohydrates in aqueous solution. The presence or absence of oxygen in the solution is important, so precautions must be taken to maintain either evacuated or oxygenated systems. Apparently, the predominant chemical reactions are oxidation and scission of carbon-carbon bonds. This is indicated by the fact that the following compounds have been reported as decomposition products of glucose by one or more authors (7, 26-28): gluconic acid, glucosone, arabonic acid, arabinose, erythrose, 1,3-dihydroxy acetone, glycol aldehyde, glyoxal, formaldehyde, carbon dioxide, and carbon monoxide. In addition, 2-oxogluconic acid, lyxose, oxalic acid, and formic acid have been obtained from mannose (29, 30).

Yield-dose curves for the products are used to distinguish the primary products from the secondary products. Phillips and Griddle (30) showed that irradiation of deaerated aqueous mannose solutions gave mannonic acid, glucosone, and two, three, and four-carbon aldehydic fragments as primary products. In

the presence of oxygen, though, scission between $C_1$ and $C_2$ took place to give formaldehyde and arabinose as primary products instead of glucosone (29).

Reductones have been proposed as products to account for the absorption at 265 to 275 mμ commonly observed with irradiated carbohydrate solutions (7, 31, 32). The proposed mechanism involves hydrogen abstraction:

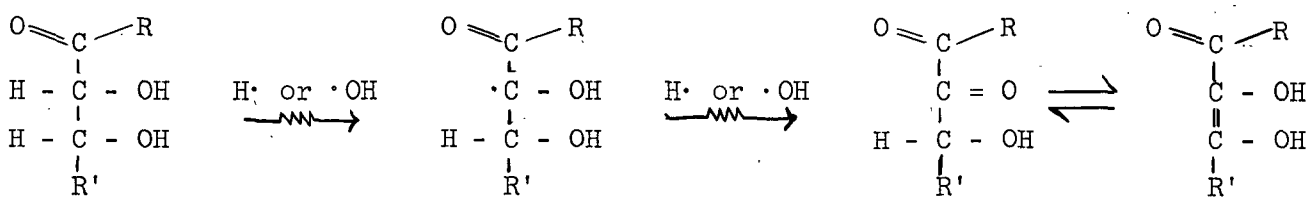


The most likely reductone formed from glucose would be xyloascorbic acid, although any enediol structure would likely give the observed absorption in the ultraviolet. Coleby (32) isolated xyloascorbic acid as a product of the irradiation of gluconolactone.

Reduction is generally not reported, but apparently it is possible because Michelakis (33) reported small amounts of methane and ethane in the gas produced upon irradiation of an aqueous solution of glucuronic acid.

In an attempt to find the position on the pyranose ring most favorable for dimerization, Bailey, Barker, Lloyd, and Moore (34) measured the rate of dimerization of model tetrahydropyranols. The conclusion reached was that dimerization proceeds much more readily through a primary hydroxyl group than a secondary hydroxyl group. A similar study (35) indicated that the rate of polymerization was still greater if a carbonyl group was attached to $C_6$ instead of a primary alcohol group. If a secondary hydroxyl group occupied the reducing position of a pyranose ring, though, polymerization proceeded readily, presumably due to the ready oxidation of this site to the lactone or acid.

# EXPERIMENTAL METHODS

## RADIATION SOURCE

All irradiations were conducted by the High Voltage Engineering Corporation. Most of the work was done at their Rockford, Illinois laboratory, but one run was made at their Burlington, Massachusetts laboratory.

A Linac Mark I accelerator, built by Applied Radiation Corporation, Oak Creek, California, was used at Rockford. This is a linear accelerator which is capable of producing 1 to 12 million electron volt (Mev.) electrons. 8.5 Mev. electrons were used in all the work with this machine, but certain details differed among irradiations. For example, a diffused beam was used for the second irradiation and a scanned beam was used for the fourth irradiation. These variables could not be avoided, but it is felt that they did not affect the nature of the product formed to any great extent. They were simply the result of a series of improvements made on the radiation facilities by the High Voltage Engineering Corporation personnel. The details of each irradiation are given in Appendix I.

A series of belts made up the conveyor system at Rockford, as shown in Fig. 6. The belt which runs under the accelerator could either be used as part of a continuous system, or could be used as a reversible conveyor. In the latter case, the samples were placed on the reversible belt, and passed back and forth under the beam until the desired dose was built up. Both the continuous and reversible systems were used.

A Van de Graaff "GS" accelerator was used at Burlington. The major difference between this machine and the linear accelerator is that it produced a steady

beam of 1.5 Mev. electrons instead of a pulsed beam of 8.5 Mev. electrons. The details of this irradiation are also given in Appendix I.

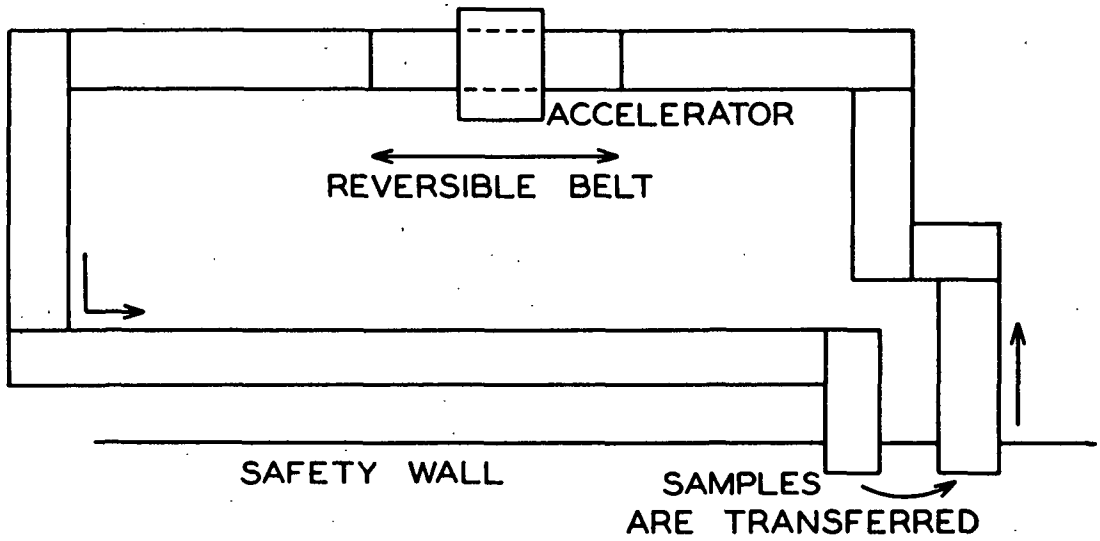


Figure 6. Conveyor Belt at Rockford

High Voltage personnel conducted the dosimetry for each irradiation. Cobalt glass dosimetry, which had previously been calibrated by Argonne National Laboratories, was used at Rockford. Blue cellophane, polyvinyl chloride, and the Faraday cup were used at Burlington.

## PREPARATION OF SOLUTIONS FOR IRRADIATION

The two types of containers used for the solutions were polyethylene bags and glass tubes. These are shown in Fig. 7. No difference was noticed in the results obtained with the two types of container.

The polyethylene bags were used for most irradiations because they enabled treatment of a large volume of solution at a minimum sample thickness. Since the polyethylene bags are known to be somewhat permeable to oxygen, the glass tubes were used in the study of the effect of oxygen on the yield of polymer.

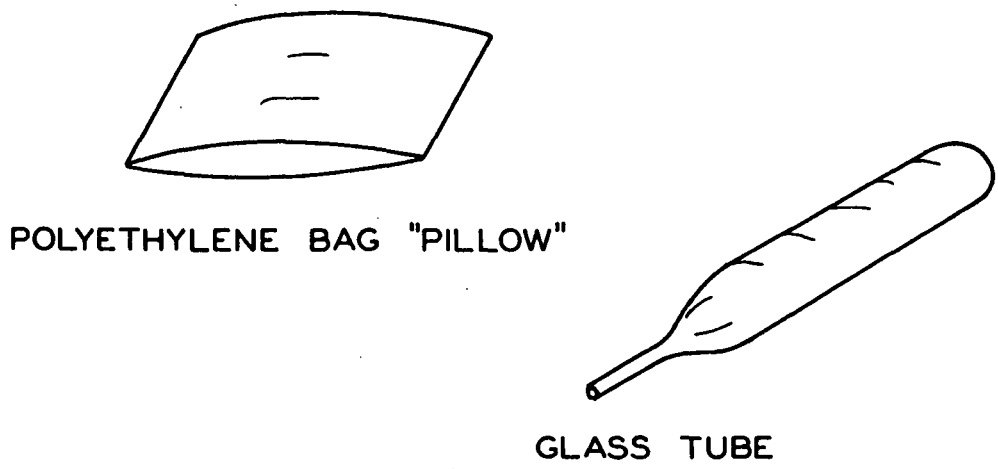


Figure 7. Containers for Irradiation

The deaerated glucose solutions were prepared by boiling 1.0% glucose solutions at 100°C. for about 5 min. The flasks were stoppered, cooled to room temperature, and then placed in a nitrogen box. Oxygen was removed from the atmosphere of the nitrogen box until it gave an Orsat analysis for oxygen of approximately zero. The polyethylene bags, which had previously been placed in the nitrogen box, were each filled with 400 ml. of solution and closed by heat sealing. This gave a "pillow" measuring approximately 5 by 7-1/2 by 3/4 inches. The bags were stored in the nitrogen box until the night before the trip to Rockford, at which time they were sealed in larger polyethylene bags and removed from the box. This provided an atmosphere of nitrogen around the small bags and therefore cut down the rate of diffusion of oxygen into the solutions during the trip to Rockford.

Just before the bags were removed from the nitrogen box, one bag was opened, and the oxygen content of the solution measured. The oxygen content was measured by the short Theriault modification of the Winkler test (36). Since the presence

of glucose interfered slightly with the test, a calibration curve was determined to correct the oxygen contents. The correction was small.

The glass tubes were made from 25 by 250 mm. test tubes. After alternately evacuating and filling the glass tubes with nitrogen 3 times, they were filled with about 75 ml. of deaerated glucose solution. Finally, the tubes were sealed off in a gas flame. When the tubes were placed on their side, the solution depth was about 3/4 inch.

One irradiation was conducted with 1.5 Mev. electrons at Burlington, Massachusetts, so this required some modifications in sample preparation. Since lower energy electrons were used, only 100 ml. of solution were put into the polyethylene bags. This presented a depth of about 1 cm. of solution to the electron beam. The bags were packed in 5-gallon drums which were lined with large polyethylene bags. The drums were flushed with nitrogen before being loaded with bags of solution, and then after loading, the large polyethylene bag liners were heat sealed shut. The drums were then sealed and shipped to Burlington by air express.

## ANALYSIS OF WHOLE IRRADIATED SOLUTIONS

After irradiation, the solutions were analyzed for pH and solids content. Solids contents were determined by evaporating a 5-ml. aliquot of solution to dryness at 50°C. in vacuo. pH was measured on a Beckman model H 2 glass electrode pH meter.

Paper chromatography of the irradiated solutions was run in ethyl acetate – pyridine – water (8:2:1, v/v) and butanol – acetic acid – water (4:1:5, v/v). The spots were revealed by dipping the chromatograms in silver nitrate according

to the method of Trevelyan, Proctor, and Harrison (37). Streaked chromatograms were obtained, but a spot for unreacted glucose and for polymer, which stayed on the starting line, could generally be detected.

To determine the yield of nondialyzable material, twenty-five milliliter aliquots of the irradiated solutions were placed in bags made of Fischer dialyzer tubing (seamless cellulose tubing: Fischer Scientific Company). All dialyzer tubing was taken from the same roll to minimize the variation of pore size between pieces of tubing. The bags were immersed in approximately 300 ml. of water which was changed daily. Paper chromatography of the solutions in the bags revealed that 3 days were sufficient to complete dialysis. The amount of nondialyzable material was found by evaporating an aliquot of the solutions in the bags to dryness.

## ISOLATION OF POLYMERS

The polymers were isolated for characterization by precipitation with ethanol. The same procedure, with minor variations, was used for each polymer, so the detailed procedure will be given only for Polymer No. 11.

Five hundred milliliters of whole Solution No. 11 were evaporated almost to dryness on a rotary evaporator. Complete dryness was not obtained, since it was feared that difficulty would be encountered in redissolving the polymer. Another 500 ml. of whole solution were added to the flask, and the evaporation process repeated. After evaporation again, it was estimated that about 1 ml. of water remained with the solids. Nine more milliliters of water were added to give a sirup, and then 450 ml. of absolute ethanol added to precipitate the polymer. The 45/1 ratio of ethanol/water is quite large, but this was used to maximize the yield of polymer without precipitating out glucose. The resulting flocculent

precipitate was separated by centrifugation and then washed twice with 20 ml. of each of the following: 45/1 ratio of ethanol/water solution, absolute ethanol, absolute diethyl ether, and low boiling petroleum ether. A few drops of hydrochloric acid were added to aid precipitation during the washing steps. With Polymer 9 the electrolyte was required to get the initial precipitation of polymer from the ethanol solution. Finally, the precipitate was dried in vacuo at 30°C. The absence of simple sugars in the isolated polymers was verified by paper chromatography. A yield of 10.2% was obtained for Polymer No. 11.

## ANALYSIS OF POLYMERS

### LIGHT SCATTERING

#### Choice of Solvent

The solubility of Polymer 9 was studied in a number of solvents in an attempt to find a suitable one for light-scattering measurements. The acetate of Polymer 9 was also made by the pyridine – acetic anhydride method of Heyne and Whistler (38) and described by Koleske (39). The results of the solubility tests on the polymer and its acetate are given in Appendix II. All solutions of the acetate were so dark colored though, that they could not be used for light-scattering measurements. Dimethyl sulfoxide, formamide, pyridine, and water dissolved the unacetylated polymer, but the pyridine and formamide solutions were considerably darker in color than those of water and dimethyl sulfoxide. Water was chosen over dimethyl sulfoxide for most of the work because dimethyl sulfoxide is very hygroscopic and would be expected to pick up water from the atmosphere during measurements, thus introducing possible solvent complications (40). One run was made, however, in 98% dimethyl sulfoxide to check the possibility of aggregation. Two per cent water was added in an attempt to reduce the

rate of moisture pickup from the air. Goring and Timell (41) used this technique with hemicelluloses.

Although the aqueous solutions of the polymers were amber colored, they were well within the limits of absorption allowed without having to apply an absorption correction (42). This is illustrated in Fig. 8. Since the most concentrated solution of 9 used for light scattering was about 0.1% instead of 0.69%, this polymer was also well within the absorption limits.

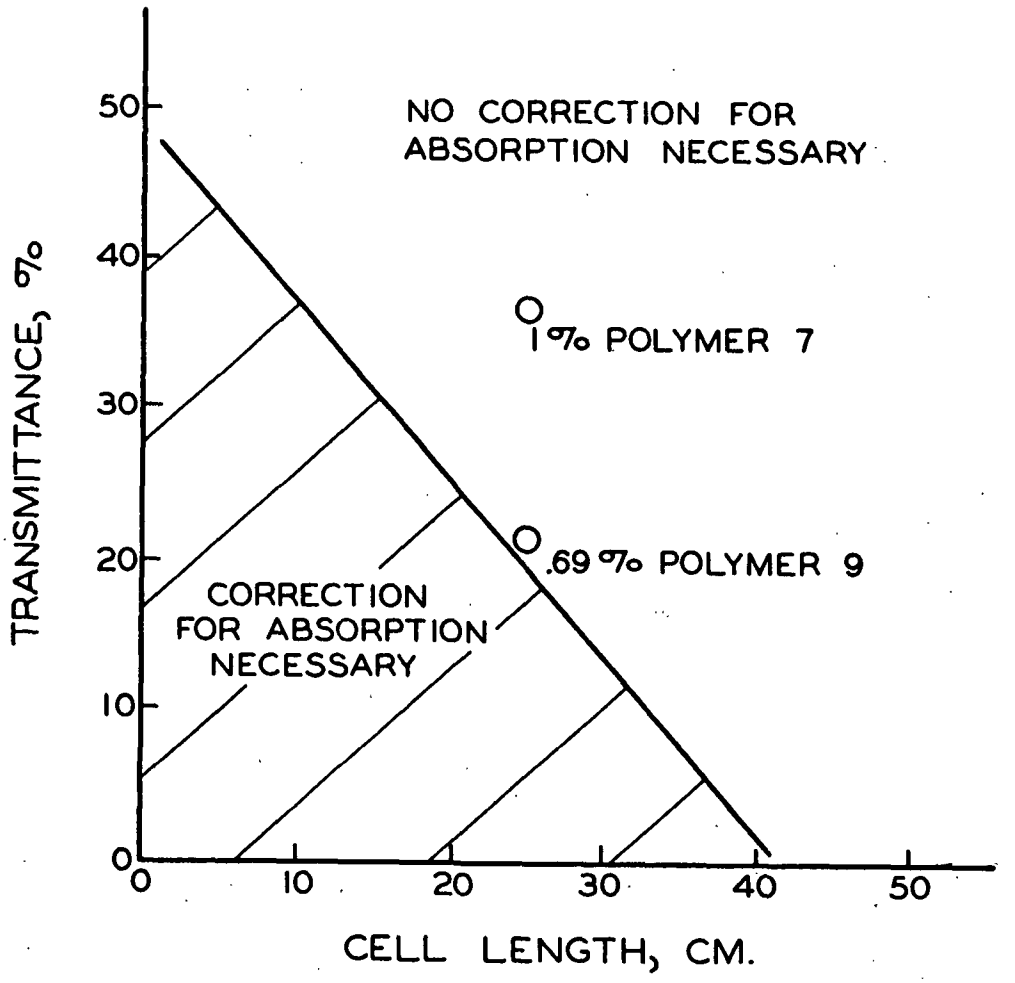


Figure 8. Transmittance Requirements for Light Scattering (42)

Clarification of Solvent

As is well known, the removal of dust particles from water is a difficult task. The procedure finally adopted in this work was repeated filtration of distilled water through a 2500 A. Polypore filter. A Polypore pressure filtration funnel was used to filter the water about 12 times, after which it was collected in a small separatory funnel. For the highest molecular weight material, the solvent exhibited a turbidity of less than 1% of the value for a 0.1% solution. For the lower molecular weight materials, the turbidity of the solvent was a larger percentage since the scattering of the solutions was less. Usually the solvent exhibited a turbidity of roughly 6% that of a 1.0% solution of Polymer 11. The dissymmetry of the clarified water was generally in the range of 1.2 to 1.8. Although this is rather high, it apparently did not effect the dissymmetry measurements on the polymer which lay in the range 1.05 to 1.20.

Clarification of Solutions

Solutions of the polymers were made up to approximately 1.0% in distilled water and then centrifuged in a laboratory centrifuge equipped with a high-speed head* which produced a centrifugal force of about 12,000 g. The solutions were carefully removed from the centrifuge cells with a syringe, and placed in the Polypore filtering apparatus. The solutions were filtered through 4500 A. pore size Polypore filters 5 times, with the last filtration being made directly into the light-scattering cell. A sample of the last filtrate was taken for a solids content determination.

In some cases the solvent was filtered directly into the light-scattering cell, and the solution into the small separatory funnel. When this was done,

*International Equipment Company part No. 296, 4 place, 40° angle head. Maximum radius 6.4 cm., minimum radius 2.5 cm., average radius 4.95 cm.

solution was added to the solvent for light-scattering measurements instead of the solvent being added to the solution. The methods were found to be equally satisfactory.

Light-Scattering Apparatus

Light-scattering measurements were made on a Brice-Phoenix Photometer (Series 1937). Since the polymer solutions exhibited very high absorption with light of 436 mμ wavelength, measurements were made with 546 mμ wavelength light.

The light-scattering instrument was calibrated earlier by Swenson (43) and other workers (39, 44). As a further check, the Rayleigh ratio, $R_{90} = (3\tau/16\pi)$, was determined for benzene, where $\tau$ is the turbidity exhibited by benzene. A value of $16.9 \times 10^{-6}$ was obtained for $R_{90}$, which checks favorably with the literature (45). As another check, the molecular weight of McCormick's B-3 polystyrene (46) was measured in toluene. The data, given in Appendix III, gives a molecular weight within 10% of the value reported by McCormick.

Calculations

Molecular weights were calculated by Debye's method of dissymmetry (40, 42, 47, 48) which employs the equation:

$$\frac{Hc}{\tau} = \frac{1}{MP_\theta} + 2A_2c + \ldots\ldots \qquad (48)$$

where $M$ is the weight average molecular weight, $\tau$ the excess turbidity due to the dissolved polymer, $c$ the concentration of polymer in g./ml. and $A_2$ the second virial coefficient. $P_\theta$ is a correction factor which depends on the size and shape of the particle as well as the angle of observation, $\theta$, and $H$ is a constant given by the following equation for 546 mμ light:

$$H = 6.18 \times 10^{-5} n_o^2 (dn/dc)^2 \qquad (49)$$

where $n_o$ is the refractive index of the solvent and $dn/dc$ the refractive index gradient. The apparent turbidity of the solutions was calculated from:

$$\tau = 1.21 (n^2 Rw/Rc)\, a\, F \frac{G_{90}}{G_o} \frac{r}{r'} \qquad (50)$$

where $G_{90}/G_o$ is the ratio of galvanometer deflections for the light scattered at 90° and 0°; $F$ is the product of the transmittances of the neutral filters used in determining the scattering ratio; $a$ is a constant relating the working standard to the opal glass reference standard; $n$ is the refractive index of the solvent, $Rw/Rc$ is an experimentally determined correction for incomplete compensation of refraction effects, and $r/r'$ is a calibration factor relating the small light-scattering cell to the large cell. The excess turbidity, upon which the molecular weight depends, is the apparent turbidity of the solution minus that of the solvent.

To determine the molecular weight, $Hc/\tau$ is plotted against $c$ and the $y$ intercept equated to $1/MP_\theta$. For 90° scattering, then, the apparent molecular weight is calculated from:

$$M = \frac{1}{\text{intercept}} \times \frac{1}{P_{90}} \qquad (51)$$

A value for $1/P_{90}$ is determined from the dissymmetry of scattering, $Z$, which is the ratio of scattering intensities at 45 and 135°. Dissymmetry was calculated from the equation:

$$Z = \frac{\left(F \frac{G_{45}}{G_o}\right)_{\text{solution}} - \left(F \frac{G_{45}}{G_o}\right)_{\text{solvent}}}{\left(F \frac{G_{135}}{G_o}\right)_{\text{solution}} - \left(F \frac{G_{135}}{G_o}\right)_{\text{solvent}}} \qquad (52)$$

Since $\underline{Z}$ is a function of concentration, it must be extrapolated to zero concentration to get the intrinsic dissymmetry $[\underline{Z}]$. Beattie and Booth (49) have tabulated values of $1/\underline{P}_{90}$ as a function of $[\underline{Z}]$ for different shaped particles. For values of $[\underline{Z}]$ less than 2.0, there is very little difference in $1/\underline{P}_{90}$ for coils, rods, spheres, or disks. The tables of Beattie and Booth (49) are for monomolecular solutions, but in another publication (50) they treat polymolecular systems of coils. For values of $[\underline{Z}]$ less than 2.0, the values of $1/\underline{P}_{90}$ for monomolecular and most polymolecular systems differ by less than 10%. Therefore, in this thesis, values of $1/\underline{P}_{90}$ were taken from Beattie and Booth's values for monomolecular spherical molecules. The reason for choosing a spherical shape will be apparent later.

If appreciable fluorescence is present, turbidities and molecular weights will be too high unless the scattering ratios are corrected for fluorescence. Brice, et al. (51) developed a method for correcting the scattering ratio for fluorescence. If the ratio of the horizontal component to the vertical component of the scattered light is approximately equal to the ratio for the fluorescent light, the corrected scattering ratio, $\underline{CSR}$, may be calculated from the equation:

$$CSR = 0.5\left[\left(F\frac{G_{90}^{V}}{G_{o}^{V}}\right)_{solution} - \left(F\frac{G_{90}^{V}}{G_{o}^{V}}\right)_{solvent} - \frac{\left(F\frac{G_{90}^{H}}{G_{o}^{H}}\right)_{solution} - \left(F\frac{G_{90}^{H}}{G_{o}^{H}}\right)_{solvent}}{\left[\left(F\frac{G_{90}^{H}}{G_{o}^{V}}\right)_{solution} - \left(F\frac{G_{90}^{H}}{G_{90}^{V}}\right)_{solvent}\right] AF}\right] \qquad (53)$$

where AF indicates measurements taken with an auxilary cut off filter and placed between the cell and the phototube, and H and V represent the horizontal and vertical components of the light. The horizontal and vertical components are measured by placing a Polaroid lens between the cell and the photometer tube. The corrected scattering ratio replaces $G_{90}/G_o$ in Equation (51).

In the absence of fluorescence, the light scattered at 90° will be completely polarized in the vertical plane if the particles are isotropic. For anisotropic particles, however, in which the polarizabilities along various directions in the particle are not equal, the scattered light will not be perfectly polarized in the vertical direction, but will exhibit a weak component in the horizontal direction. The depolarization factors were calculated by the equation:

$$\rho_u = \frac{\left(F\frac{G_{90}^H}{G_o^H}\right)_{solution} - \left(F\frac{G_{90}^H}{G_o^H}\right)_{solvent}}{\left(F\frac{G_{90}^V}{G_o^V}\right)_{solution} - \left(F\frac{G_{90}^V}{G_o^V}\right)_{solvent}} \qquad (54)$$

Values of $\rho_u$ were extrapolated to zero concentration, to give $(\rho_u)_o$, which enabled calculation of the Cabannes factor, $C_u$, by the following Equation (48):

$$C_u = \frac{6-7(\rho_u)_o}{6+7(\rho_u)_o} \qquad (55)$$

The apparent molecular weight is multiplied by the Cabannes factor to obtain the true molecular weight. The Cabannes factor generally has a value greater than 0.9, and thus imparts a correction of less than 10% to the molecular weight. Although the Cabannes factor was not intended for use with solutions that exhibit fluorescence, the correction was applied to the data on Polymer 11. Results were

obtained which were similar to those obtained on the same polymer by applying the fluorescence correction alone, thus supporting the accuracy of Brice's method.

All calculations were carried out with the aid of the I.B.M. 1620 computer.

Refractive Index Gradient

The refractive index gradient, $dn/dc$, was measured, in most cases, on a Rayleigh interferometer (Baird Associates, Cambridge, Mass.) at 546 mμ. Interference fringes were matched at several concentrations, and $dn/dc$ calculated from the relation (39):

$$dn/dc = \left[(D-D_o)/47\right] \lambda/c\ L \qquad (56)$$

where

$D$ = instrument drum reading for the solution

$D_o$ = instrument drum reading for the solvent

$\lambda$ = wavelength of light used; $5.46 \times 10^{-5}$ cm.

$c$ = solution concentration, g./ml.

$L$ = cell length; 1.00 cm.

Plots of $(D - D_o)$ versus $c$ were made and a straight line drawn through the points. In cases where the straight line did not pass through the origin, a parallel line was drawn through the origin and points taken from this line for use in the above equation. A sample calculation is given in Appendix IV.

The solutions of Polymer 9 in water and dimethyl sulfoxide possessed enough color so that it was difficult to match the fringes on the Rayleigh interferometer. In these cases, the refractive index of several solutions of different concentration was measured with a Bausch and Lomb dipping refractometer, and $dn/dc$ obtained from a plot of refractive index versus concentration. White light was used as a source, and the temperature was held at 25°C. by means of a circulating

water bath. The A prism was used with the water solution and the D prism with the 98% dimethyl sulfoxide solution. The data are given in Appendix IV.

## OSMOMETRY

### Osmometer

A Mechrolab Model 501 High Speed Membrane Osmometer was used for all osmotic pressure measurements. This is a dynamic method, and the principle of operation is shown in Fig. 9. Solvent flow through the membrane is detected by focusing an optical system on the section of capillary where a small bubble has been introduced. The light intensity changes sharply with movement of the air bubble. With aqueous solutions it is necessary to coat the capillary with a small amount of wetting agent to obtain smooth movement of the bubble (52). Pluronic L-62 (Wyandotte Chemical Company) was used in this work. The change of light intensity activates a servo motor which adjusts the pressure on the bottom of the membrane by adjusting the height of the elevator. A counter reads the position of the elevator, and the osmotic pressure is the difference between the reading for the solution and the pure solvent. A Sargent Recorder S-72150 was used to record the position of the elevator.

Dynamic measurement of osmotic pressure offers advantages over the static method. In addition to greatly increasing the speed of measurements, it increases the accuracy of measurement where molecules are present which can permeate the membrane (53). This is because measurement is made before the molecules have time to permeate the membrane. Staverman, et al. (54-57) have concluded that a measurement should be made as soon as possible after putting the solution into the osmometer. The pressure observed will be less than the theoretical osmotic pressure, because of the Staverman effect (53, 58, 59), but will be closer to the theoretical pressure than values obtained by the static method. The

Staverman effect is the observation that molecules capable of permeating the membrane do not contribute their full share to the osmotic pressure even if they have not permeated the membrane at the time of measurement.

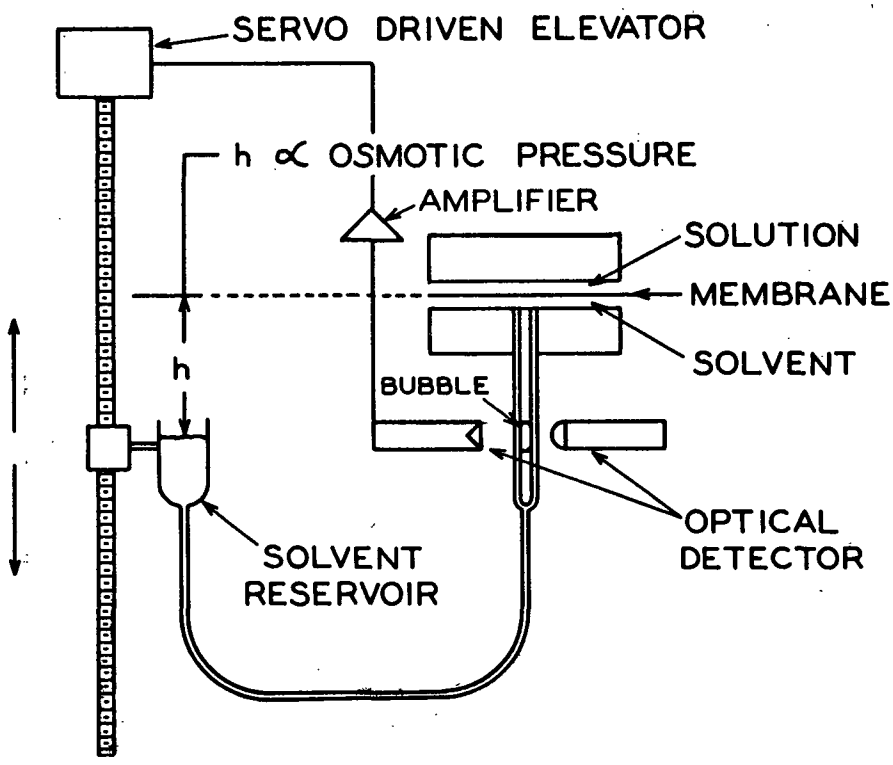


Figure 9. Mechrolab High Speed Membrane Osmometer. (Courtesy of Mechrolab, Inc., Mountain View, Cal.)

Solutions

In order to reduce the polyelectrolyte effect (60-62) the polymers were dissolved in 0.33N potassium chloride and neutralized to approximately pH 7 with a few drops of 0.1N potassium hydroxide. All solutions were made up by weight.

Membranes

After some exploratory work with S & S 0-7, 0-8, B-19, and B-20 membranes (Schleicher and Schuell Company, Keene, New Hampshire) the B-20 membrane was chosen. The B series membranes are recommended for aqueous solutions, and B-20 has an average pore size of 50 A.

Calculations

The concentration dependence of the osmotic pressure is represented by the series:

$$\frac{\pi}{c} = \frac{RT}{M}(1 + Ac + Bc^2 + \ldots.) \qquad (57)$$

where $\pi$ is the osmotic pressure in g./sq. cm., $c$ the concentration in g./cc., $R$ the gas constant, $T$ the absolute temperature, $M$ the molecular weight, and $A$ and $B$ the second and third virial coefficients. The molecular weight is calculated from the equation:

$$M = \frac{RT}{(\pi/c)_o d_1 g} = \frac{8.315 \times 10^7}{980.7} \times \frac{T}{(\pi/c)_o d_1} \qquad (58)$$

where $d_1$ is the density of the solvent and $g$ is the acceleration due to gravity. The subscript zero indicates that the value $\pi/c$ must be taken at zero concentration. The equation can be simplified by making up the solutions by weight (i.e., $c$ is in g./kg.). For a temperature of 37°C., the simplified equation becomes:

$$M = \frac{26,300}{(\pi/c)_o}$$

VISCOMETRY

Viscosities were measured at 30.000 ± 0.005°C. in a Ubbelohde viscometer, Cannon size 50, of the small volume type. The specific viscosity, $\eta_{sp}$, was calculated from the efflux times by the equation:

$$\eta_{sp} = \frac{t - t_o}{t_o} \tag{59}$$

where $t$ is the efflux time for the solution and $t_o$ that for the solvent. The intrinsic viscosity $[\eta]$, was obtained by extrapolation of a plot of $\eta_{sp}/c$ versus $c$ to zero concentration, according to the following definition of intrinsic viscosity:

$$[\eta] = \lim_{c \to 0} (\eta_{sp}/c) \tag{60}$$

where $c$ is the concentration in grams per deciliter.

Since the difference in efflux time between the solutions and solvent was a mere 2 to 3 seconds for most solutions, there was some scatter to the data. The scatter was minimized, though, by plotting $(\eta_{sp}/c)$ versus $c$ on semilogarithmic graph paper, as is often done. It was not felt that going to a size 25 viscometer would increase the difference in efflux times between the solvent and solution enough to justify the expected increase in difficulty in maintaining a clean viscometer. Reproducible data could be obtained with the size 50 viscometer only if it was cleaned scrupulously with alcoholic potassium hydroxide followed by hydrogen peroxide – hydrochloric acid cleaning solution before each measurement. Each concentration was made up separately by weight, and the measurement made in a clean viscometer.

The kinetic energy correction was calculated by the following equation from Timell (63) and Schulz (64):

$$\eta_{sp} = \eta^1_{sp} \left[ \frac{F_o}{1 - F_o} \cdot \frac{t + t_o}{t} + 1 \right] \tag{61}$$

where $\eta_{sp}$ is the apparent specific viscosity, $\eta^1_{sp}$ the corrected value, $t$ the efflux time of the solution in seconds, and $t_o$ the efflux time of the solvent. $F_o$ is calculated from the formula:

$$F_o = \frac{M \cdot d_o \cdot V}{8\pi \cdot \eta_o \cdot t_o \cdot L} \qquad (62)$$

where m, the kinetic energy coefficient, is given the value unity, $d_o$ is the density of the solvent, V the volume of the viscometer bulb in cc., $\eta_o$ the viscosity of the solvent in poises, $t_o$ the efflux time of the solvent in seconds, and L the length of the capillary in cm. Since the kinetic correction changed the value for the specific viscosity by less than 0.5%, it was neglected.

CHEMICAL MEASUREMENTS

Elemental analyses were performed in duplicate by the Geller Microanalytical Laboratories, Charleston, West Virginia. Carbon was measured as $CO_2$, hydrogen as $H_2O$, and oxygen by difference. The analyses were corrected for ash where applicable.

Carboxyl groups were measured by potentiometric titration with 0.01N sodium hydroxide. Nitrogen was passed over the solutions during titration to prevent any reaction with carbon dioxide in the air. The end point was taken as the position of maximum slope in the pH versus ml. of titrant curve. The pH at the end point varied from about 6.5 to 7.5, depending on the particular polymer titrated. Polymer 9 gave such a poor titration curve that the carboxyl content could not be determined.

Infrared absorption spectra were run on a Perkin-Elmer Model 21 recording spectrophotometer. Sodium chloride optics were used, and the samples were run in solid potassium bromide pellets.

Ultraviolet absorption spectra were measured in aqueous solution on a Beckman DK-2 recording spectrophotometer.

FRACTIONATION

Fractionation Procedure

Fractionation was performed on Sephadex, manufactured by AB Pharmacia, Uppsala, Sweden. Sephadex is a cross-linked dextran gel which has been used to successfully fractionate proteins (65-67), oligosaccharides (68), and polysaccharides (69). It comes in several pore sizes, and the proper pore size is selected according to the molecular weight range of the material to be fractionated. A column chromatographic procedure is generally employed in which the lower molecular weight molecules diffuse selectively into the smaller pores of the Sephadex, and hence take a longer time to reach the bottom of the column. The larger molecules are excluded from the small pores and come out in the early fractions. Molecules which are excluded from all the pores come out in the void volume of the column. The void volume is usually determined by measuring the elution volume for a high molecular weight solute which is known to be completely excluded from the gel.

Sephadex was chosen over precipitation for fractionation because exploratory work with precipitation indicated that difficulty would be encountered in obtaining an even weight distribution among the fractions. Sephadex also has the advantage that, if free of adsorption effects, it comes close to separating molecules on the basis of size alone. Precipitation depends on solubility which is also affected by the chemical composition and physical form of the material. The use of eluents containing salts has been found to improve the separation of acidic oligosaccharides (66). Exploratory work with Polymer 11, though, indicated that similar results were obtained in the presence and absence of salt.

About 2 g. of Polymer 11 were dissolved in 100 ml. of water and subjected to the clarification procedure described in the light-scattering section. Some

dilution of the sample was necessary to avoid sample loss during clarification. A 100-ml. aliquot of the solution containing 1.5550 g. of polymer was placed on a 4-1/2 by 15 in. column of Sephadex G-25, and elution started with distilled water. Since the solute was colored, it was easy to follow its progress as it passed down the column. Solute started to appear in the effluent after 1260 ml. had been collected. This is close to the void volume figure of 1300 ml. which was quoted for this particular column (70). Two hundred milliliter fractions were collected until a total of 10 fractions had been collected. This accounted for 95.4% of the solids placed on the column.

The supernatant liquid left from the ethanol precipitation of Polymer 11 was also fractionated on the column of Sephadex G-25. A similar procedure was used.

Analysis of the Fractions

The pH of each fraction was measured, and the solids content determined by evaporation of an aliquot to dryness. The polymers in each fraction were isolated by freeze-drying and the molecular weights measured by light scattering and osmometry. Elemental analyses, infrared and ultraviolet absorption spectra, and carboxyl content were also determined on each fraction.

# RESULTS AND DISCUSSION

## THE EFFECT OF DIFFERENT CONDITIONS OF IRRADIATION

### DOSE

The yield of polymer, measured as either the amount of nondialyzable material, the amount of ethanol precipitate, or the amount of immobile material on a paper chromatogram, increased with dose. The effect of dose on the amount of nondialyzable material and ethanol precipitate is shown in Fig. 10.

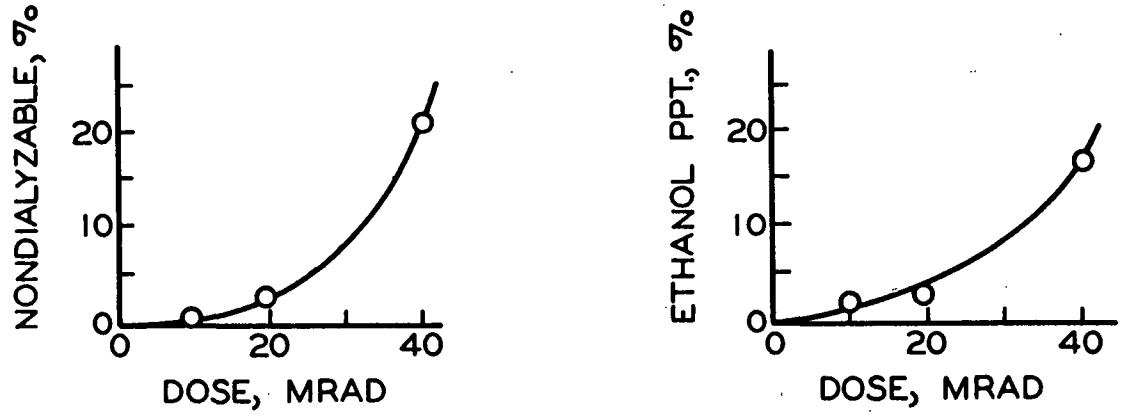


Figure 10. The Effect of Dose on Yield of Polymer. Data are on Samples 5, 6, and 7

It also appears that the average molecular weight of the polymer increases with dose. The above data on the yield of nondialyzable material suggests that the molecules grow in size as they receive a higher dosage. A large increase in nondialyzable material is obtained in going from 20 to 40 Mrads, as if this represents a threshold at which many more molecules become large enough to be stopped by the dialysis membrane. Work on some of the other polymers isolated by ethanol precipitation indicated that, as a general rule, the average molecular weight increased as the yield of ethanol precipitate increased. This is shown in Table III.

Infrared absorption spectra, given in Fig. 11, show the total carbonyl absorption in the region 1760 - 1720 cm.$^{-1}$ to increase with dose. The two polymers were formed under identical conditions except that one received a dose of 20 Mrads and the other 40 Mrads. In a later section the absorption in this region will be shown to be due to at least two types of carbonyl, the absorption of which both increase as the polymer grows in size.

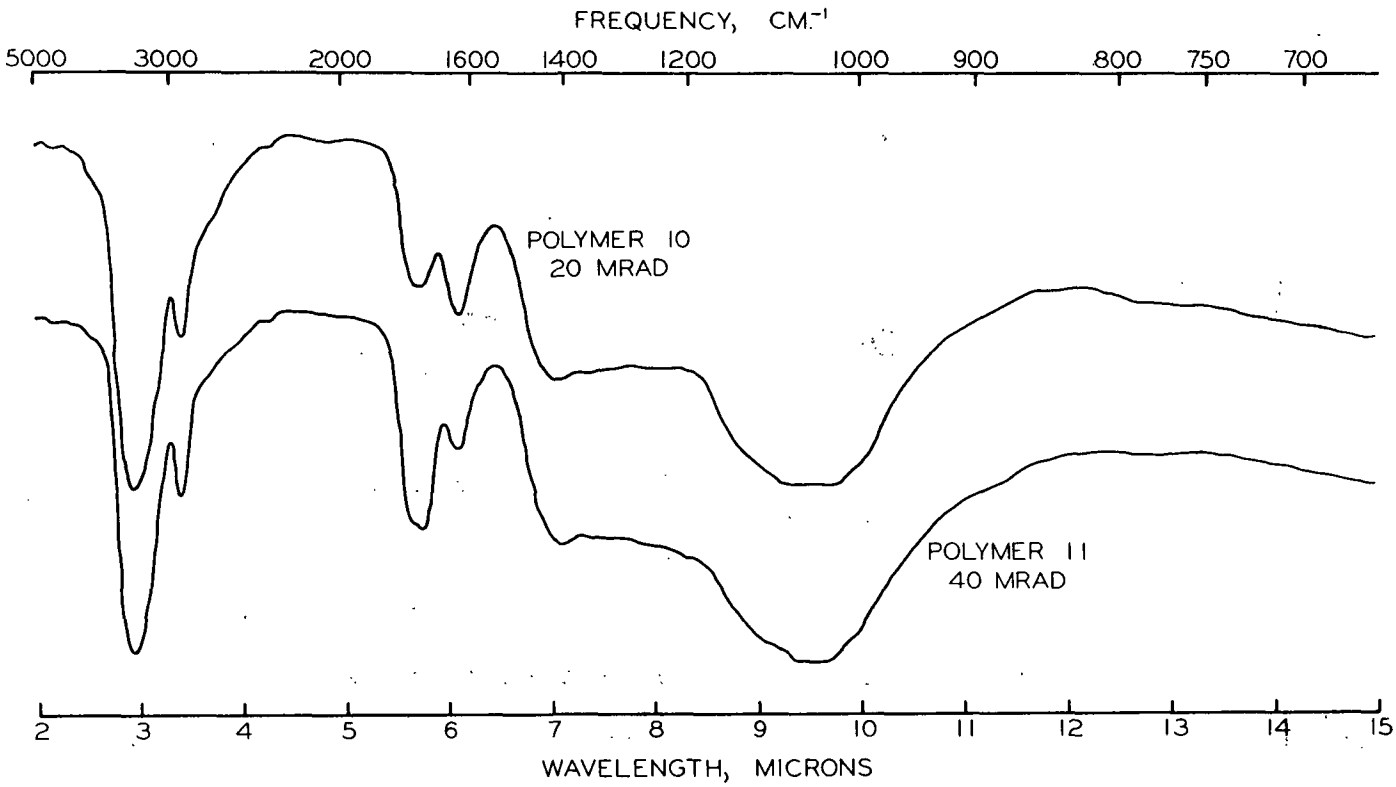


Figure 11. Infrared Absorption Spectra of Polymers 10 and 11

DOSE RATE

The effect of different dose rates on the yield of polymer is shown in Table II.

TABLE II

THE EFFECT OF DOSE RATE ON YIELD

| Sample No. | Dose Rate | Nondialyzable Material, % |
|---|---|---|
| | Total Dose: 20 Mrad | |
| 10 | 1 Mrad/pass; 1 pass/5.5 min. | 0.8 |
| 6 | 1 Mrad/pass; 1 pass/0.78 min. | 2.7 |
| 8 | 4 Mrad/pass; 1 pass/3.12 min. | 2.8 |
| | Total Dose: 40 Mrad | |
| | Dose Rate | |
| 11 | 1 Mrad/pass; 1 pass/5.5 min. | 3.8 |
| 12 | 2 Mrad/pass; 1 pass/5.5 min. | 3.2 |
| 7 | 1 Mrad/pass; 1 pass/0.77 min. | 21.3 |
| 13 | 2 Mrad/pass; 1 pass/0.6 min. | 28.7 |
| 9[a] | 1 Mrad/pass; 1 pass/0.64 min. | 60.0 |

[a]Irradiation conducted at Burlington on the Van de Graaff accelerator; all others at Rockford on the linear accelerator.

It can be seen that, in general, increasing the dose rate increased the yield of polymer. When the frequency of the passes under the beam was increased (compare Samples 10 and 6 or 11 and 7), a larger yield was obtained. The apparent inconsistencies between Samples 6 and 8 and between 11 and 12 are thought to be due to the shortcomings of dialysis as a measure of polymer yield. Increasing the dose rate would tend to increase the concentration of hydrogen and hydroxyl free radicals in solution, which in turn would tend to increase the concentration of sugar free radicals. This would make coupling of the free radicals more likely, and hence increase the yield of polymer. The high yield of polymer from the Burlington treatment can be accounted for by a similar explanation. The

steady beam at Burlington would tend to give a higher concentration of free radicals than a pulsed beam, and also the rate of energy loss per unit path length is greater for the 1.5 Mev. electrons used at Burlington than for the 8.5 Mev. electrons used at Rockford [see Equation (1)].

The other factor that must be considered in analyzing the effect of dose rate is that the heat built up in the samples was greater at the higher dose rates. All irradiations were conducted at ambient temperature, with no temperature control. Higher temperatures would be expected to increase the mobility of the sugar radicals, and thus make coupling more likely.

The molecular weights of three polymers each made at 40 Mrad but different dose rates are given in Table III. The same explanation used for the effect on yield can be used to explain the effect of dose rate on molecular weight.

TABLE III

THE EFFECT OF DOSE RATE ON YIELD AND MOLECULAR WEIGHT

Total Dose: 40 Mrad

| Polymer | Dose Rate | Yield, % ethanol ppt. | Light-Scattering Molecular Weight |
|---|---|---|---|
| 11 | 1 Mrad/pass; 1 pass/5.5 min. | 10.2 | 9,800 |
| 7 | 1 Mrad/pass; 1 pass/0.77 min. | 16.6 | 140,000 |
| 9 | 1 Mrad/pass; 1 pass/0.64 min. | 41.8 | 5,000,000 |

The effect of dose rate found in this work is exactly opposite to the effect reported for more conventional free radical polymerizations. For example, Collinson and Swallow (21), report that increasing the dose rate lowers the rate of polymerization of styrene because it increases the rate of chain termination by initiating radicals. Increasing the temperature of a conventional free radical polymerization also usually lowers the molecular weight due to an increase in the rate of chain termination (60). However, the proposed mechanism for radiation-induced

polymerization of glucose is the very mechanism by which the more conventional free radical polymerizations are terminated – i.e., by free radical coupling. The data on the effect of dose rate, therefore, support the proposed mechanism of hydrogen abstraction from the carbohydrate followed by coupling of free radicals.

OXYGEN CONTENT OF THE SOLUTIONS

The effect of small amounts of dissolved oxygen on the yield of polymer is given in Table IV.

TABLE IV

THE EFFECT OF OXYGEN

| Sample No. | Oxygen Content, p.p.m. | Nondialyzable Material, % |
|---|---|---|
| 1 | 0.6 | 1.2 |
| 4 | 7.8 | 2.9 |

Both samples were irradiated to 20 Mrads in glass tubes. The low yields of Table IV are typical of the 20-Mrad treatment. The difference in yield between the two samples is thought to be due to variation in pore size between pieces of dialyzer tubing rather than to the effect of oxygen. The fact that polymer was obtained in the presence of oxygen is surprising since other workers (1-10) using gamma-rays have found the presence of oxygen to inhibit polymerization. Apparently, at the high doses and dose rates employed in this work, the small amounts of dissolved oxygen are used up early in the process, and subsequent reactions occur as if oxygen were absent.

GLUCOSE CONCENTRATION

From Table V it can be seen that the per cent yield of polymer dropped by a factor of roughly 10 when going from a 1.0% to a 10.0% glucose solution.

TABLE V

THE EFFECT OF GLUCOSE CONCENTRATION

| Sample No. | Concentration, % | Nondialyzable Material, % |
|---|---|---|
| 1 | 1.0 | 1.2 |
| 3 | 10.0 | 0.09 |

Both irradiations were to 20 Mrad at 1 Mrad/pass and 1 pass/.782 min.

This is the result predicted for an indirect mechanism where the radiation decomposes the solvent molecules, and the resulting products attack the solute molecules (16).

## THE PHYSICAL NATURE OF THE MOLECULES

The molecular weights and intrinsic viscosities for three of the polymers formed at 40 Mrads are summarized in Table VI.

TABLE VI

MOLECULAR WEIGHT AND VISCOSITY DATA ON WHOLE POLYMERS

| Polymer | dn/dc | Z | Molecular Weight, light scattering | [η], dl./g. |
|---|---|---|---|---|
| 11 | 0.166 | 1.1 | 9,800 | 0.024 |
| 7 | 0.200 | 1.6 | 140,000 | 0.026 |
| 9 | 0.215 | 2.35 | 5,000,000 | 0.205 |
| 9[a] | -0.135 | 1.7 | 2,500,000 | |

[a]Measured in 98% dimethyl sulfoxide; all others in water.

### MOLECULAR WEIGHT

Light-scattering measurements on the polymers indicated that they were of much higher molecular weight than previously imagined. Barker, Lloyd, and Stacey (71) suggested that, on the basis of viscosity measurements, their polymer had a molecular weight in the range 1200 to 4000. This was a very rough approximation,

for, as they pointed out, no reliable constants were available for estimation of molecular weight from viscosity data. The molecular weights given by Barker, et al. would correspond to a degree of polymerization of 6 to 22, and would hence border on the range of an oligosaccharide rather than a true high polymer. Light-scattering measurements on Polymers 11, 7, and 9 in water and 9 in 98% dimethyl sulfoxide indicate that the materials are truly high polymers. The light-scattering data are presented in Fig. 12 through 16.

Very low second virial coefficients were obtained for the polymers in water, thus indicating very little polymer – solvent interaction (40). The polymer is apparently on the threshold of precipitation as evidenced by the negative second virial coefficients noticed for Polymers 11 and 9. Other authors (43, 72) have attributed negative second virial coefficients to aggregation effects, and Tanford (73) presents a theoretical discussion which predicts negative coefficients where aggregation takes place. The fact that a molecular weight of 2,500,000 was obtained in 98% dimethyl sulfoxide in comparison to 5,000,000 in water indicates that although some aggregation did occur in water, the polymer is indeed of very high molecular weight. The higher second virial coefficient obtained in 98% dimethyl sulfoxide indicates a more highly solvent-swollen molecule in this solvent.

The values for $dn/dc$ in Table VI increase with molecular weight, reflecting a change in the chemical composition of the molecules with molecular weight. The same result was found with the fractions of Polymer 11, which will be discussed in a later section.

A test for fluorescence on Polymers 7 and 9 indicated a negligible amount of fluorescence. However, Polymer 11, the lowest molecular weight polymer, exhibited a great deal of fluorescence. Therefore, for Polymer 11 the 90° scattering ratios were corrected for fluorescence by the method of Brice, et al. (51). For comparison purposes, plots of $Hc/\tau$ versus $c$ are given using

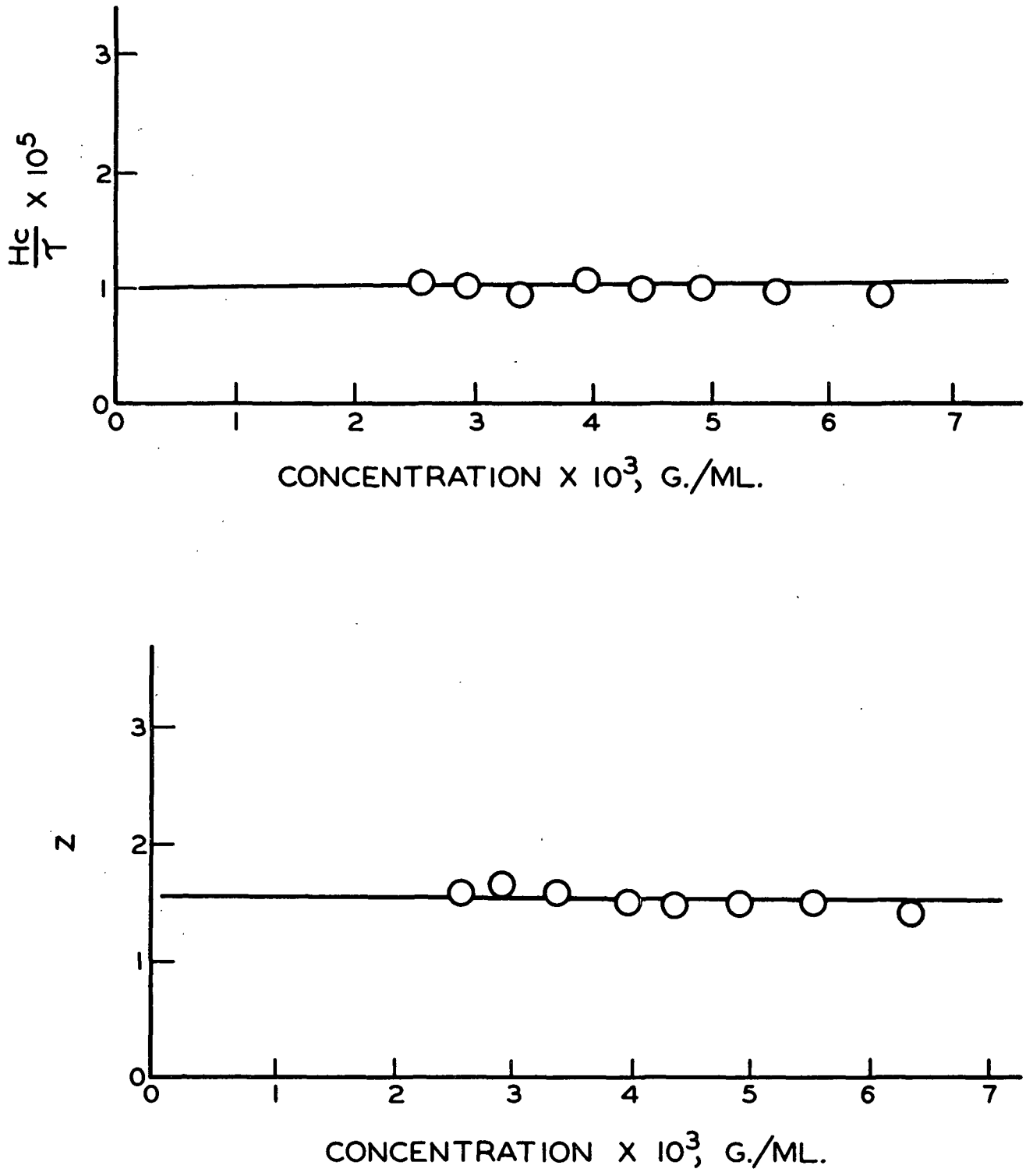


Figure 12. Light-Scattering Data on Polymer 7 in Water

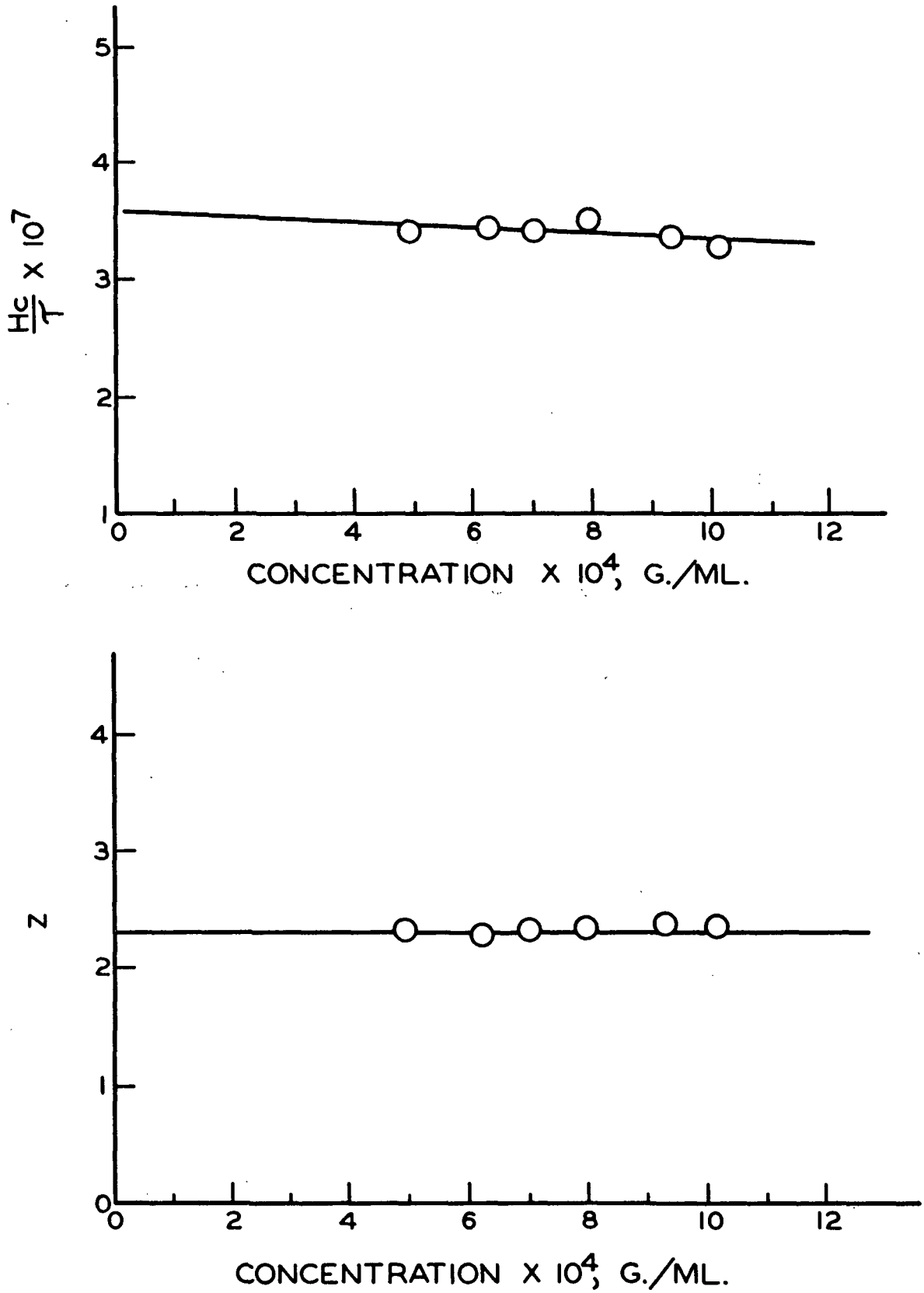


Figure 13. Light-Scattering Data on Polymer 9 in Water

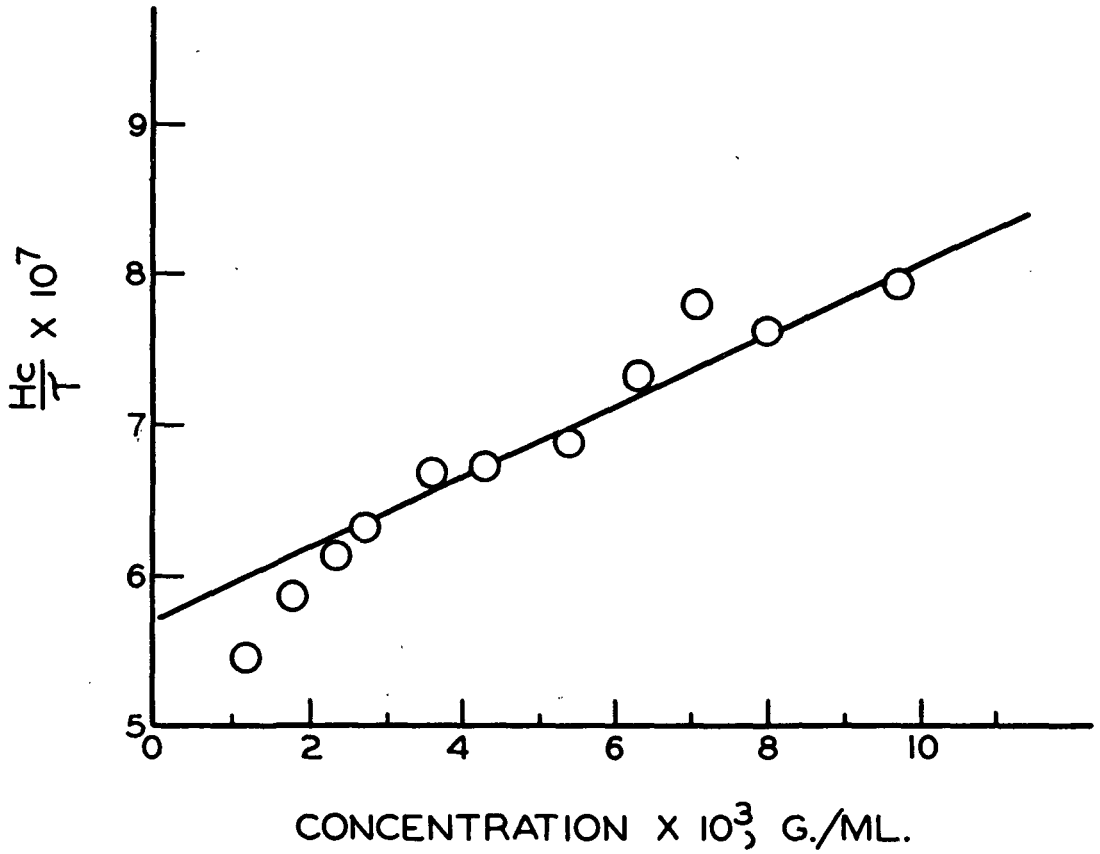


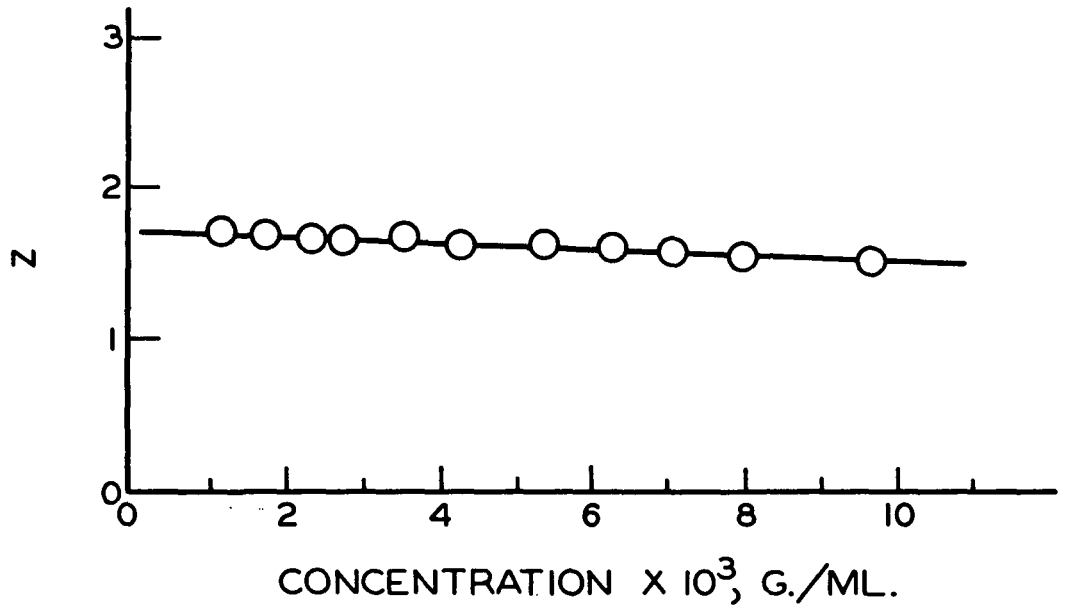


Figure 14. Light-Scattering Data on Polymer 9 in 98% Dimethyl Sulfoxide

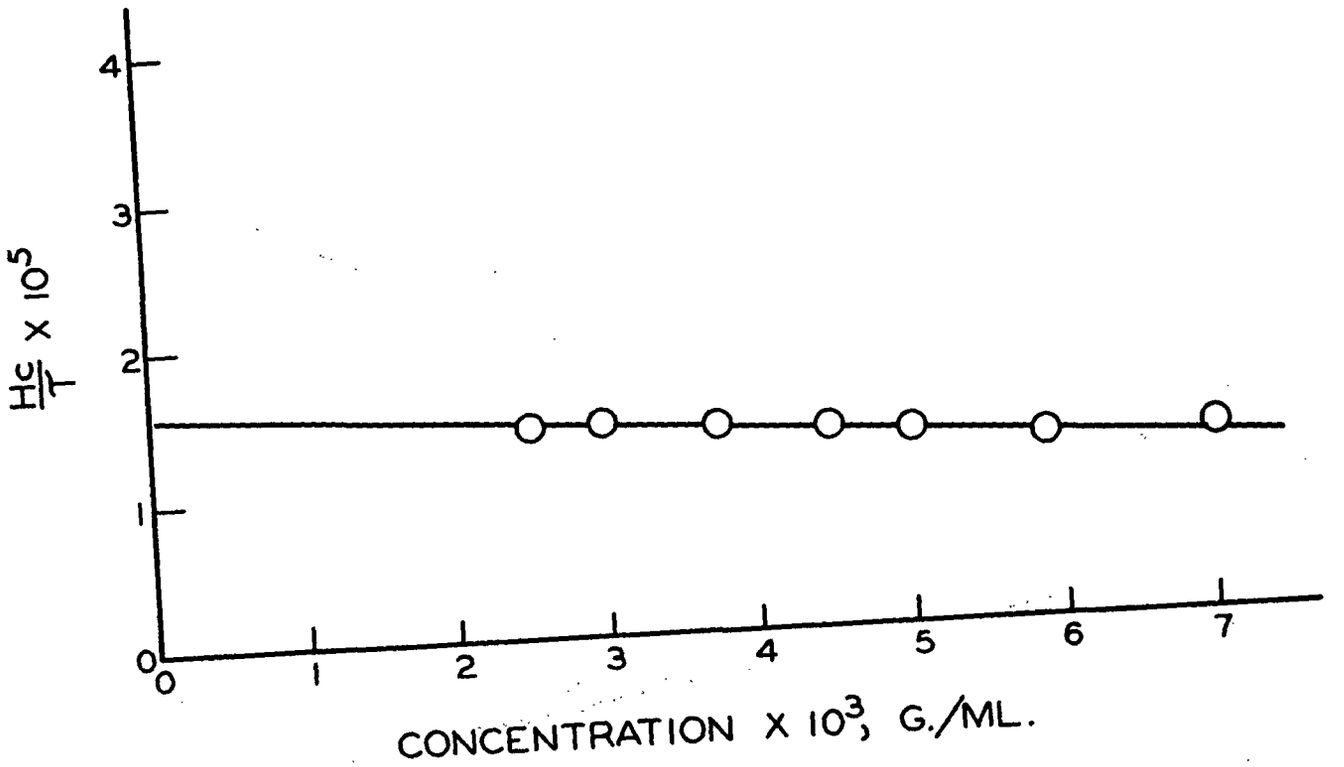


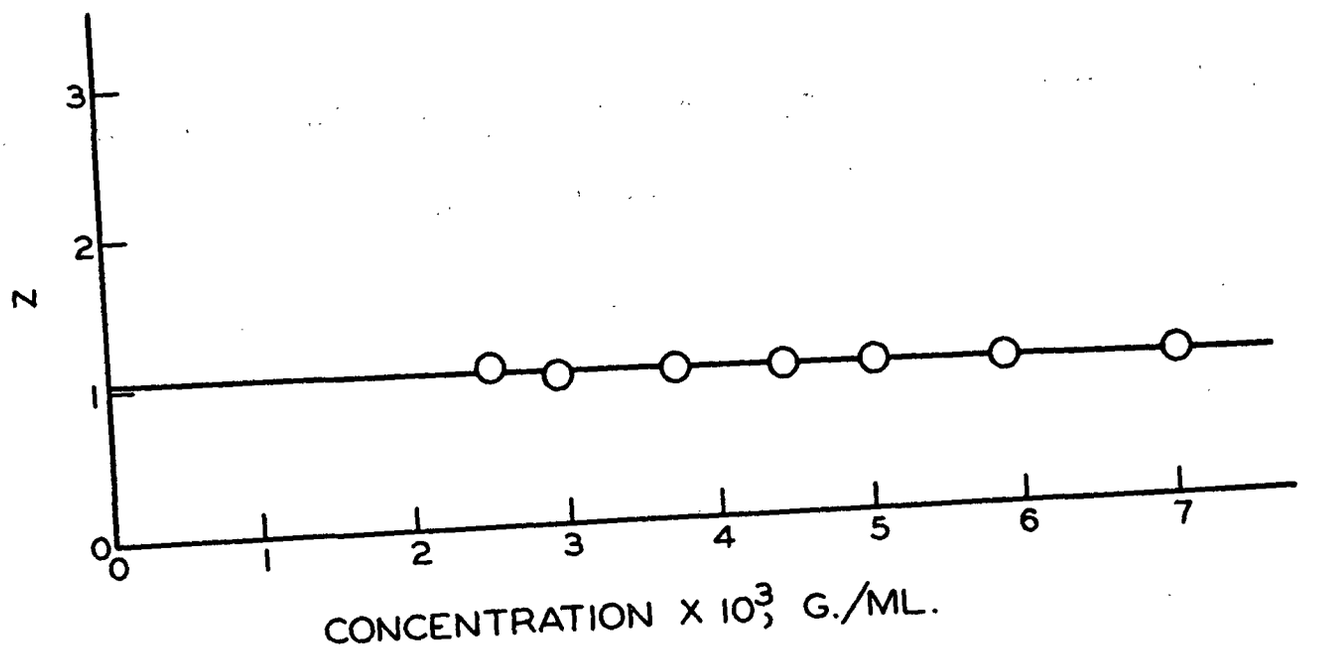


Figure 15. Light-Scattering Data on Polymer 11 in Water

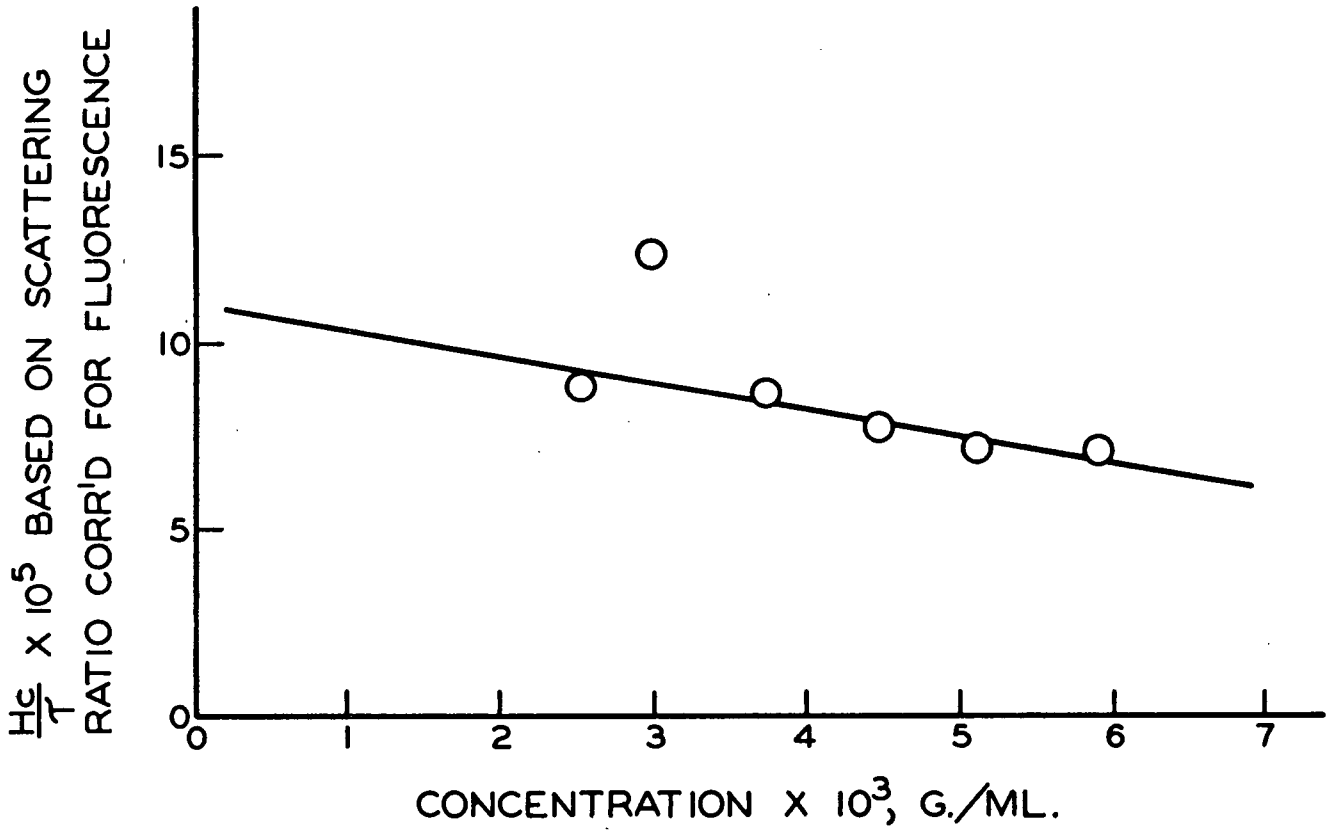


Figure 16. Light-Scattering Data on Polymer 11 in Water

both the corrected and uncorrected scattering ratios. The fact that Polymer 11 exhibited fluorescence and Polymers 7 and 9 did not is puzzling. The only major difference between the three appears to be molecular weight. However, Moacanin, et al. (74) noticed that fluorescence was greater for low molecular weight lignosulfonate molecules than for higher molecular weight ones. The same thing appears to be true for the system studied in this thesis.

The number average molecular weight of Polymer 11, measured on the membrane osmometer, was 2000. The accuracy of this value was confirmed by measurements on a vapor-pressure osmometer, as described in Appendix VI. Since the weight average molecular weight was 9800, this gives an $\overline{M}_w/\overline{M}_n$ ratio of 4.9, which is quite reasonable for branched molecules. For a normal distribution of linear polymers, a ratio of 2.0 would be expected, but as the distribution gets broader, a larger ratio is expected (73). In fact, Flory (60) and Erlander and French (75) have applied a statistical analysis to the molecular weight distribution of branched molecules and concluded that the ratio $\overline{M}_w/\overline{M}_n$ becomes very large for broad distribution of highly branched molecules such as amylopectin and glycogen. Data on the weight average and number average molecular weights on polymers in the literature is presented in Table VII, along with that for Polymer 11.

TABLE VII

COMPARISON OF WEIGHT AND NUMBER AVERAGE MOLECULAR WEIGHTS

| Polymer | $\overline{M}_w$ Light Scattering | $\overline{M}_n$ Osmometry | $\overline{M}_w/\overline{M}_n$ |
|---|---|---|---|
| Polymer 11 | 9,800 | 2,000 | 4.9 |
| Polyacrylonitrile-polyvinyl acetate copolymer (76) | 435,000 | 40,800 | 10.6 |
| Branched polyethylene (77) | 350,000 | 32,000 | 10.9 |
| Starch amylopectin (78) | 80,000,000 | 300,000 | 267 |

It appears then, that the molecular weight distribution of Polymer 11 is broader than a normal distribution, but is sharper than many branched polymers reported in the literature.

EVIDENCE FOR BRANCHING

Although the polymers had high light-scattering molecular weights, they had very low intrinsic viscosities. This is shown in Fig. 17. The possibility of a high molecular weight compound with a low intrinsic viscosity is quite reasonable when the properties of highly branched molecules are considered. Highly branched molecules retain low intrinsic viscosities even at high molecular weights. For example, Goring (79) obtained an intrinsic viscosity of 0.08 dl./g. for a dioxane-hydrochloric acid lignin molecule of 50,000 molecular weight in pyridine. Similarly, Greenwood and Robertson (80) report an intrinsic viscosity of 0.10 dl./g. for glycogen of 4,800,000 molecular weight in 1.0N potassium hydroxide. Methylation studies on this material indicated that there were approximately 2500 branches per molecule (i.e., a branch every 10 anhydroglucose units).

Goring's (79, 81) conception of the lignin molecule is that of a molecule so highly branched that it assumes a spherical shape in solution. For hard, nonswelling spheres, the intrinsic viscosity is given by

$$[\eta] = 0.025\ \bar{V}$$

where $\bar{V}$ is the specific volume of the material. The intrinsic viscosity is seen to depend only on the specific volume and not the size of the spheres. When the sphere is a macromolecule comprised of a porous, solvent-swollen network, $\bar{V}$ becomes the volume of the swollen macromolecule per unit weight of solute. Thus, $\bar{V}$, and hence $[\eta]$, increases with the swelling of the molecule in the solvent.

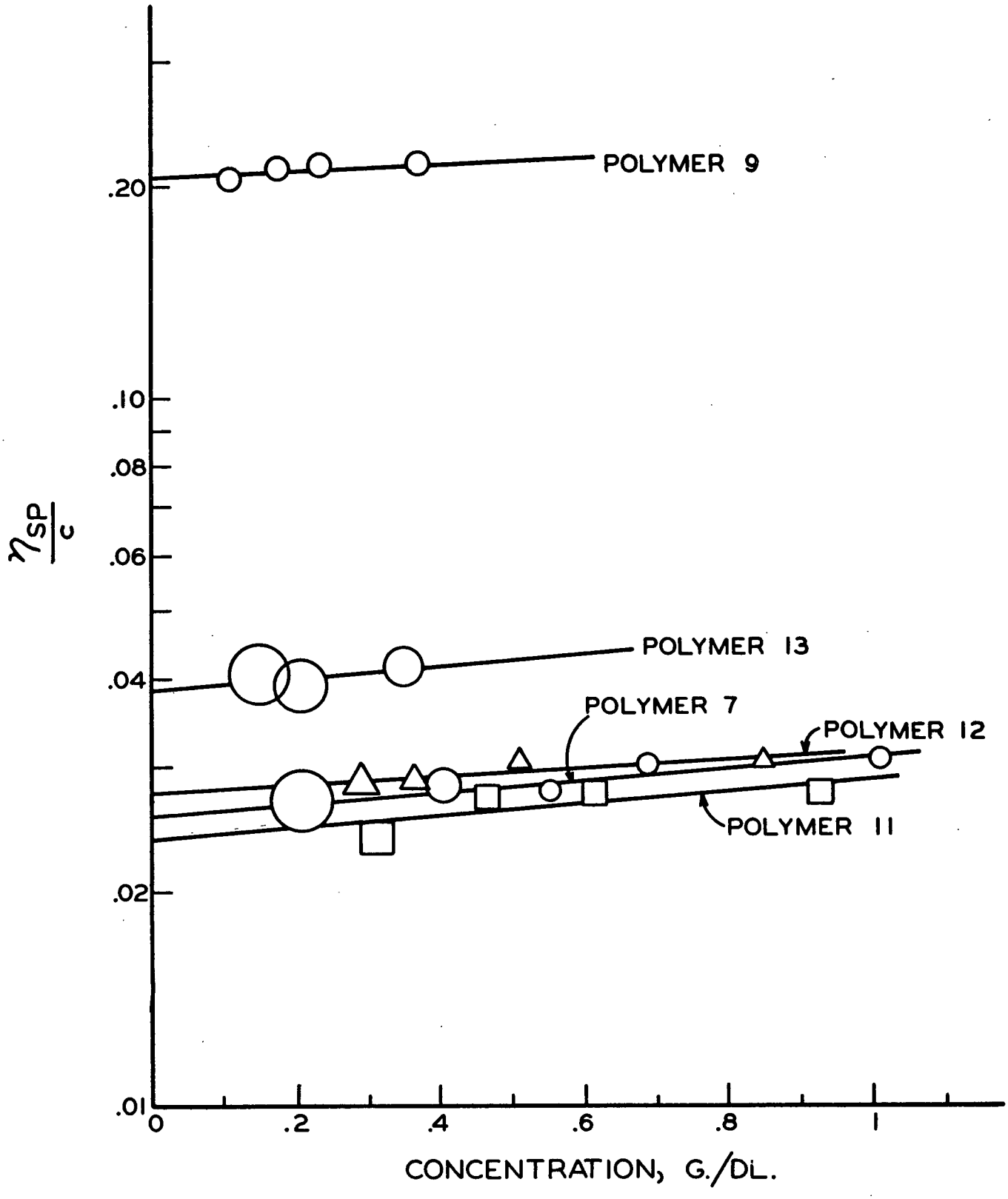


Figure 17. Viscosity Data on Polymers in Water at 30°C. The Size of the Data Points Represents the Error in $\eta_{sp}/c$ Introduced by an Error of 0.1 Sec. in the Measured Efflux Time

The results on polymers formed by irradiation of glucose solutions suggest that the configuration of the molecule lies somewhere between that of a hard sphere and a random coil. The low second virial coefficients obtained in the light-scattering work are consistent with this hypothesis.

## THE POLYELECTROLYTE EFFECT

### Osmometry

A marked polyelectrolyte effect was encountered in the osmotic pressure measurements, as shown in Fig. 18. In one case the polymer was dissolved in water to give a solution of pH 2.5; in another case it was dissolved in 0.33N potassium chloride and partially neutralized; and in the third case it was dissolved in 0.33N potassium chloride and neutralized to pH 7.3. It can be seen from the figure that negative slopes were obtained unless the polymer was run in the presence of salt and also neutralized. The curve for the water solution is below the others because a more porous membrane was used which apparently led to diffusion and a large Staverman effect. In water, apparently hydrogen ions dissociate from the carboxyl groups as dilution proceeds and thus act as separate osmotic species to cause spurious results. If the polymer is neutralized and run in the presence of salt, normal results are obtained.

Other authors (60, 61, 62) have also found it necessary to run polyelectrolytes in the presence of salt. For example, Strauss and Foss (61) found the ratio of $\pi/c$ to increase with dilution when poly-4-vinyl-N-n-butylpyridinium bromide was run in 93% ethanol solution. The explanation given was that at the more dilute concentrations the bromide ions diffused away from the polymer and acted as a separate osmotic species. The addition of lithium bromide suppressed the dissociation, and gave results similar to those for a neutral polymer. In addition to producing a slightly positive slope, the addition of the salt shifted the curve to slightly lower osmotic pressure values.

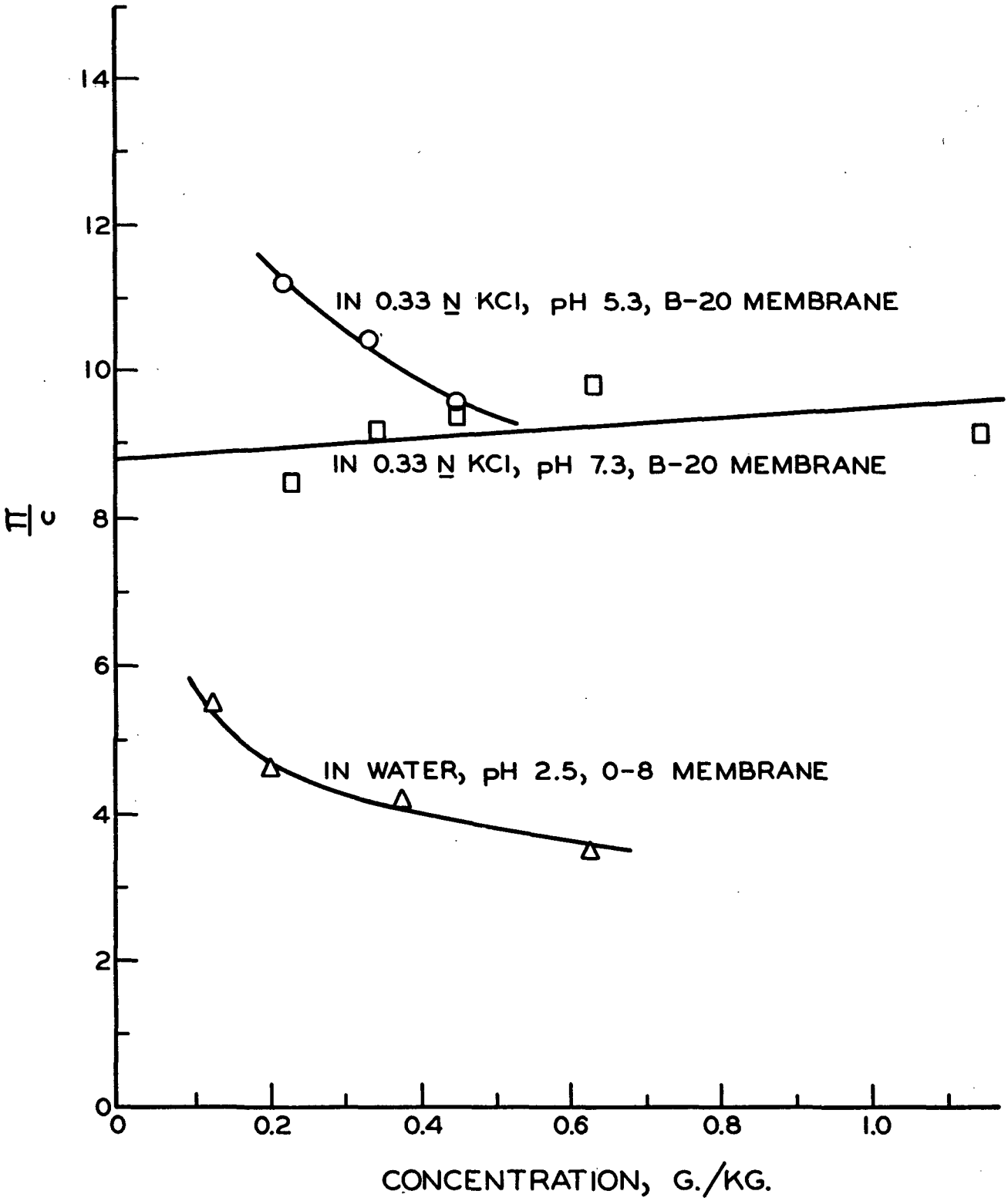


Figure 18. Osmotic Pressure Data on Polymer 11, Fraction 3

Light Scattering

It is customary to dissolve polyelectrolytes in salt solution for light-scattering measurements (40) to reduce the interaction between solute molecules. Because of the electrostatic repulsion of like charges, the distance of closest approach of two ionized molecules in solution is greater than that of two molecules in the nonpolar systems. This restriction places some degree of order on the system, and there is a decrease in the extent of concentration fluctuations. Since the theory of light scattering is based on refractive index fluctuations, and hence concentration fluctuations, the scattering of interacting molecules is less than the theoretical value. For example, Guinand, et al. (82) found the intensity of the 90° scattering of polyacrylic acid to be 1/50th the value for the unionized acid. Doty and Steiner (83, 84) developed a theory for charged macromolecules, and found it to fit qualitatively the light-scattering measurements taken on bovine serum albumin. The latter is a protein which carries a charge of about 50 protons per molecule. The authors found the $Hc/\tau$ versus $c$ plot for bovine serum albumin to rise steeply from the intercept at zero concentration, then bend over and gradually become horizontal at higher concentrations. In addition, the dissymmetry fell sharply from unity at zero concentration, passed through a minimum, and then rose slowly at higher concentrations. When the material was dissolved in salt, interaction between the solute molecules was reduced and normal light-scattering results were obtained.

Light-scattering measurements were taken on Polymer 11, Fraction 2 under three conditions: (1) dissolved in water, (2) dissolved in 0.33N potassium chloride, and (3) dissolved in 0.33N potassium chloride and neutralized to pH 7.8. The results are given in Fig. 19 through 21. The data points based on

the scattering ratio corrected for fluorescence were rather erratic, as seen in Fig. 19. The maximum deviation in $Hc/\tau$ in Fig. 19 is such that the molecular weights differed by about 25%. Plots of $Hc/\tau$ versus $c$ using the uncorrected scattering ratio typically gave plots with little deviation. It can be seen from Fig. 19-21 that the peculiar results obtained by Doty and Steiner were not obtained for the polymer in water. Greater negative slopes were obtained in the $Hc/\tau$ versus $c$ curves in the presence of salt, suggesting that more aggregation occurred under these conditions. Anacker, et al. (85) found the degree of aggregation of dodecyltrimethylammonium bromide to increase in the presence of salt. The molecular weights calculated from the corrected scattering ratios are given for Polymer 11, Fraction 2 in Table VIII.

TABLE VIII

THE EFFECT OF SALT ON LIGHT SCATTERING

| Conditions of Measurement | Molecular Weight |
|---|---|
| Dissolved in water; pH 2.5 | 12,000 |
| Dissolved in 0.33N KCl; pH 2.7 | 22,000 |
| Dissolved in 0.33N KCl; pH 7.8 | 19,000 |

Since the peculiar results noted by Doty and Steiner were not obtained, and since the degree of aggregation appeared to be greater in the presence of salt, no more light-scattering work was done in the presence of salt. It is believed the salt had little effect on the light-scattering results because the charge per molecule was much less than that for the bovine serum albumin. Titration data indicated the maximum number of carboxyl groups expected per molecule was about 19 for Polymer 11.

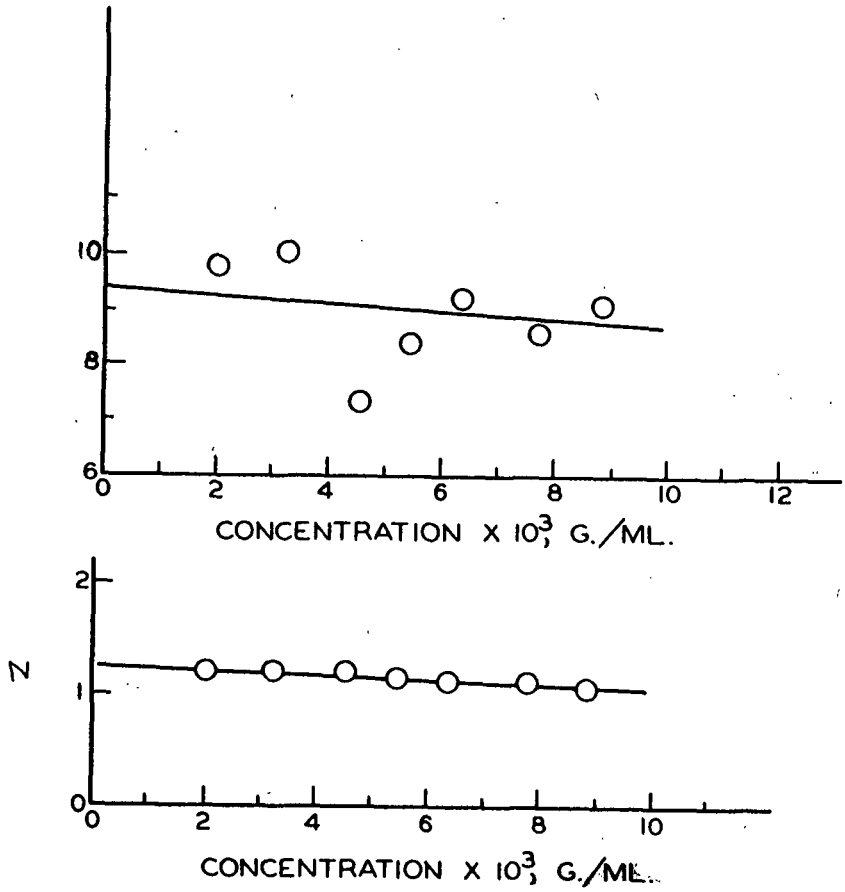


Figure 19. Light-Scattering Data on Polymer 11, Fraction 2 in Water pH = 2.5

Viscometry

Usually, with polyelectrolytes, the charges on the molecules cause them to expand in dilute solution, thus giving a viscosity larger than would be expected for the molecule in the absence of charge (60). The ratio $\eta_{sp}/c$ often increases with dilution in such a manner that the curve appears asymptotic to the ordinate axis. The addition of salt to the system usually suppresses the effect, and normal curves are obtained.

As seen from Fig. 17, although no attempt was made to suppress the polyelectrolyte effect with salt, the linear plots suggest that polyelectrolyte effects upon viscosity were negligible. Apparently, the molecules are too highly branched and compact to expand significantly during dilution.

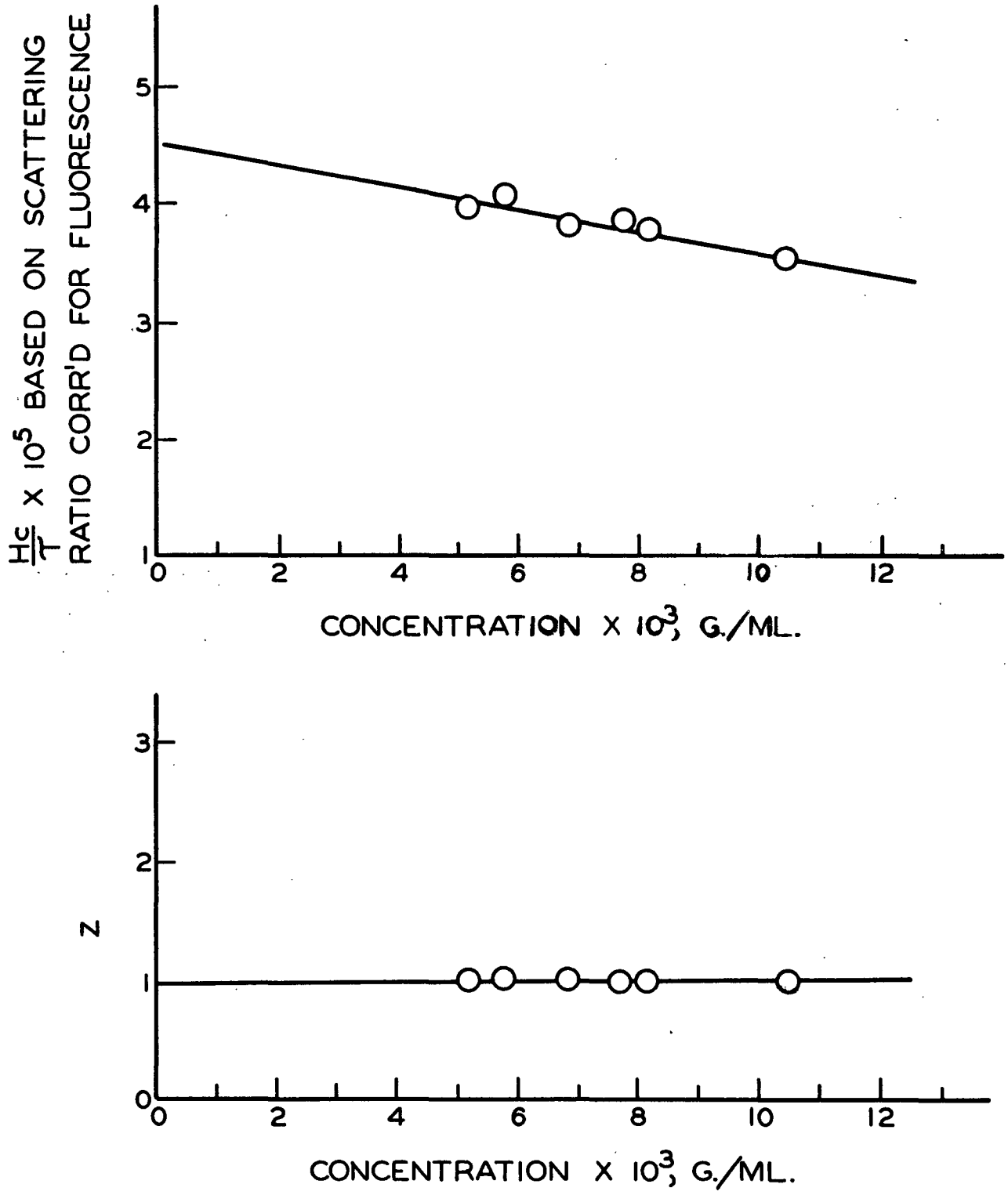


Figure 20. Light-Scattering Data on Polymer 11, Fraction 2 in 0.33N KCl, pH = 2.7

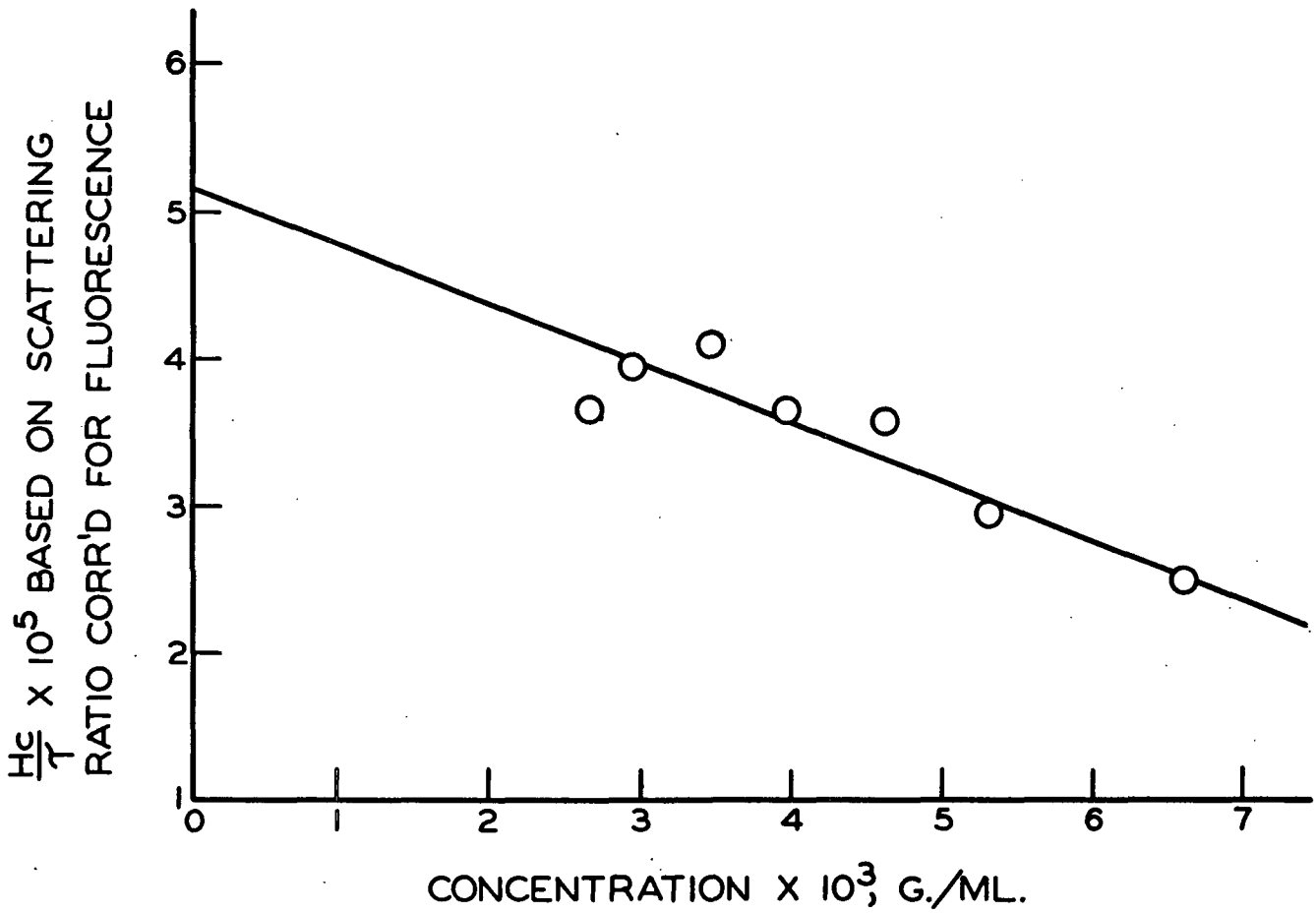


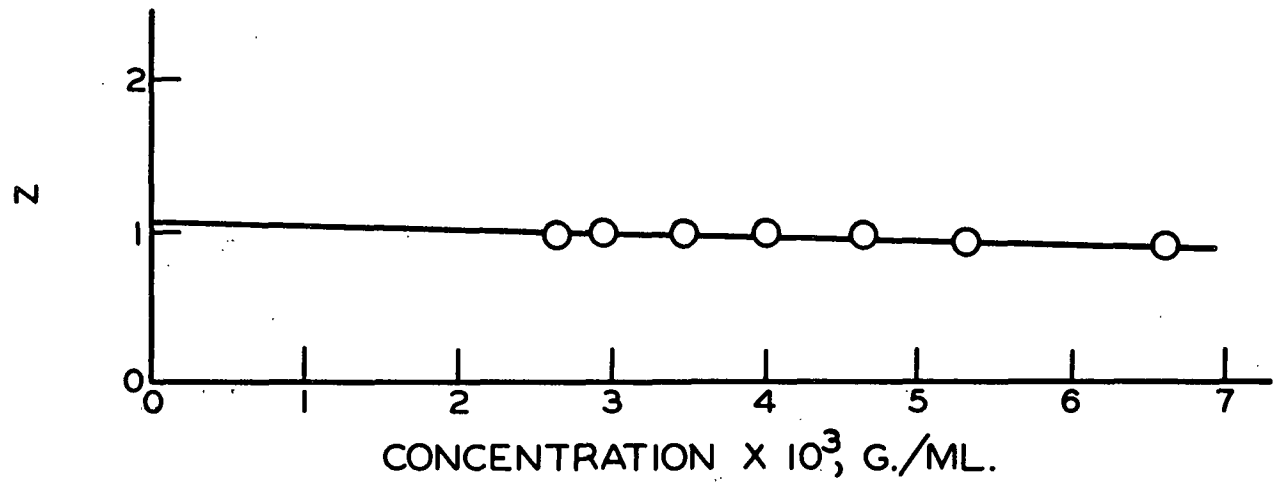


Figure 21. Light-Scattering Data on Polymer 11, Fraction 2 in 0.33N KCl and Neutralized to pH 7.8

FRACTIONATION

The solids distribution obtained upon fractionation of Polymer 11 is shown in Fig. 22. The manufacturers of Sephadex claim that, as a general rule, molecules larger than 5,000 in molecular weight should be excluded from G-25 gel and hence come out in the void volume of the column, which in this case was 1300 ml. If a dilution factor of 2/1 is assumed, Fraction 1 would be expected to be of molecular weight greater than 5,000, Fraction 2 about 5,000, and Fraction 3 slightly less than 5,000, etc. Too many other factors are involved to apply the rule strictly, but it may be used as a rough approximation. The fact that the diagram is skewed toward the early fractions indicates that most of the material was of higher molecular weight.

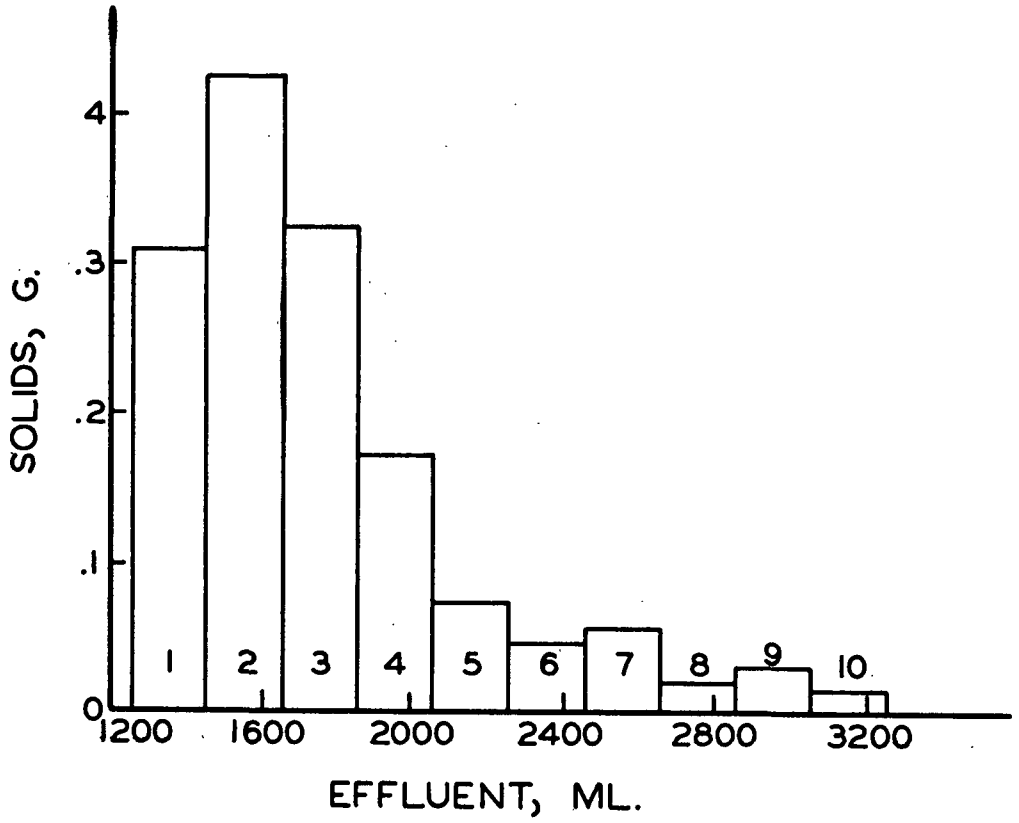


Figure 22. Fractionation of Polymer 11 on Sephadex G-25. Void Volume of the Column = 1300 ml.

The molecular weights of the fractions were measured by light scattering and osmometry. The results are summarized in Table IX. The osmometry data are given in Fig. 23. Since the light-scattering plots for the fractions are similar to those already presented, they are given in Appendix V.

TABLE IX

MOLECULAR WEIGHT DETERMINATIONS ON FRACTIONS OF POLYMER 11

| Fraction | Yield, g. | $dn/dc$ | $[\eta]$ | $\bar{M}_w$, light scattering | $\bar{M}_n$, osmometry |
|---|---|---|---|---|---|
| 1 | .3100 | .185 | 1.10 | 13,000 | 4,900 |
| 2 | .4260 | .167 | 1.25 | 12,000 | 3,800 |
| 3 | .3240 | .165 | 1.05 | 4,200 | 2,900 |
| 4 | .1740 | .163 | 2.00 | 21,000 | |
| 5 | .0780 | | | | 2,200 |
| whole polymer | | .166 | 1.10 | 9,800 | 2,000 |

The fractions after Fraction 5 contained too little material for molecular weight determinations, but they would be expected to follow the same trend established in the first five fractions. The high dissymmetry found for Fraction 4 indicates that dust was probably present in this sample, so the high light-scattering molecular weight for Fraction 4 should be discounted. Such high sensitivity settings for the photometer were required with these low molecular weight materials that the readings were exceptionally sensitive to small amounts of dust.

The values for $dn/dc$ were determined very carefully, as shown by the sample calculation in Appendix IV. As was the case with the whole polymers, $dn/dc$ increases with molecular weight, thus indicating a variation in chemical composition among the fractions. Any of the chemical changes that occur in the molecule as it grows in size could account for the change in $dn/dc$. These changes will be discussed later.

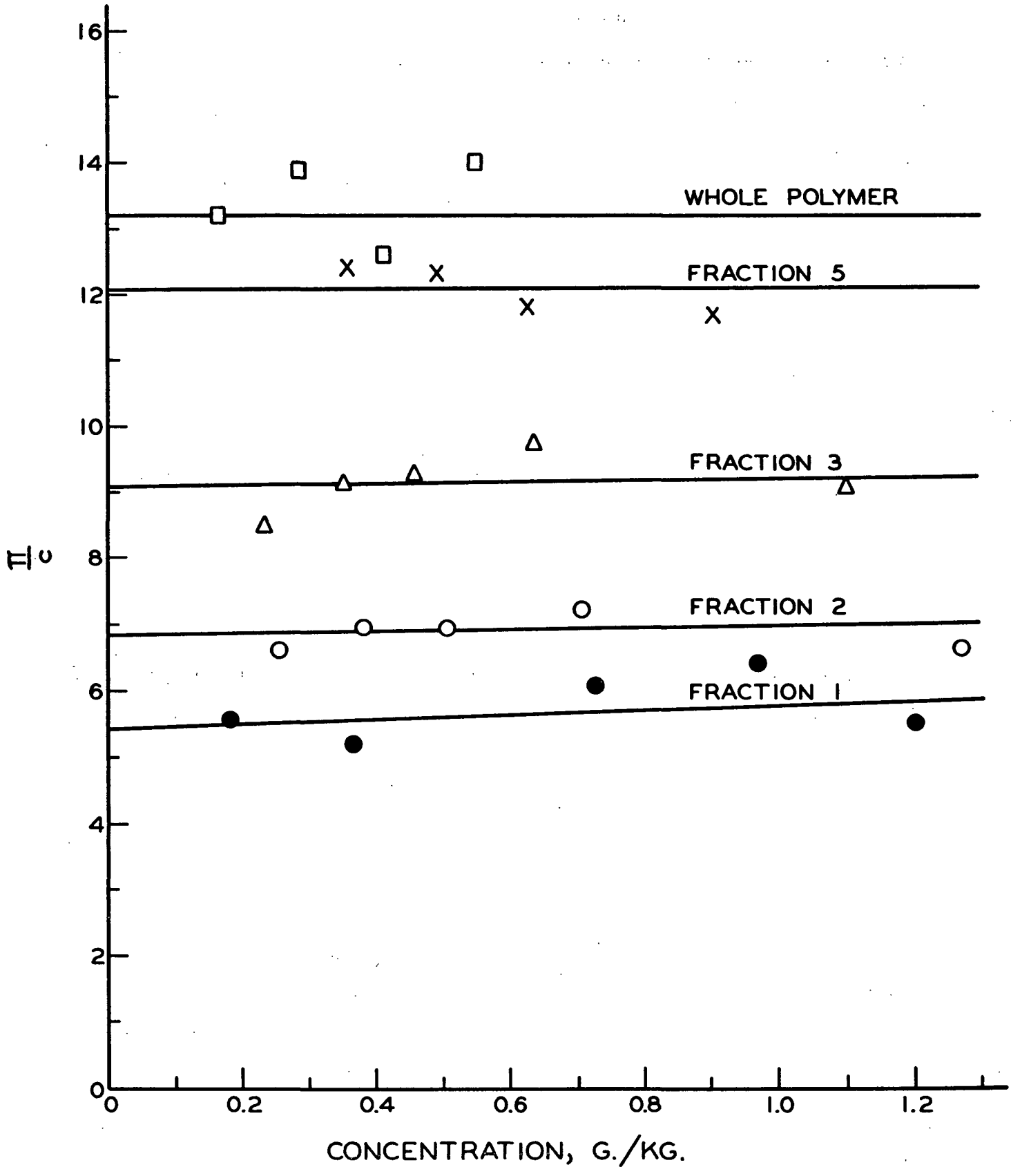


Figure 23. Osmotic Pressure Data on Fractions of Polymer 11. All Solutions Were in 0.33N KCl and Neutralized to Approximately pH 7

The value of 2,000 for the molecular weight of the whole polymer determined by osmometry is reasonable when it is recalled that 10 fractions were taken, and that the number average molecular weight is very sensitive to small amounts of low molecular weight material.

The osmometry data of Table IX clearly indicate that fractionation by molecular weight was obtained on the Sephadex column. The ratios of $\overline{M}_w/\overline{M}_n$ for the fractions range from about 1.4 to 3.2, and are therefore less than the ratio of 4.9 for the whole polymer. As expected, the fractions are apparently less polymolecular than the whole polymer.

## THE CHEMICAL NATURE OF THE MOLECULES

### COMPARISON OF THE POLYMERS WITH THOSE OF BARKER ET AL.

Since the net effect of the passage of gamma-rays and electrons through matter is considered to be similar, the polymers produced in this thesis would be expected to be similar in over-all nature to those produced by Barker, et al. (1). An indication of this is the fact that the results of an attempted acid hydrolysis were similar to those reported by Barker, et al. Polymer 2 was treated with 1N hydrochloric acid at 100°C. for three hours, during which time the solution darkened and a brown precipitate gradually formed. The infrared absorption spectrum of the precipitate is shown in Fig. 24, and can be seen to be similar to that of the original material except for a slight decrease in the intensity of the carbonyl absorption. Paper chromatography of the neutralized supernatant liquid in ethyl acetate – pyridine – water (8:2:1 v/v) indicated a large spot of immobile material. No glucose was found, but a very light streak was present indicating the possible presence of trace amounts of mobile material.

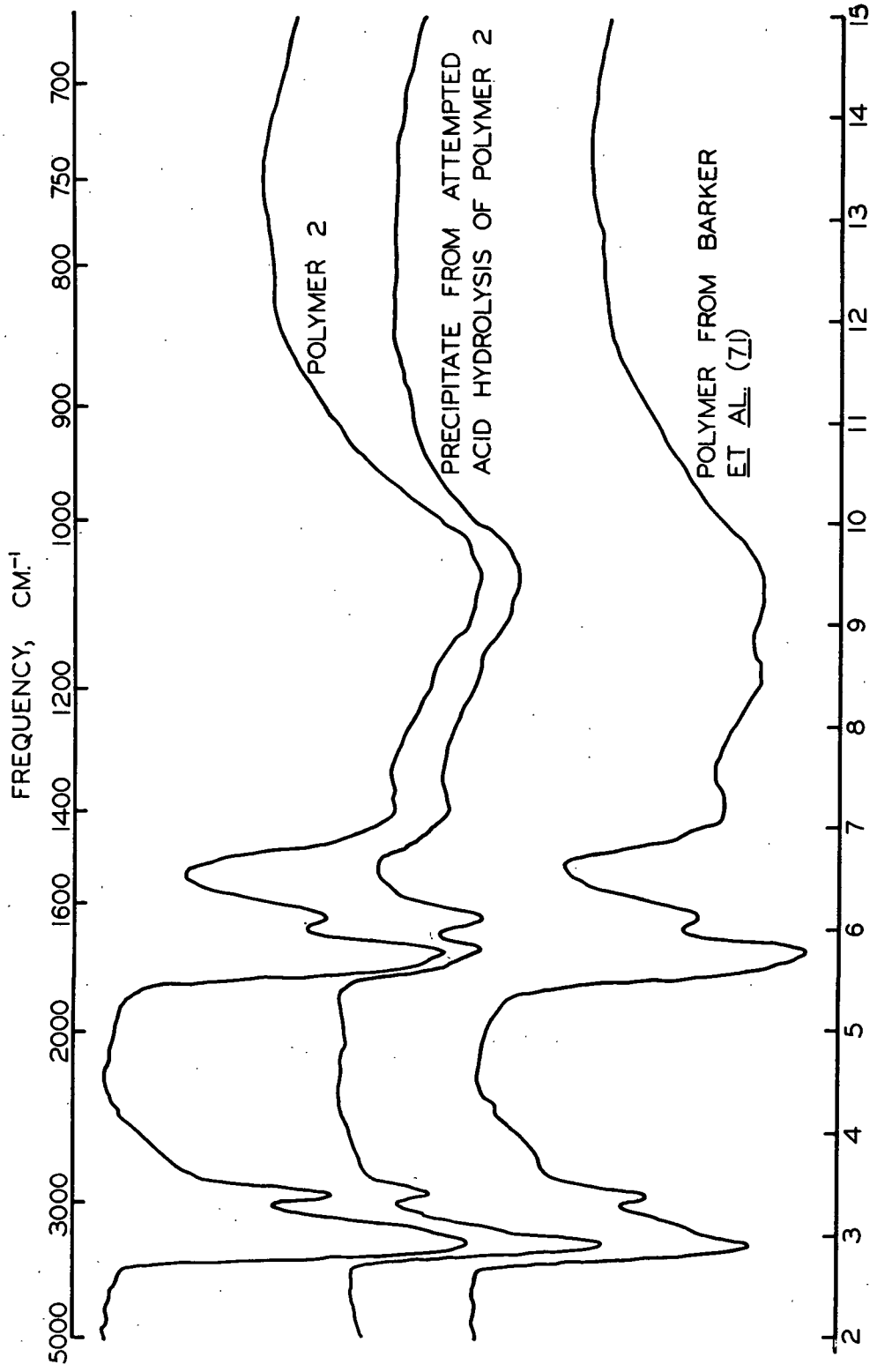


Figure 24. Infrared Absorption Spectra

The fact that the polymers produced in this work are similar to those of Barker, et al. is conclusively demonstrated by examination of the infrared absorption spectrum of a sample of Dr. Barker's polymer (71) shown in Fig. 24. The spectrum is similar to that of Polymer 2 except for a slight difference in intensity of carbonyl absorption.

For comparison purposes, curves for glucose, cellulose, and starch are presented in Fig. 25. It can be seen that the absorption spectrum for the radiation-induced polymer is less detailed than those for glucose, cellulose, and starch, which indicates that it is chemically more complex than the naturally occurring materials. Perhaps more than one monomer is incorporated into the polymer, and perhaps more than one type of polymeric linkage is involved. From the carbonyl absorption at approximately 1720 $cm.^{-1}$, the radiation-induced polymers appear to be more highly oxidized than the naturally occurring polymers. The carbonyl band is quite broad, suggesting the presence of more than one kind of carbonyl group. This was shown to be the case by fractionation of Polymer 11.

The infrared absorption spectrum can be used to reveal information on the possible presence of unsaturation in the radiation-induced polymer. In contrast to the strong carbonyl absorption in the infrared, the C=C stretching vibration gives rise only to a weak band in nonconjugated compounds (88). The position of this band is generally 1680-1620 $cm.^{-1}$. In considering carbon-carbon double bonds it is often helpful to look in the region 690-970 $cm.^{-1}$ for C-H out-of-plane deformation bands. The exact position of absorption in this region depends on the substitution at the double bond, and as the degree of substitution increases, the number of characteristic frequencies is reduced. Unsaturation in completely substituted olefins of the nature $R_1R_2C{=}CR_3R_4$ is very difficult to

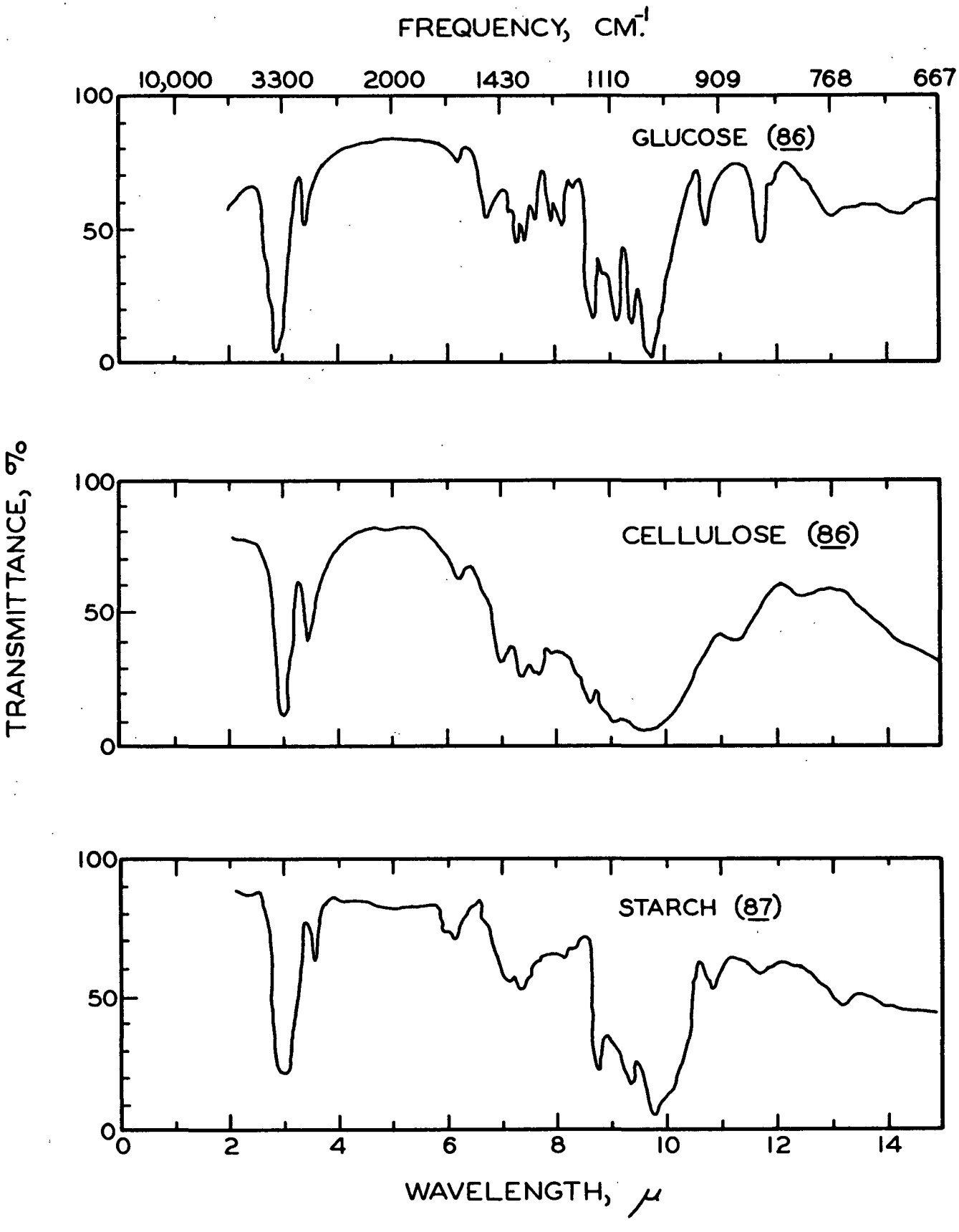


Figure 25. Infrared Absorption Spectra

detect, as the only remaining characteristic frequency is the C=C stretching mode, the intensity of which is considerably reduced by the symmetry around the double bond.

Polymer 2 can be seen to absorb weakly at 1630 cm.$^{-1}$, but this is also the region of absorption of water, which is very likely present in trace amounts. Examination of the 690-970 cm.$^{-1}$ region eliminates all double bonds except the completely substituted type, of which an enediol would be the most likely.

Free OH stretching gives rise to a sharp absorption band in the region 3650-3590 cm.$^{-1}$. Intermolecular hydrogen bonding decreases the frequency to 3400-3200 cm.$^{-1}$ and broadens the absorption peak. As seen from Fig. 24 and 25 all the compounds considered exhibit broad absorption at approximately 3370 cm.$^{-1}$, indicating intermolecular hydrogen bonding.

## ANALYSIS OF FRACTIONS

The chemical properties of the fractions of Polymer 11 were studied in an attempt to further elucidate the structure of the polymer. A necessary assumption in this analysis is that the high molecular weight material is formed from the low molecular weight material. Since all evidence points to the fact that a more severe radiation treatment gives a higher molecular weight product, this assumption seems reasonable.

### Carboxyl Content

The carboxyl content of the fractions is plotted in Fig. 26. The fraction numbers are plotted in reverse order so that the molecular weight increases in the plot from left to right. The carboxyl groups are seen to be associated mainly with the higher molecular weight material, and hence are thought to be the result

of a secondary reaction which takes place on the molecule as it grows in size. If the polymer was a polymer of gluconic acid as postulated by Barker, et al. (1, 8), the carboxyl content of the fractions would be expected to be about the same.

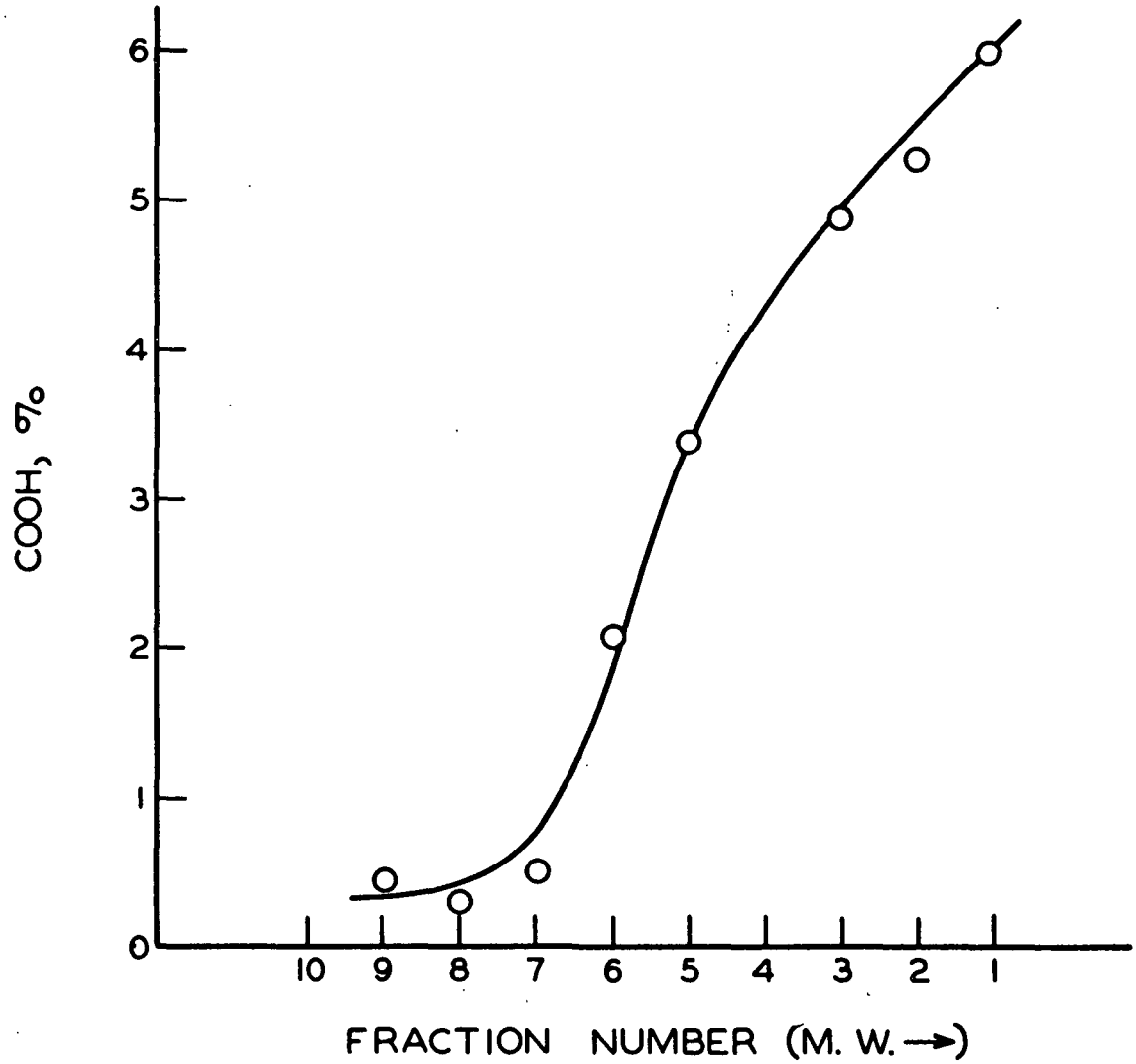


Figure 26. Carboxyl Content of the Fractions of Polymer no. 11 (Fractions 10 and 4 Were Not Measured Because of Insufficient Sample)

Infrared Absorption Spectra

The infrared absorption spectra, given in Fig. 27, show that as the molecular weight of the polymer increases, the carbonyl absorption band increases in intensity

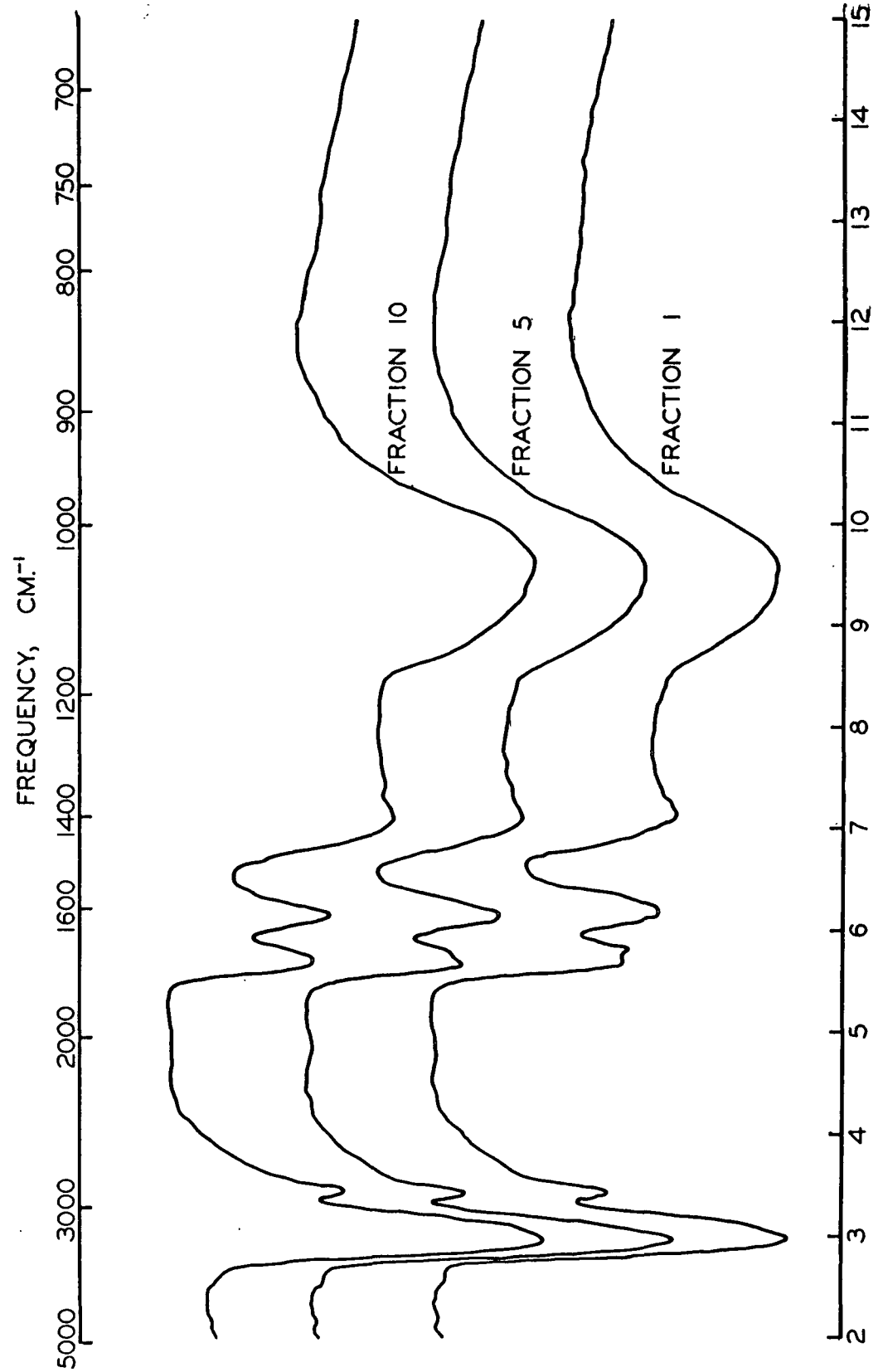


Figure 27. Infrared Absorption Spectra of the Fractions of Polymer 11

and gradually splits into two peaks. Since the carboxyl content increases with molecular weight, it would be expected that the peak at 1720 cm.$^{-1}$ was due to the carboxyl group. This falls into the range of 1725-1700 cm.$^{-1}$ quoted by Bellamy (88) for saturated aliphatic acids. The peak at 1760 cm.$^{-1}$, though, is too high to be in the normal aldehyde or ketone range, but is in the range of esters and lactones. Bellamy gives 1740-1720 and 1725-1705 cm.$^{-1}$ as the position for saturated aldehydes and ketones, respectively, and 1750-1735 and 1780-1760 cm.$^{-1}$ for $\delta$ and $\gamma$ lactones, respectively. The lactone is considered more likely than an ester because the polymer is resistant to acidic and alkaline hydrolysis (1), and because Barker, Lloyd, and Stacey (8) found evidence of lactone formation in the polymer. Sodium borohydride reduction by the method for lactones (89) reduced the intensity of the peak at 1760 cm.$^{-1}$, but left a peak at 1730 cm.$^{-1}$. The peak at 1620 cm.$^{-1}$ is due to the salt of a carboxylic acid.

Ultraviolet Absorption Spectra

The absorption of the fractions in the ultraviolet is shown in Fig. 28. The spectra show a maximum at 264 mμ, which is within the region of 260-270 mμ reported by Barker, et al. (1). The fact that the absorption extends out into the visible region of the spectrum suggests the presence of a double bond conjugated with the carbonyl group. Carbonyl groups in themselves do not cause absorption in the visible region.

The specific extinction coefficient at 265 mμ was calculated for each fraction and is plotted in Fig. 29. If the absorption at 265 mμ is due to an enediol structure as suggested by Grant and Ward (7), the production of the enediol increases with molecular weight; most likely this is the result of radical attack on the polymer molecule as it grows in size.

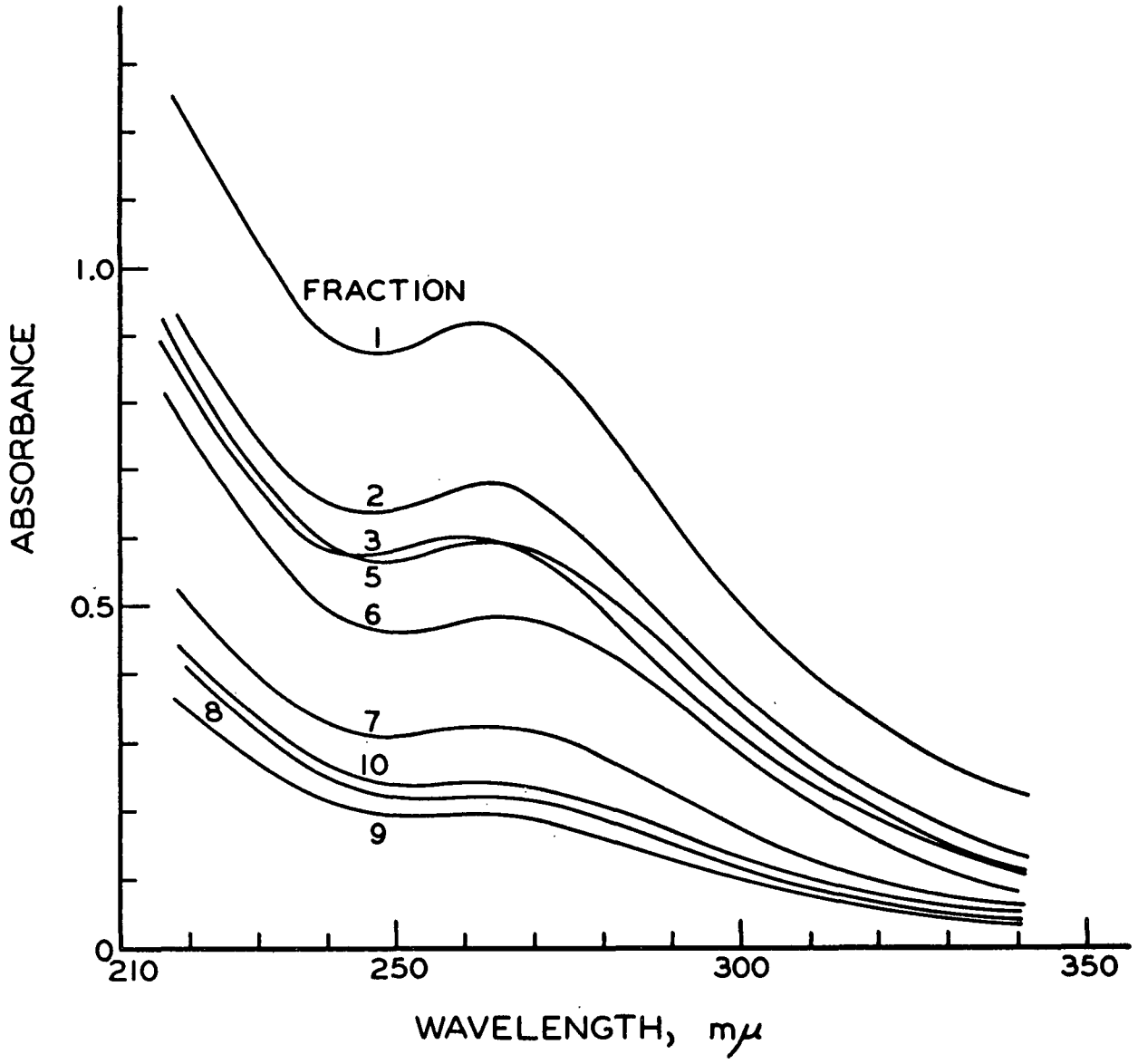


Figure 28. Ultraviolet Absorption Spectra for Fractions of Polymer 11 (Concentration = $1.8 \times 10^{-4}$ g./ml.)

Elemental Analyses

The results of the elemental analyses on the fractions are given in Table X and Fig. 30. For comparison purposes, the elemental compositions of some pertinent carbohydrates are given in Table XI.

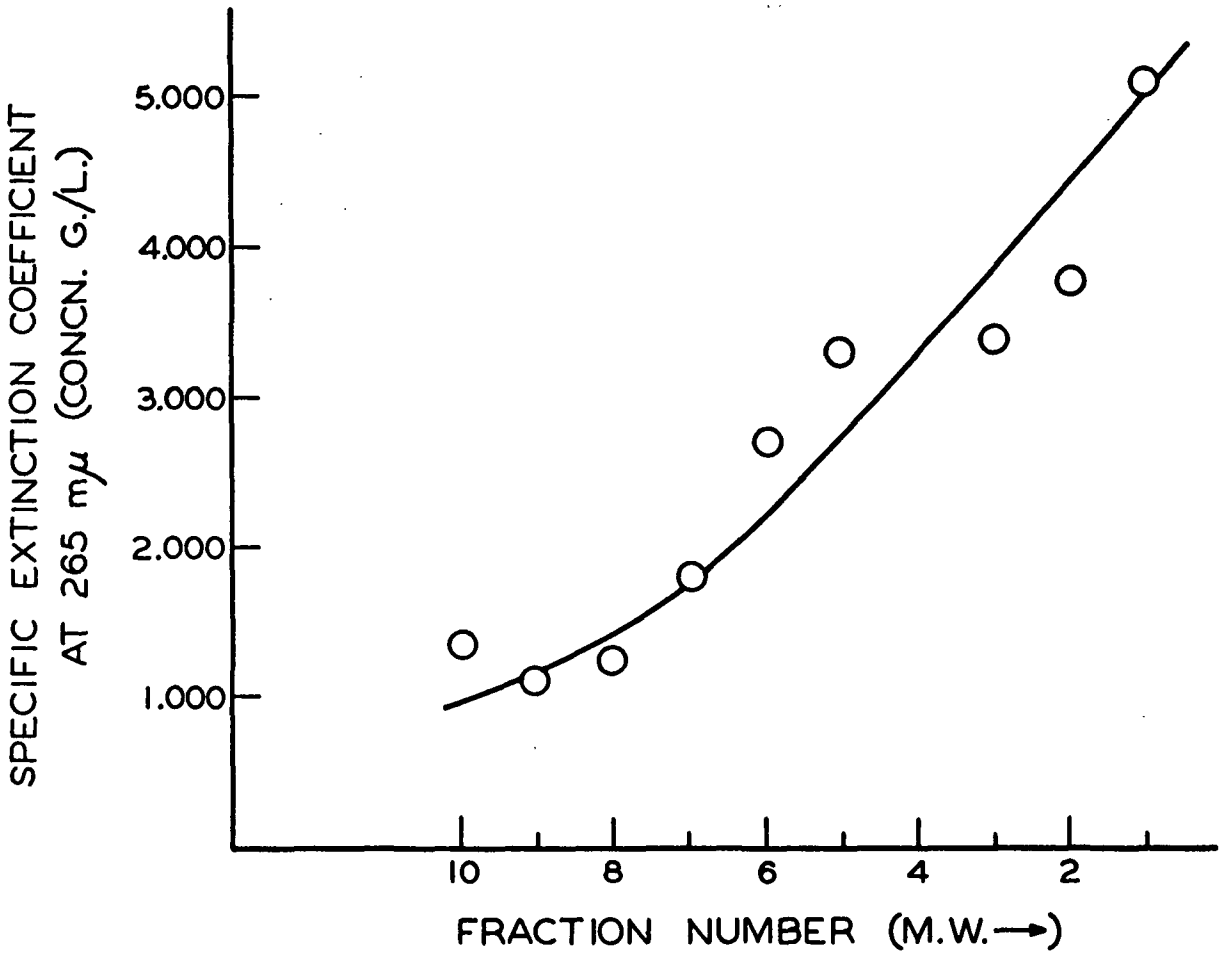


Figure 29. The Specific Extinction Coefficient at 265 mμ for Fractions of Polymer 11

The elemental analyses of the low molecular weight fractions come closest to fitting the composition of gluconolactone. Surprisingly enough the oxygen content of the fractions decreases with molecular weight in spite of the fact that the carboxyl content increases. At the same time the carbon content increases probably as a result of the loss of hydrogen and oxygen.

TABLE X

ELEMENTAL ANALYSIS OF POLYMER 11

| Fraction | Carbon, % | Hydrogen, % | Oxygen, %[a] |
|---|---|---|---|
| 1 | 46.13 | 5.42 | 48.41 |
| 2 | 44.53 | 5.54 | 49.93 |
| 3 | 45.19 | 5.64 | 49.17 |
| 5 | 44.32 | 5.65 | 50.03 |
| 6 | 44.25 | 5.61 | 50.14 |
| 7 | 44.82 | 5.27 | 49.91 |
| 8 | 42.24 | 5.56 | 52.21 |
| 9 | 41.75 | 5.76 | 52.80 |
| 10 | 41.35 | 5.80 | 52.85 |

[a]By difference.

TABLE XI

ELEMENTAL COMPOSITION OF CARBOHYDRATES

| Compound | C, % | H, % | O, % |
|---|---|---|---|
| Glucose | 40.0 | 6.7 | 53.3 |
| Gluconic acid | 36.7 | 6.1 | 57.1 |
| Gluconolactone | 40.4 | 5.6 | 53.9 |

If the ratio of moles of hydrogen per mole of carbon and the ratio of moles of oxygen per mole of carbon are plotted against the fraction number, the results shown in Fig. 31 are obtained. The only way the loss of oxygen can be accounted for is by the loss of hydroxyl groups or oxygen-rich fragments such as carbon dioxide or formic acid. Dehydration could account for some of the oxygen loss, but not all of it. If dehydration alone were taking place, the slope of the plot for the loss of oxygen would be one-half that for the loss of hydrogen. If carbon dioxide were lost from gluconolactone, the carbon content would increase to 44.8% and the oxygen content would decrease to 47.7%.

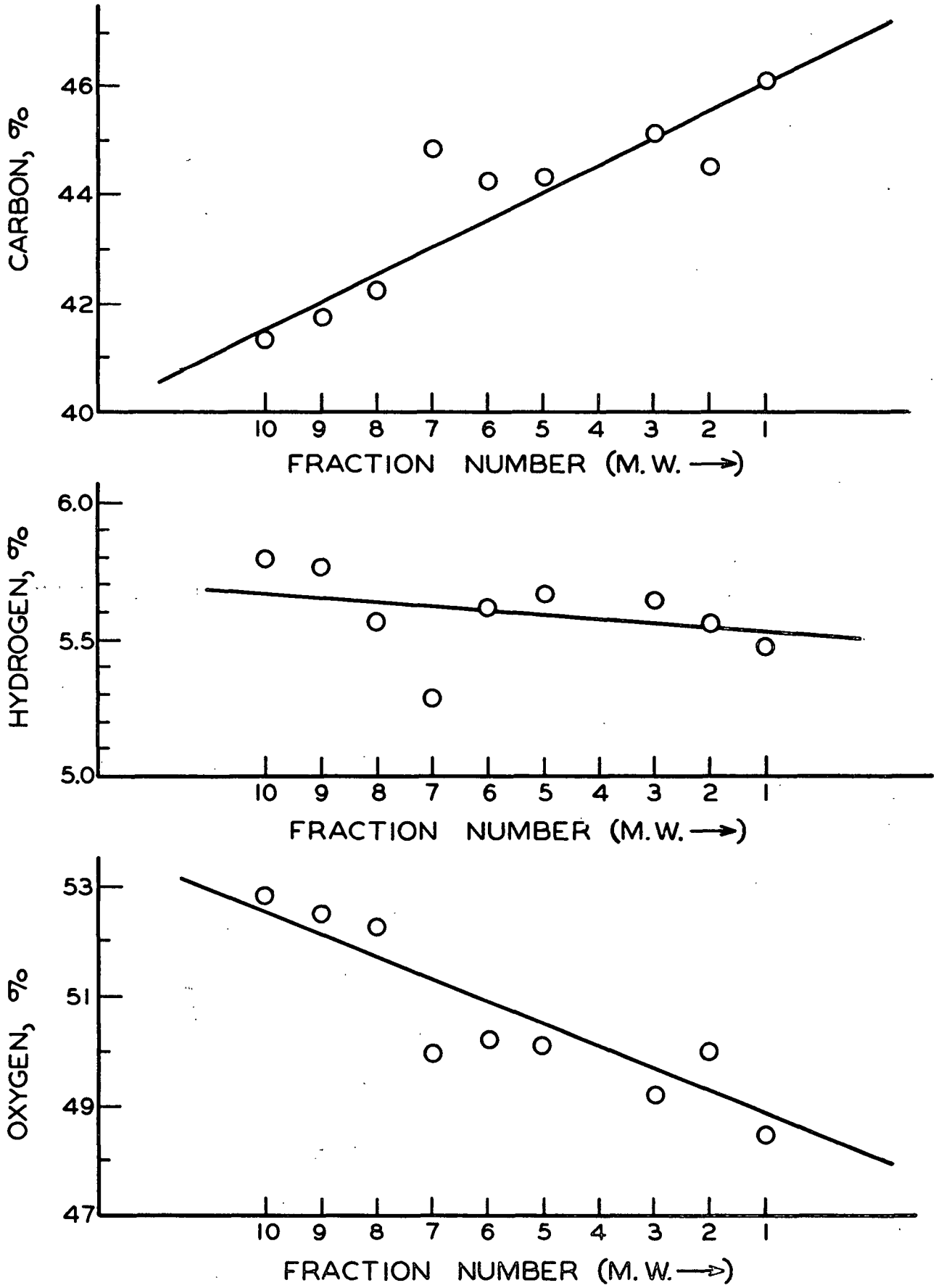


Figure 30. Elemental Analyses of Fractions of Polymer 11

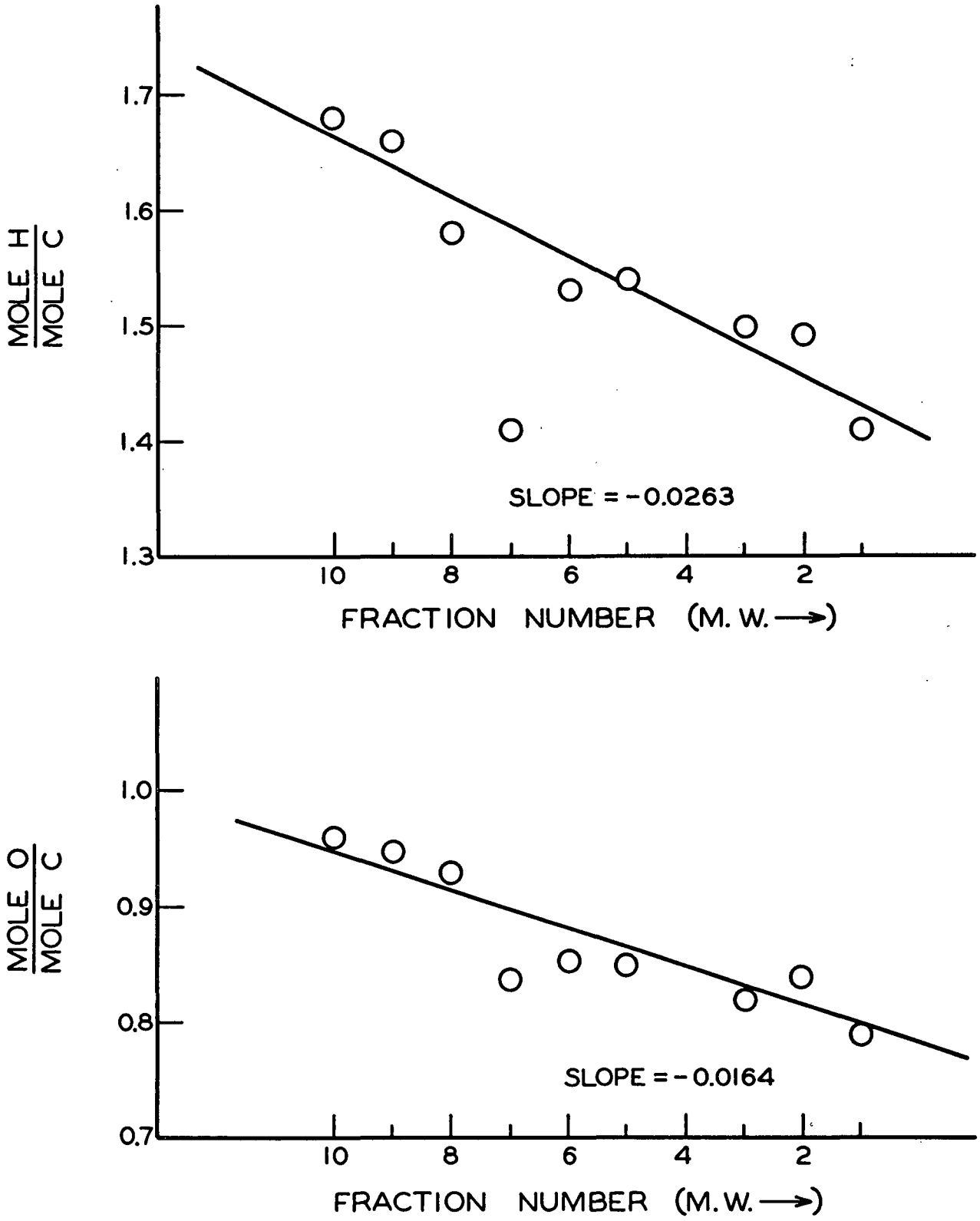


Figure 31. Elemental Analyses of the Fractions on a Mole Basis

The elemental analysis and infrared data both appear to be consistent with the hypothesis that gluconolactone is incorporated into the polymer in the early stages of formation. Although neither gluconic acid or gluconolactone were isolated as products of irradiation in this study, other workers (7, 27) have established gluconic acid as a product. Also, it may be recalled that Barker, et al. (1) obtained slightly a larger yield of polymer from gluconolactone than from glucose.

## FRACTIONATION OF THE SUPERNATANT FROM ETHANOL PRECIPITATION

The supernatant left from the ethanol precipitation of Polymer 11 was fractionated on the column of G-25 Sephadex. An approximately normal distribution of solids was obtained among the 20 fractions taken. Paper chromatography showed that unreacted glucose appeared in Fraction 7 and lasted through Fraction 14. A low molecular weight acidic material appeared in Fractions 8 through 17.

The polymers in Fractions 1 through 6 showed the same trends in carboxyl content, elemental analyses, and ultraviolet and infrared absorption spectra as noted for the polymers precipitated by the ethanol. The molecular weight of Fraction 1 was estimated by osmometry to be about the same as that for Fraction 4 of the ethanol precipitate. The original ethanol precipitation apparently did not give a sharp fractionation on the basis of molecular weight alone.

## MISCELLANEOUS NEW CHEMICAL INFORMATION

During the course of the thesis several miscellaneous chemical tests were run on the polymers. The results of these tests do not contribute to the main theme of the thesis, but should be reported for the benefit of other workers in

the field. This work may be considered supplementary to the more extensive chemical analysis by Barker, et al. (1).

Molisch Test

Glucose and Polymers 9 and 7 were each subjected simultaneously to the Molisch test for carbohydrates. The test employs α-naphthol in the presence of sulfuric acid, and gives a pink color with monosaccharides, oligosaccharides, and many polysaccharides. The color is due to condensation products between α-naphthol and furfural or hydroxymethyl furfural. Functional derivatives, such as acids, do not give a test.

Polymers 7 and 9 gave negative tests. This is not surprising though, when it is recalled that the polymer is resistant to acid hydrolysis, thus preventing the formation of furfural or hydroxymethyl furfural.

Optical Rotation

Polymer 7 exhibited no detectable optical rotation when a 0.26% aqueous solution was examined with sodium light on a Zeiss Winkel polarimeter. This is somewhat surprising since the naturally occurring polysaccharides are usually optically active. For example, soluble starch and glycogen have specific rotations of + 375 and 366°, respectively, in aqueous solution (90). Cellulose has a specific rotation of -46° in a 1:1 mixture of water and Triton B (90). It may be that the polymer is heterogeneous enough that the optical rotations of different portions of the molecule cancel each other, and the net effect is no rotation.

Treatment with Hydrobromic Acid

The treatment used by Hough, Jones, and Wadman (91) to demethylate methylated sugars was tried on Polymer 11. The polymer was dissolved in 47% hydrobromic acid and heated on a boiling water bath for 2 hours. During the heating a dark brown

precipitate formed similar to that noted upon treatment with 1N hydrochloric acid. After neutralization, paper chromatography of the supernatant liquid revealed a trace of material which was apparently glucose. The yield, estimated by visual observation, was about 0.2%.

The results suggest the presence of a small number of ether linkages in the polymer. Since the yield was very low, though, most of the linkages are still thought to be carbon-carbon bonds.

# CONCLUSIONS

Irradiation of aqueous glucose solutions with high energy electrons produces a highly branched, high molecular weight, acidic polymer. Molecular weights can be produced which are much higher than previously expected, and are definitely in the high polymer range.

A wide range of molecular weights may be produced, depending on the conditions of irradiation. For example, the weight average molecular weights of the polymers produced in this thesis ranged from 9,800 to 5,000,000. Increasing either the dose or the dose rate appears to increase the molecular weight of the product. As would be expected, the distribution of molecular weights within a given product is quite broad. For instance, the polymer which had a 9,800 weight average molecular weight had a number average molecular weight of 2,000, thus giving a $\overline{M}_w/\overline{M}_n$ ratio of 4.9.

In addition to being heterogeneous with respect to molecular weight, the polymers are heterogeneous in chemical composition. The carboxyl content increases with molecular weight and is therefore thought to be the result of secondary attack on the molecule which takes place as it grows in size. This is opposed to the earlier hypothesis that the repeating monomer unit during the initial stages of polymerization was gluconic acid. Infrared spectroscopy and elemental analysis data are consistent with the hypothesis that gluconolactone is incorporated into the polymer in the early stages of formation. Secondary attack then results in the formation of carboxyl groups, enediol groups, and the loss of oxygen-rich fragments.

## SUGGESTIONS FOR FUTURE WORK

A tremendous amount of work remains to be done before the system is fully understood, but the most immediate work that is needed is a more thorough chemical analysis of the fractions of the polymer. Hydroxyl and carbonyl content and periodate oxidation data would contribute significantly to the knowledge of the nature of the changes that take place in the molecule as it grows in size.

All the experimental facts pointing toward a carbon-carbon bond in the polymer are negative evidence (i.e., resistance to hydrolysis, etc.). In order to pinpoint the nature and location of the polymeric bond, dimers will have to be isolated and studied. Brooks (92) has suggested that periodate oxidation of dimers formed from L-mannose might shed some light in this area.

In interpreting the results of the analysis of the fractions, it was necessary to assume that the high molecular weight material was derived from the low molecular weight material. A check on this would be to irradiate a solution of low molecular weight polymer to see if a high molecular weight polymer is formed. Analysis of the solution for low molecular weight fragments would indicate the nature of the radiation-induced degradation.

Temperature control of the solutions during irradiation would enable one to separate this variable in the effect of dose rate on the molecular weight of the product. A series of irradiations at different temperatures and different dose rates would be necessary to establish the effect of each variable.

## POLYMER NOMENCLATURE

During the course of the laboratory work, the solutions and polymers were each given a hyphenated number. The first number referred to the page of the research notebook on which the sample was first described, and the second number referred to the particular sample on that page. For example, 67-5 referred to Sample 5 on page 67. For the written thesis the polymers are renumbered as follows:

| Old Number | | New Number |
|---|---|---|
| 67-5 | | 1 |
| 67-9 | | 2 |
| 68-1 | Research | 3 |
| 70-1 | Notebook | 4 |
| 71-1 | No. 2101 | 5 |
| 71-2 | | 6 |
| 71-3 | | 7 |
| 71-4 | | 8 |
| 125-1 | | 9 |
| 34-1 | | 10 |
| 34-2 | Research | 11 |
| 34-3 | Notebook | 12 |
| 34-4 | No. 2215 | 13 |

## ACKNOWLEDGMENTS

The author wishes to express his sincere appreciation for the guidance and encouragement offered by his Thesis Advisory Committee: Dr. E. J. Jones, Chairman, Dr. J. W. Green, and Mr. E. E. Dickey. Appreciation is also expressed to Mr. H. A. Swenson who took an active interest in the thesis throughout its progress.

Thanks are also due the following:

Dr. S. A. Barker of The University of Birmingham, Birmingham, England for his gift of a sample of his polymer.

Mr. Keith Clark and Mr. Robert Carpenter of The High Voltage Engineering Corporation for their assistance in the irradiation of the samples.

Mr. Lowell Sell of the Institute Analytical Group for infrared and ultraviolet spectroscopy.

Mr. Charles Schmitt of the Institute Cellulose Chemistry Group for instruction in the use of the Brice-Phoenix Photometer and the Mechrolab High Speed Osmometer.

## LITERATURE CITED


1. Barker, S. A., Grant, P. M., Stacey, M., and Ward, R. B., J. Chem. Soc. 1959:2648-54.

2. Burr, J. G., J. Phys. Chem. 61:1477-80(1957).

3. McDonell, W. R., and Newton, A. S., J. Am. Chem. Soc. 76:4651-8(1954).

4. Phillips, G. O., and Criddle, W. J., J. Chem. Soc. 1962:2733-9.

5. Phillips, G. O., and Criddle, W. J., J. Chem. Soc. 1961:3763-70.

6. Grant, P. M., and Ward, R. B., J. Chem. Soc. 1959:2654-8.

7. Grant, P. M., and Ward, R. B., J. Chem. Soc. 1959:2871-6.

8. Barker, S. A., Lloyd, I. R. L., and Stacey, M., Rad. Res. 17:619-24(1962).

9. Leavitt, F. C., J. Polymer Sci. 51:349-57(1961).

10. Miller, A. A. Crosslinking of cellulosic materials by irradiation. U. S. patent 2,898,891 (July, 1959).

11. Hillend, W. J. Electron radiation of aqueous methyl cellulose solutions. Doctor's Dissertation. Appleton, Wisconsin, The Institute of Paper Chemistry, 1963. 73 p.

12. Charlesby, A. Atomic radiation and polymers. Oxford, England, Pergamon Press Ltd., 1960. 556 p.

13. Chapiro, A. Radiation chemistry of polymeric systems. New York, Interscience, 1962. 712 p.

14. Hollaender, A. Radiation biology. Vol. 1, part 1. New York, McGraw-Hill, 1954. 621 p.

15. High Voltage Engineering Corporation. High voltage electron-beam processing. Bulletin P. Burlington, Mass., 1959. 31 p.

16. Bovey, F. A. The effects of ionizing radiation on natural and synthetic high polymers. New York, Interscience, 1958. 287 p.

17. Allen, A. O., J. Phys. Chem. 52:479-90(1948).

18. Hart, E. J., J. Chem. Ed. 34:586-93(1957).

19. Hart, E. J., Nucleonics 19:45-8(Oct., 1961).

20. Kuppermann, A., Nucleonics 19:38-42(Oct., 1961).

21. Collinson, E., and Swallow, A. J., Chem. Revs. 56:471-568(1956).

22. McDonell, W. R., and Sheffield, G., J. Chem. Phys. 23:208(1955).

23. Jayson, G. G., Scholes, G., and Weiss, J., J. Chem. Soc. 1957:1358-68.

24. Allen, J. T., Hayon, E. M., and Weiss, J., J. Chem. Soc. 1959:3913-9.

25. Phillips, G. O. Radiation chemistry of carbohydrates. In Wolfrom's Advances in carbohydrates. Vol. 16. p. 13. New York, Academic Press, Inc., 1961.

26. Phillips, G. O., Nature 173:1044-5(1954).

27. Phillips, G. O., Moody, G. J., and Mattok, G. L., J. Chem. Soc. 1958:3522-34.

28. Phillips, G. O., Mattok, G. L., and Moody, G. J., Proc. U. N. Intern. Conf. Peaceful Uses At. Energy, 2nd, Geneva, 1958, 29:92-8(1959); C.A. 54:19113b.

29. Phillips, G. O., and Criddle, W. J., J. Chem. Soc. 1960:3404-12.

30. Phillips, G. O., and Criddle, W. J., J. Chem. Soc. 1962:2733-9.

31. Naik-kurade, A. G., Livingston, G. E., Francis, F. J., and Fagerson, I. S., Food Research 24:618-32(1959); C.A. 54:7913b.

32. Coleby, B., Chem. and Ind. 1957:111-12.

33. Michelakis, A. M. The effect of ionizing radiations on certain carbohydrates and related substances. Doctor's Dissertation. Columbus, Ohio. The Ohio State University, 1959. 168 p.

34. Bailey, A. J., Barker, S. A., Lloyd, I. R. L., and Moore, R. H., Rad. Res. 15:532-7(1961).

35. Bailey, A. J., Barker, S. A., and Stacey, M., Rad. Res. 15:538-45(1961).

36. American Public Health Association, American Water Works Association, and Water Polution Control Federation. Standard methods for the examination of water and wastewater. 11th ed. p. 316. New York, American Public Health Association, 1960.

37. Trevelyan, W. E., Proctor, D. P., and Harrison, J. S., Nature 166:444-5 (1950).

38. Heyne, E., and Whistler, R. L., J. Am. Chem. Soc. 70:2249-52(1948).

39. Koleske, J. V. The configuration and hydrodynamic properties of fully acetylated guaran. Doctor's Dissertation. Appleton, Wis., The Institute of Paper Chemistry, 1963. 175 p.

40. Stacey, K. A. Light scattering in physical chemistry. London, Butterworths Scientific Publications, 1956. 230 p.

41. Goring, D. A. I., and Timell, T. E., J. Phys. Chem. 64:1426-30(1960).

42. Phoenix Precision Instrument Company. The new Brice-Phoenix light scattering photometer. Operation manual OM-1000. Philadelphia, Pa., The Co., 1955. 52 p.

43. Swenson, H. A., Morak, A. J., and Kurath, S. F., J. Polymer Sci. 51:231-45(1961).

44. Cornell, R. H. The uniformity of substitution during the emulsion xanthation of cellulose and the solution properties of the corresponding diethylacetamide derivatives. Doctor's Dissertation. Appleton, Wis., The Institute of Paper Chemistry, 1960. 122 p.

45. Kratohvil, J. P., Dezelic, Gj., Kerker, M., and Matijevic, E., J. Polymer Sci. 57:59-78(1962).

46. McCormick, H. W., J. Polymer Sci. 36:341-9(1959).

47. Debye, P., J. Appl. Phys. 15:338-42(1944).

48. Oster, G. Light scattering. In Weissberger's Technique of organic chemistry. Vol. 1, part III. p. 107. New York, Interscience, 1960.

49. Beattie, W. H., and Booth, C., J. Phys. Chem. 64:696-7(1960).

50. Beattie, W. H., and Booth, C., J. Polymer Sci. 44:81-91(1960).

51. Brice, B. A., Nutting, G. C., and Halwer, M., J. Am. Chem. Soc. 75:824-8 (1953).

52. Rankin, J., Mechrolab, Inc., Mountain View, California. Personal communication, 1964.

53. Mechrolab, Inc. The Mechrolab model 501 high speed membrane osmometer. Operation manual. Mountain View, California. 1962. 27 p.

54. Staverman, A. J., Pals, D. T. F., and Kruissink, C. A., J. Polymer Sci. 23: 57-68(1957).

55. Bruss, D. B., and Stross, F. H., J. Polymer Sci. 55:381-94(1961).

56. Tung, L. H., J. Polymer Sci. 32:477-85(1958).

57. Bruss, D. B., and Stross, F. H., J. Polymer Sci. 1(Part A):2439-57(1963).

58. Staverman, A. J., Rec. Trav. Chim. 70:344-52(1951); C.A. 45:6010e.

59. Staverman, A. J., Rec. Trav. Chim. 71:623-33(1952); C.A. 46:10788a.

60. Flory, P. J. Principles of polymer chemistry. Ithaca, New York, Cornell University, 1953. 672 p.

61. Strauss, U. P., and Fuoss, R. M., J. Polymer Sci. 4:457-72(1949).

62. Fuoss, R. M. Discussions Faraday Soc. 11:125-34(1951).

63. Timell, T. E., Svensk Papperstid. 57:777-88(1954).

64. Schulz, G. V., Z. Elektrochem. 43:479-85(1937); C.A. 31:7317[9].

65. Phillips, A. W., and Gibbs, P. A., Biochem. J. 81:551-6(1961).

66. Flodin, P. Dextran gels and their applications in gel filtration. New York, N. Y., Pharmacia Fine Chemicals, Inc., 1962. 85 p.

67. Flodin, P., and Killander, J., Biochem. Biophys. Acta 63:403-10(1962).

68. Flodin, P., and Aspberg, K., In Biological structure and function. Vol. 1. p. 345. London, Academic Press, 1961.

69. Granath, K., and Flodin, P., Makromol. Chem. 48:160-71(1961).

70. Dillingham, E. O. Personal communication, 1963.

71. Barker, S. A., Lloyd, I. R. L., and Stacey, M., Rad. Res. 16:224-31(1963).

72. Horio, M., Imamura, R., and Inagaki, H., Tappi 38:216-20(1955).

73. Tanford, C. Physical chemistry of macromolecules. New York, John Wiley and Sons, Inc., 1961. 710 p.

74. Moacanin, J., Felicetta, V. F., Haller, W., and McCarthy, J. L., J. Am. Chem. Soc. 77:3470-5(1955).

75. Erlander, S., and French, D., J. Polymer Sci. 20:7-28(1956).

76. Peebles, L. H., Jr., J. Am. Chem. Soc. 80:5603-7(1958).

77. Muus, L. T., and Billmeyer, F. W., J. Am. Chem. Soc. 79:5079-82(1957).

78. Stacy, C. J., and Foster, J. F., J. Polymer Sci. 25:39-50(1957).

79. Goring, D. A. I. The physical chemistry of lignin. In Proceedings of the wood symposium (I.U.P.A.C.), Montreal, Canada, Aug., 1961. p. 233. London, Butterworths, 1962.

80. Greenwood, C. T., and Robertson, J. S. M., J. Chem. Soc. 1954:3769-78.

81. Gupta, P. R., and Goring, D. A. I., Can. J. Chem. 38:270-9(1960).

82. Guinand, S., Boyer-Kawenoki, F., Dobry, A., and Tonnelat, J., C. R. Acad. Sci., Paris 229:143-5(1949); C.A. 44:6238g.

83. Doty, P., and Steiner, R. F., J. Chem. Phys. 17:743-4(1949).

84. Doty, P., and Steiner, R. F., J. Chem. Phys. 20:85-94(1952).

85. Anacker, E. W., Rush, R. M., and Johnson, J. S., J. Phys. Chem. 68:81-93 (1964).

86. Sell, L. O. Unpublished work, 1959 and 1960.

87. Newburger, S. H., Jones, J. H., and Clark, G. R., Proc. Sci. Sect. of the Toilet Goods Assoc., No. 19 (May, 1963).

88. Bellamy, L. J. The infrared spectra of complex molecules. New York, John Wiley and Sons, Inc., 1954. 323 p.

89. Frush, H. L., and Isbell, H. S., J. Am. Chem. Soc. 78:2844-6(1956).

90. Pigman, W. The carbohydrates. New York, Academic Press, Inc., 1957, 902 p.

91. Hough, L., Jones, J. K. N., and Wadman, W. H., J. Chem. Soc. 1950:1702-6.

92. Brooks, R. D. Chemical characterization of the high polymer formed from the irradiation of aqueous glucose. Unpublished work. Appleton, Wis., The Institute of Paper Chemistry, 1963. 48 p.

93. Rezanowich, A., Yean, W. Q., and Goring, D. A. I., Svensk Papperstid. 66: 141-9(1963).

94. Hildebrand, J. H., and Scott, R. L. The solubility of nonelectrolytes. New York, Reinhold, 1950. 488 p.

# APPENDIX I

## IRRADIATION DATA

### SAMPLES 1, 2, 3, 4, 5, 6, 7, AND 8

Solution concentration: 1.0% except 3 which was 10.0%.

Containers: glass tubes for 1, 2, 3, and 4; polyethylene bags for 5, 6, 7, and 8.

Oxygen content of the solutions: 0.6 p.p.m. for all except 4 which had 7.8 p.p.m.

Date of irradiation: October 22, 1962.

Location: Rockford, Ill.

Type of machine: Linac Mark I.

Energy of electrons: 8.5 Mev.

Average beam current: 40 μa.

Width of beam: 6 inches; diffused

Pulse rate: 120 p.p.s.

Distance of samples from beam window: 14-3/4 in.

Dose rate: 1 Mrad/pass except for 8 which was 4 Mrad/pass

Dosimetry: cobalt glass

Conveyor speed: 31 in./min. except for 8 which was 7.75 in./min.

Distance of conveyor travel before reversing directions: 24 in.

Dose: 5.....10 Mrad
1, 3, 4, 6, and 8.....20 Mrad
2 and 7.....40 Mrad

### SAMPLE 9

Solution concentration: 1.0%

Containers: polyethylene bags

Oxygen content of solutions: 0.8 p.p.m.

Date of irradiation: March 1, 1963

Location: Burlington, Mass.

Type of machine: Van de Graaff "GS"

Energy of electrons: 1.5 Mev.

Beam current: 1.0 ma.

Width of beam: 13 inches; scanned

Distance of samples from beam window: 6 in.

Dose rate: 1 Mrad/pass

Dosimetry: MSC 300 blue cellophane, polyvinyl chloride, and Faraday Cup

Conveyor speed: 93 in./min.

Distance of conveyor travel before reversing direction: 24 in.

Dose: 40 Mrad

SAMPLES 10, 11, 12, AND 13

Solution concentration: 1.0%

Containers: polyethylene bags for 10, 11, and 12; glass tubes for 13.

Oxygen content of solutions: 1.8 p.p.m. for 10, 11, and 12; 0.6 p.p.m. for 13.

Date of irradiation: June 14, 1963

Location: Rockford, Ill.

Type of machine: Linac Mark I

Energy of electrons: 8.5 Mev.

Average beam current: 35 μa. for 10, and 11; 70 μa. for 12 and 13.

Width of beam: 18 inches; scanned.

Pulse rate: 60 p.p.s. for 10 and 11; 120 p.p.s. for 12 and 13.

Distance of samples from beam window: 7 inches for 10, 11, and 12; 3.5 inches for 13.

Dose rate: 1 Mrad/pass for 10 and 11; 2 Mrad/pass for 12 and 13.

A continuous conveyor system was used for 10, 11, and 12 with the samples travelling at 31 in./min. and passing under the beam every 5.5 min. The reversible conveyor, which traveled at 31 in./min. and reversed direction every 18 in. was used for 13.

Dosimetry: cobalt glass

Dose: 10.....20 Mrad
11, 12, and 13.....40 Mrad

# APPENDIX II

## SOLUBILITY STUDIES

An attempt was made to dissolve Polymer 9 and its acetate in several solvents. The results are given in Table XII.

TABLE XII

SOLUBILITY OF POLYMER 9 AND ITS ACETATE

| Solvent | δ | Reference | Polymer 9 | Acetate |
|---|---|---|---|---|
| Water | 23.4 | (93) | S | I |
| Formamide | 20.5 | (93) | S | S |
| Ethanol | 12.7 | (93) | I | I |
| Nitromethane | 12.6 | (93) | I | I |
| Dimethyl sulfoxide | 12.6 | (93) | S | |
| Acetonitrile | 11.9 | (93) | I | I |
| 1,3-Dichloro-2-propanol | 10.8 | (94) | P | P |
| Pyridine | 10.7 | (93) | S | S |
| o-Chlorophenol | 10.6 | (94) | P | P |
| Tetrachloroethane | 10.2 | (39) | I | I |
| Acetone | 10.0 | (93) | I | I |
| Ethyl lactate | 10.0 | (39) | P | I |
| Dimethyl formamide | 9.6 | (39) | P | S |
| 2-Butanone | 9.4 | (94) | I | I |
| Chloroform | 9.3 | (93) | I | I |
| Diethyl ether | 7.5 | (93) | I | I |
| 3-Bromo-1-propanol | 5.6 | (94) | P | P |
| Trifluoroethanol | | | I | S |
| Tetrahydrofuran | | | I | |
| Diglyme | | | I | |

S = soluble
P = partially soluble
I = insoluble

The tests were performed by placing a pinch of the solute in a 10 by 75-mm. test tube and adding about 1 ml. of the solvent. The solute was judged insoluble if it remained undissolved and there was no appreciable coloration of the solvent. When soluble, the material dissolved completely leaving no residual precipitate.

If, after standing overnight, part of the polymer had dissolved but swollen pieces remained, the material was listed as partially soluble. Also listed in Table XII are the solubility parameters, $\delta$. The solubility parameter is a measure of the cohesive energy of the solvent and is calculated from the energy of vaporization at zero pressure and the molar volume of the liquid (95). As seen from Table XII, there does not seem to be any correlation between the solubility parameter and the solubility of the acetate. This was also noted by Koleske (39) in his work with guaran triacetate. There does, however, seem to be a larger number of solvents for the original polymer among solvents with a high solubility parameter. In order to dissolve the acetate in trifluoroethanol, it was necessary to use the freshly prepared acetate. If allowed to stand for a period of time, it became resistant to solution. Also, after a month or so, the dry unacetylated polymer became resistant to solution in water, presumably due to intermolecular hydrogen bonding.

## APPENDIX III

### LIGHT-SCATTERING DATA ON B-3 POLYSTYRENE

The performance of the light-scattering apparatus was checked by determining the molecular weight of B-3 Polystyrene in toluene. The data give a molecular weight of 234,000 (Fig. 32) which is within 10% of the value of 214,000 obtained by McCormick (46) by sedimentation velocity experiments.

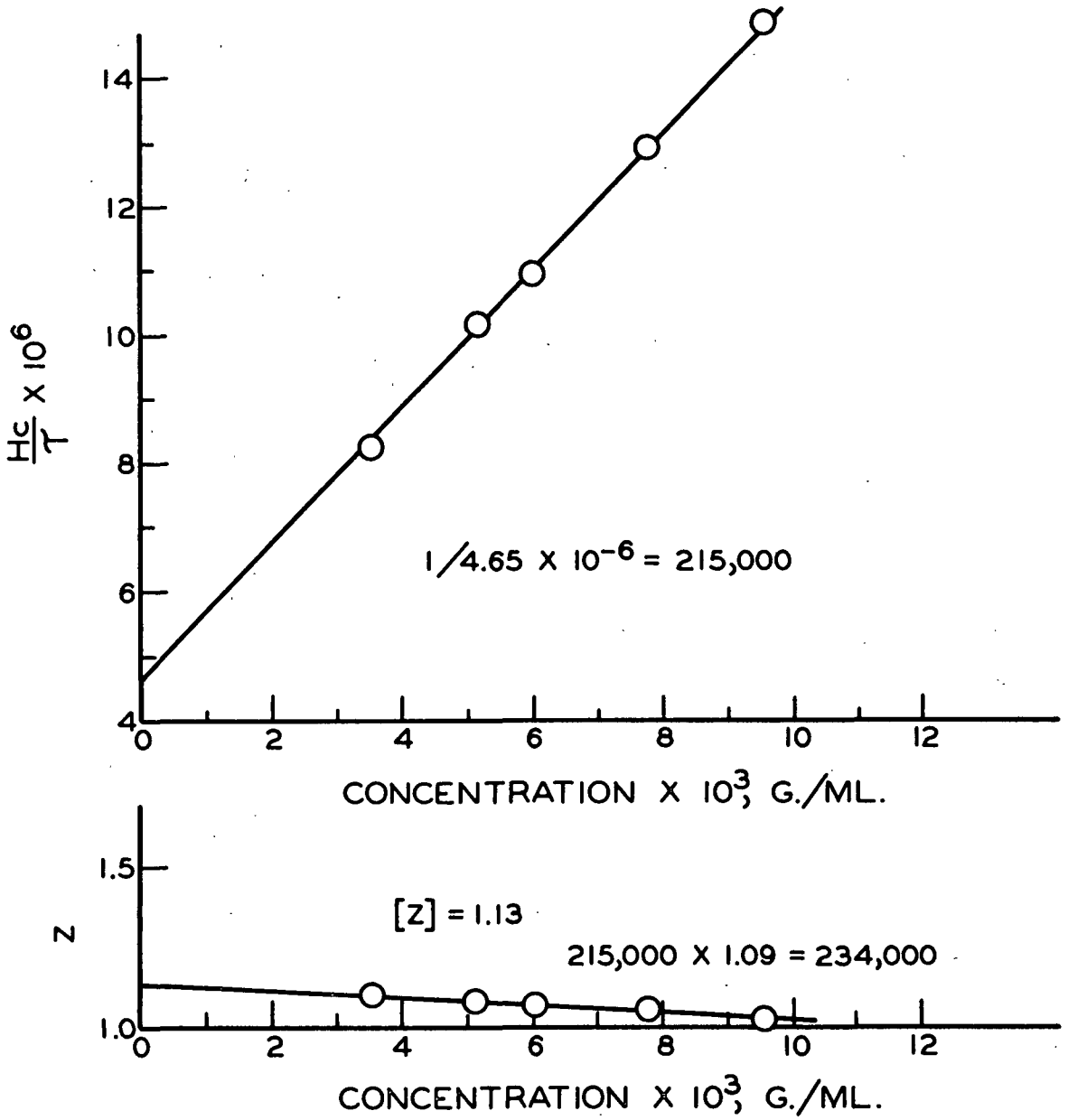


Figure 32. Light-Scattering Data on B-3 Polystyrene in Toluene

## APPENDIX IV

## REFRACTIVE INDEX GRADIENT DATA

The refractive index gradient data measured with the dipping refractometer is given in Fig. 33 and 34.

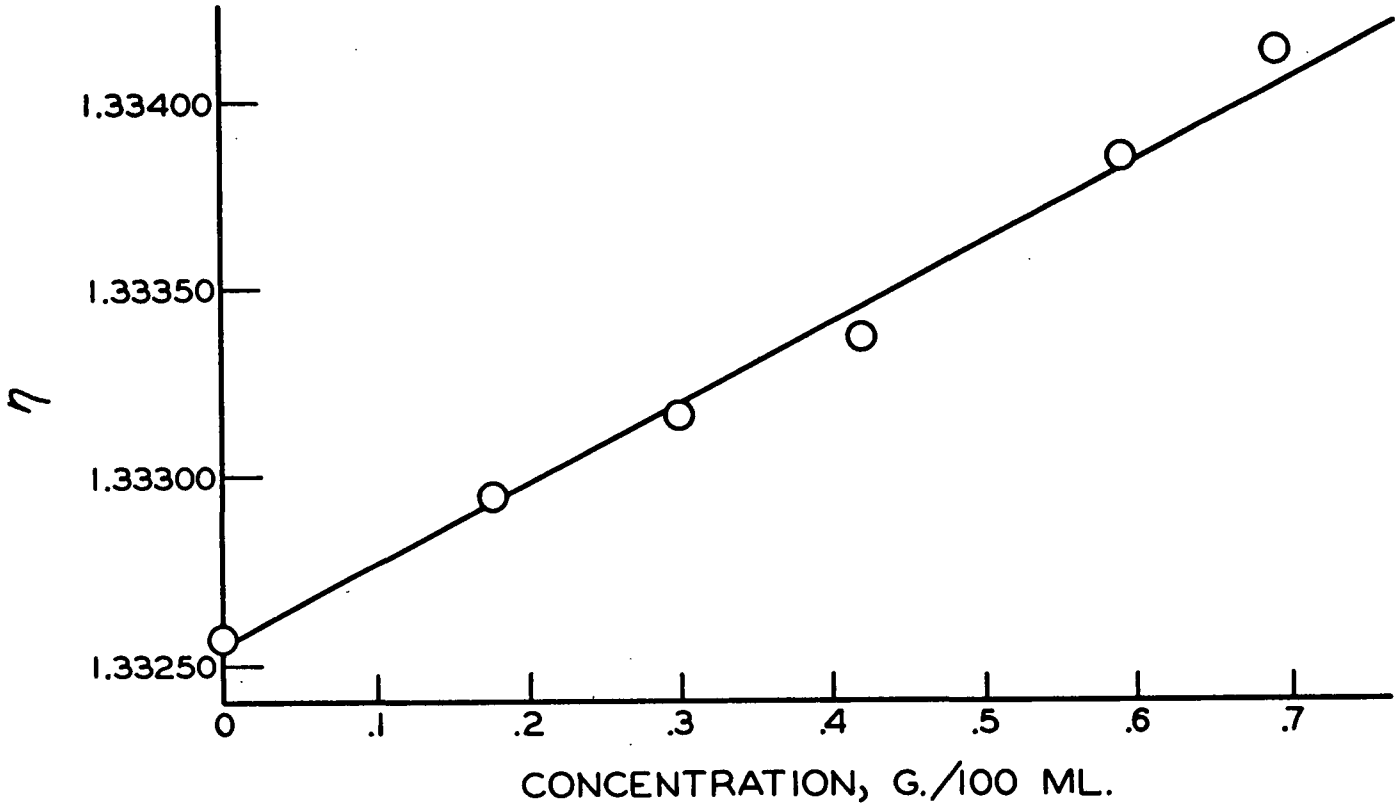


Figure 33. Determination of dn/dc for Polymer 9 in Water

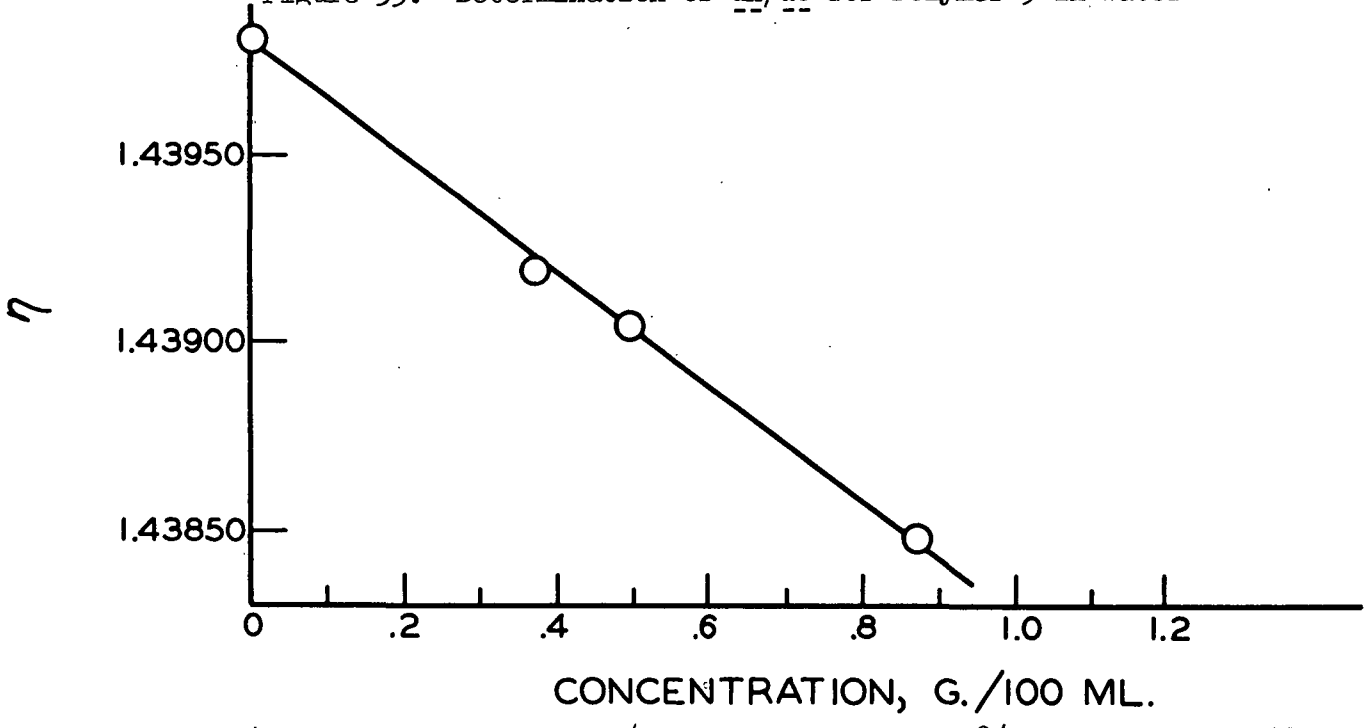


Figure 34. Determination of dn/dc for Polymer 9 in 98% Dimethyl Sulfoxide

A sample calculation is given for the determination of $\underline{dn}/\underline{dc}$ with the Rayleigh interferometer.

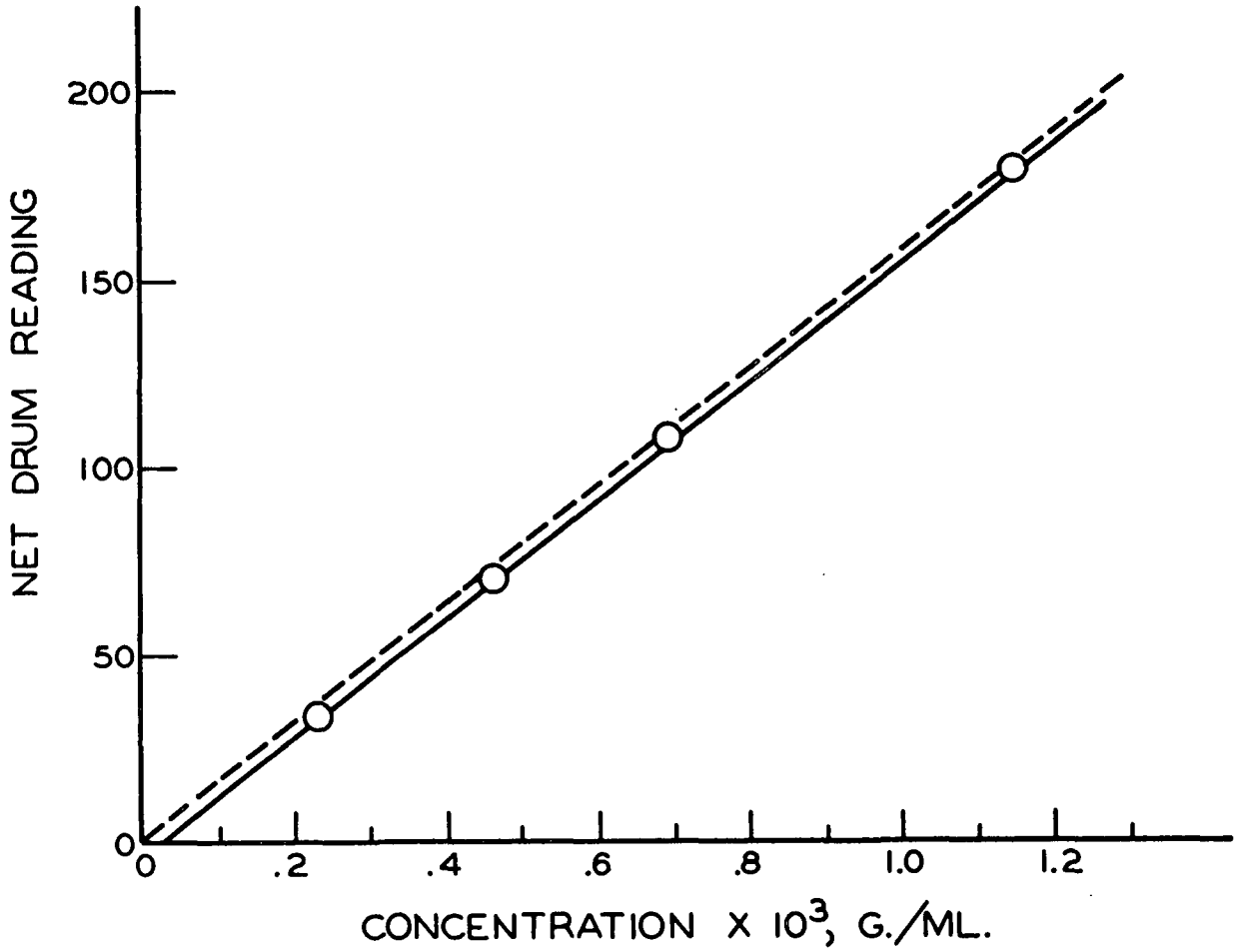


Figure 35. Rayleigh Interferometer Readings for Fraction 1 of Polymer 11 in Water

Since the line through the data points did not pass through the origin, a parallel line was drawn through the origin. This line was used for the calculation.

$$\frac{\underline{dn}}{\underline{dc}} = \frac{\text{Net drum reading x wavelength of light}}{47 \text{ x concentration}}$$

$$= \frac{92 \times 5.46 \times 10^{-5}}{47 \times 0.58 \times 10^{-5}}$$

$$= 0.185$$

APPENDIX V

LIGHT-SCATTERING DATA ON FRACTIONS OF POLYMER 11

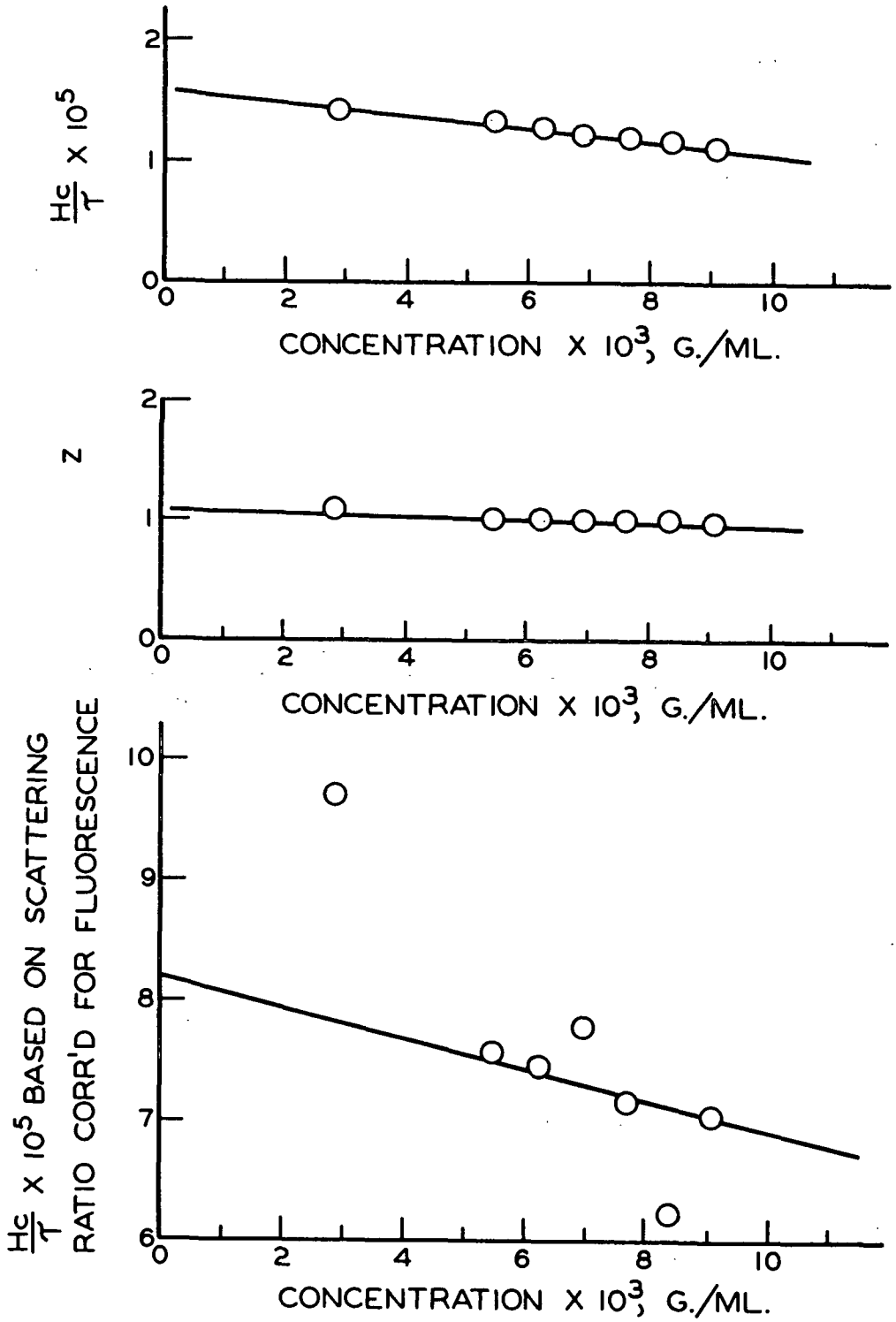


Figure 36. Light-Scattering Data on Fraction 1 of Polymer 11

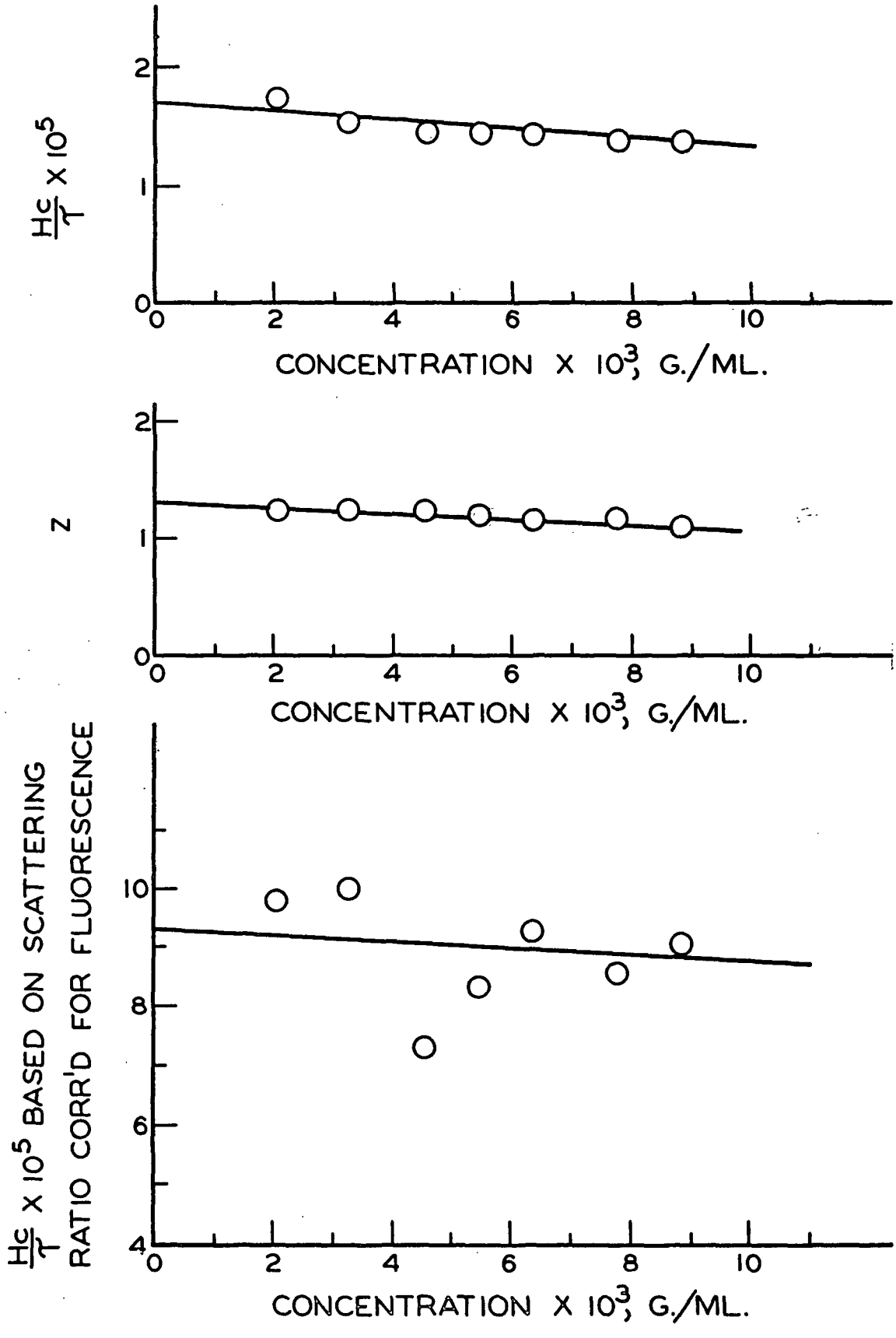


Figure 37. Light-Scattering Data on Fraction 2 of Polymer 11

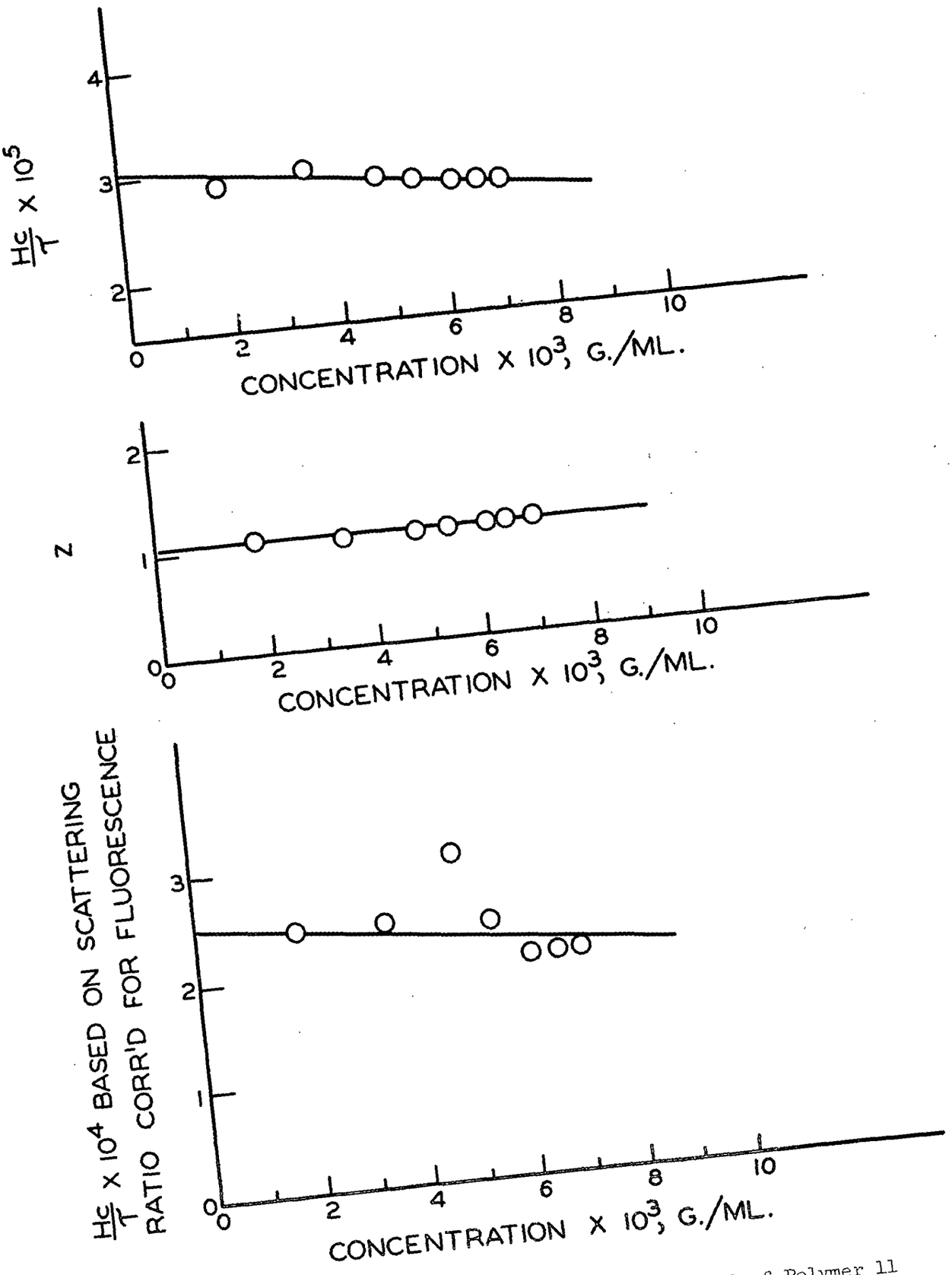


Figure 38. Light-Scattering Data on Fraction 3 of Polymer 11

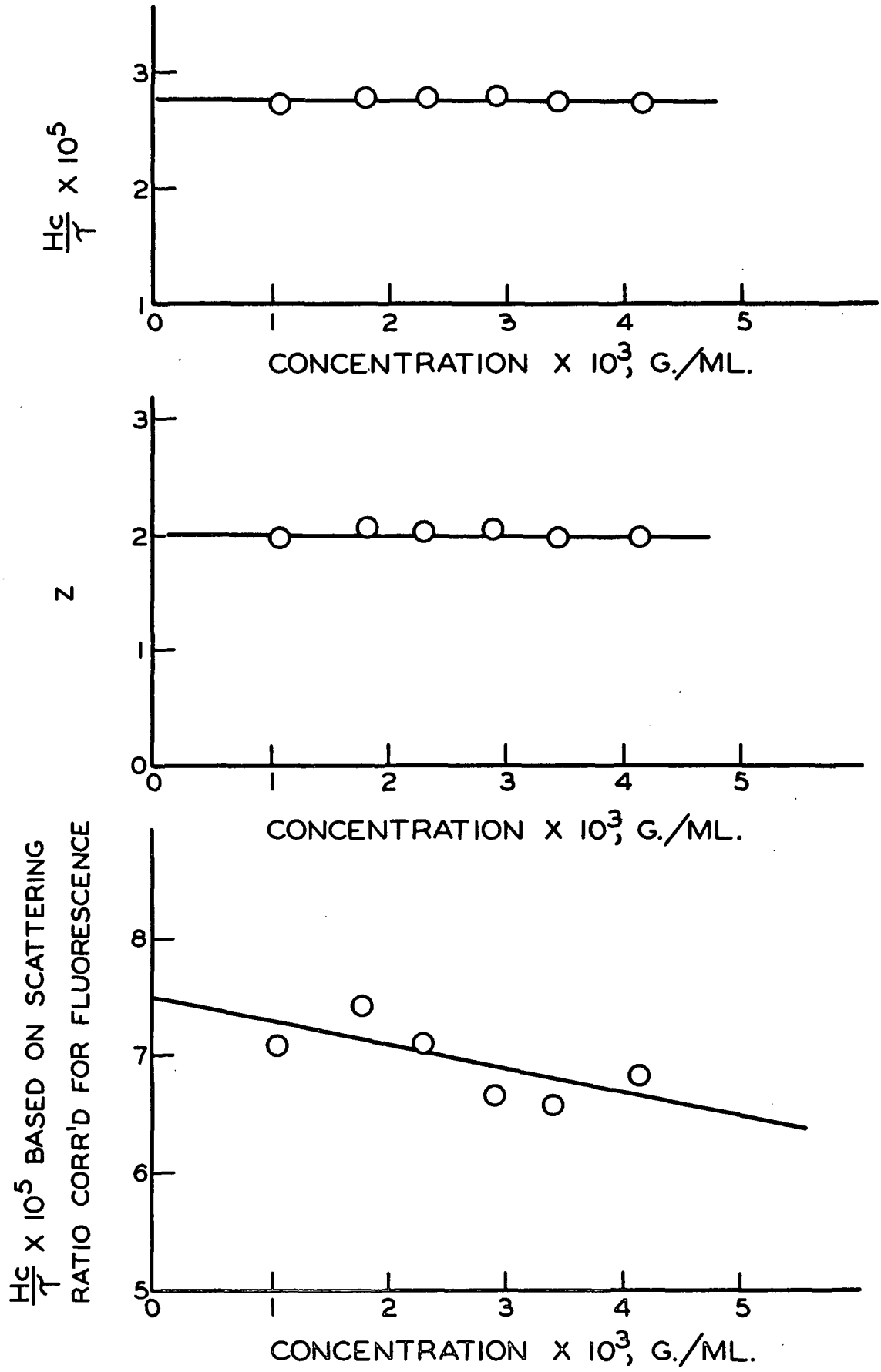


Figure 39. Light-Scattering Data on Fraction 4 of Polymer 11

## APPENDIX VI

## DETERMINATION OF MOLECULAR WEIGHTS WITH THE VAPOR PRESSURE OSMOMETER

Samples of whole Polymer 11 and Fraction 2 of Polymer 11 were sent to Mechrolab, Inc., Mountain View, Cal. for determination of molecular weight on their Model 301A Vapor Pressure Osmometer. In this osmometer, a sample of solution and pure solvent are introduced into a temperature-controlled enclosure which is saturated with solvent vapor. Since the vapor pressure of the solution is lower than that of the solvent, solvent vapor condenses on the solution, causing its temperature to rise. The change in temperature is measured by a thermistor, and the molecular weight of the solute calculated from the Clausius-Clapeyron equation.

The molecular weight of the whole polymer was measured in water by Mechrolab, and a value of 1600 obtained. The value obtained on the membrane osmometer for this sample dissolved in 0.33N potassium chloride and neutralized was 2000.

Insufficient material was available to run more than one concentration of Fraction 2 of Polymer 11 on the vapor pressure osmometer, but the molecular weight calculated from the one data point was 2300. The value obtained on the membrane osmometer was 3800.

The conclusion reached by Mechrolab, Inc., was that the molecular weights obtained for the polymers on the membrane osmometer were very realistic.